University of Alberta

Structural determinants of transport function in the facilitated hexose transporter family (SLC2A) proteins.

By

Andrei Razvan Manolescu ©

A thesis submitted to the Faculty of Graduate Studies and Research in partial fulfillment of the requirements for the degree of Doctor of Philosophy

Department of Physiology

Edmonton, Alberta

Spring 2006

Library and Archives Canada

Published Heritage Branch

395 Wellington Street
Ottawa ON K1A 0N4
Canada

Bibliothèque et Archives Canada

Direction du Patrimoine de l'édition

395, rue Wellington
Ottawa ON K1A 0N4
Canada

Your file Votre référence
ISBN: 0-494-14018-6
Our file Notre référence
ISBN: 0-494-14018-6

NOTICE:
The author has granted a non-exclusive license allowing Library and Archives Canada to reproduce, publish, archive, preserve, conserve, communicate to the public by telecommunication or on the Internet, loan, distribute and sell theses worldwide, for commercial or non-commercial purposes, in microform, paper, electronic and/or any other formats.

The author retains copyright ownership and moral rights in this thesis. Neither the thesis nor substantial extracts from it may be printed or otherwise reproduced without the author's permission.

AVIS:
L'auteur a accordé une licence non exclusive permettant à la Bibliothèque et Archives Canada de reproduire, publier, archiver, sauvegarder, conserver, transmettre au public par télécommunication ou par l'Internet, prêter, distribuer et vendre des thèses partout dans le monde, à des fins commerciales ou autres, sur support microforme, papier, électronique et/ou autres formats.

L'auteur conserve la propriété du droit d'auteur et des droits moraux qui protège cette thèse. Ni la thèse ni des extraits substantiels de celle-ci ne doivent être imprimés ou autrement reproduits sans son autorisation.

In compliance with the Canadian Privacy Act some supporting forms may have been removed from this thesis.

While these forms may be included in the document page count, their removal does not represent any loss of content from the thesis.

Conformément à la loi canadienne sur la protection de la vie privée, quelques formulaires secondaires ont été enlevés de cette thèse.

Bien que ces formulaires aient inclus dans la pagination, il n'y aura aucun contenu manquant.

Canada

Abstract

Facilitated glucose transporters (GLUT's) mediate transport of sugars across cell membranes using the chemical gradient of sugars as the driving force. Improved cloning techniques and database analyses have expanded this family of proteins to a total of 14 putative members. In this I work present the characterization of a novel hexose transporter isoform, GLUT7, which has been cloned from a human intestinal cDNA library using a PCR-based strategy. The encoded protein is comprised of 524 amino acid residues and shares 68% similarity and 53% identity with GLUT5, its most closely related isoform. When GLUT7 was expressed in *Xenopus* oocytes it showed high affinity transport for glucose and fructose. Northern blotting indicated that the mRNA for GLUT7 is present in the human jejunum and ileum, but absent from stomach, duodenum, colon and lung. Western blotting and immunohistochemistry of rat tissues using an antibody raised against the predicted C-terminal sequence confirmed this distribution and indicated that the transporter is predominantly expressed in the brush-border membrane of enterocytes. The unusual substrate specificity and high level of sequence identity with GLUT5 suggest that GLUT7 represents an intermediate between class II GLUT's and the class I member GLUT2.

Sequence alignments indicated that GLUTs 2, 5, 7 & 9 all had an isoleucine residue at position '314' (GLUT7) at the exofacial border of the helix 7, whereas the

non-fructose transporting isoforms, GLUT's 1, 3, & 4, had a valine at the equivalent position. Mutation of I314 to a valine in GLUT7 resulted in a loss of fructose transport, while glucose transport remained completely unaffected. Similar results were obtained with GLUT's 2, 5, 9 and 11. Energy minimization modeling of GLUT7 indicates that I314 projects from TM7 into the lumen of the aqueous pore where it could form a hydrophobic interaction with Tryptophan 89 from TM2. A valine residue at '314' appears to produce a narrowing of the vestibule compared to isoleucine. It is proposed that this hydrophobic interaction across the pore forms a selectivity filter restricting the access of some hexoses to the substrate binding site/s within the aqueous channel.

Acknowledgements

In everything that I have accomplished in my career so far, I have been influenced, helped and motivated by numerous people and my Ph.D. program is no exception. Here is the place to express my public gratitude to those people that have helped me to become a more complete researcher and ultimately a more complete physician.

First of all, I would like to thank to Dr. Chris Cheeseman, which is not a very easy task. It is so hard for me to pinpoint the most important thing that I am grateful for to Dr. Cheeseman because there were so many of them. He passed to me his passion and excitement for research, revealed to me the priceless value of "digging out" old and sometimes undeservedly forgotten research, taught me to price any experimental result as insignificant as would appear at a first look. He guided my academic growth by offering me support when I searched for it but also, giving me the possibility to make and learn from my own mistakes. Above all, I have received from him countless lessons of life that "molded" me beyond the purpose of a Ph.D. program. For all of these, I will always feel indebted to him and I only hope that someday I will be capable to pay this "debt" forward by being capable of offering the same the wisdom and patience to my students.

I would also, like to thank my family, my grandparents, my great-aunt and my father, who lovingly guided and supported me throughout my whole education. They cultivated in me from a very young age, the thirst for knowledge, the desire to ask questions, and the drive to challenge myself continuously in search for answers. For the past five years and from 10,000 km they have been continuously supporting me and putting up with numerous "three o'clock in the morning" phone calls, when I needed to share with them my excitement produced by some experimental results.

Aside from my parents, I have a special "thank you" for my medical school mentors that seeded in me the passion for medicine, which "irremediably" and definitive

"contaminated" me. Here, I have to mention Dr. Adrian Botan, who was the first one to influence me in choosing medicine as a profession. He, along with Dr. Dan Peretianu, Dr. Nicolae Wavernia, Dr. Mihail Isvoranu, Dr. Anton Mihail and Dr. Nicolae Efimov have been living examples of what it takes to be a complete physician.

I am extremely thankful for the substantial help and support received during my Ph.D. from Dr Sandy McEwan who shared with me his enthusiasm regarding basic science and particularly, opened to me the field of nuclear imaging. I will always feel a debt of gratitude.

I have a special thank you for my external reviewers Dr. Jean Yves Lapointe and Dr. Greg Gross for critically reading my thesis and sharing with me their very valuable opinions. I also, have to thank Dr. Howard Young and Dr. Joanne Lemieux who had a critical impact on my understanding of the structure of membrane proteins. Moreover, I would like to thank my committee members, Dr. Jim Young and Dr. Joe Casey for their guidance and advice during my Ph.D.

I am extremely grateful to Dr. Xing -Zhen Chen and Dr. Qiang Li for passing me their hands on experience in molecular biology. Also, a very special "thank you" goes to my fellow colleague Marie-Laure Baudet with whom I shared countless late hours of work and discussion regarding "science, life and their consequences".

This list would not be complete without mentioning the people that have been around me in Dr. Cheeseman's laboratory. Firstly, I would like to thank to Mrs. Debbie O'Neil who literally was part of my "other family"- the "lab family". She spiced up my Ph.D. by making it fun and pleasurable. Moreover, she has been a real team mate for me by offering support and help when needed. Moreover, I would like to thank Anita Au and Ania Stepczinski, former summer students in our lab, for helping me in some of my projects and for their good-hearted friendship.

I would like to thank the staff of our departmental office led by Mrs. Tella Findley for all the help and support that they offered to me during my Ph.D. program.

I would like to thank to University of Alberta and J.B. Collip- Muttart Diabetes Research and Training Centre for their financial support.

I would also like to thank to my best friends Alexandru and Ramona Bortnowschi, and Anna Kuranicheva for continuously supporting and encouraging me in all my endeavors during my Ph.D. program.

I would like to thank Melissa Slugoski, for her love, support and devotement. She has been my "fixed point", continuously helping me to "crystallize" my hypotheses to a final form, patiently teaching me how "to agree to disagree" and constructively bringing my feet on the ground.

I am also thankful to Tara, for her unconditional love and quietly supporting presence in my life.

Table of Contents

Chapter 1 Introduction..... 2

1.1 EVOLUTION OF THE CARRIER CONCEPT..... 3

1.2 KINETIC MODEL..... 13

1.3 HISTORY OF MOLECULAR CLONING AND CHARACTERIZATION OF GLUTs... 18

1.3.1 Phylogenetic class I..... 21

1.3.1.1 GLUT1..... 21

1.3.1.2 GLUT2..... 22

1.3.1.3 GLUT3..... 23

1.3.1.4 GLUT4..... 24

1.3.2 Phylogenetic class II..... 26

1.3.2.1 GLUT5..... 26

1.3.2.2 GLUT7..... 27

1.3.2.3 GLUT9..... 28

1.3.2.4 GLUT11..... 29

1.3.3 Phylogenetic class III..... 30

1.3.3.1 GLUT6..... 30

1.3.3.2 GLUT8..... 31

1.3.3.3 GLUT10..... 32

1.3.3.1 GLUT12..... 34

1.3.4 Other sugar transport proteins related to the GLUT family..... 34

1.3.4.1 GLUT14..... 34

1.3.4.2 HMIT..... 34

1.4 TOPOLOGY MODEL AND 3-D MODELING..... 36

1.5 DETERMINANTS OF FACILITATIVE HEXOSE TRANSPORT..... 42

1.5.1 Particular positions of hexose ring structures necessary for binding and or transport 42

1.5.2 Key amino acids for GLUT structure/ function..... 44

1.5.2.1 Hydrophilic residues with functional importance..... 44

1.5.2.2 The role of aromatic residues in non hydrophilic substrate-transporter interactions..... 49

1.5.2.3 The role of proline residues in conformational changes..... 50

1.5.2.4 Hydrophobic residues with structural-functional importance..... 52

1.6 SUMMARY 61

Chapter 2 Methods..... 64

2.1 MULTIPLE SEQUENCE ALIGNMENTS OF PROTEIN PRIMARY STRUCTURES..... 65

2.2 PHYLOGENETIC TREE CONSTRUCTION..... 69

2.3 HOMOLOGY BUILDING..... 70

2.4 MOLECULAR DYNAMIC SIMULATION..... 71

2.5 TRANSPORT CHANNEL PREDICTION..... 72

2.6 SUBSTRATE DOCKING..... 72

2.7 ISOLATION OF cDNA ENCODING HUMAN GLUT7 GENE..... 73

2.8 SITE DIRECTED MUTAGENESIS..... 75

2.9 PREPARATION OF OOCYTES..... 78

2.10 EXPRESSION RECOMBINANT HGLUT7 PROTEIN IN *XENOPUS LAEVIS* OOCYTES..... 80

2.11 NORTHERN BLOTTING..... 81

2.12 PREPARATION OF ISOLATED PLASMA MEMBRANES..... 82

2.13 WESTERN BLOTTING AND IMMUNOHISTOCHEMISTRY..... 82

2.14 RADIOTRACER FLUX ASSAY..... 84

2.15 KINETIC ANALYSIS..... 84

Chapter 3 Results..... 86

3.1 CLONING OF HGLUT7 (SLC2A7)..... 87

3.1.1 GLUT7 functional studies..... 87

3.1.2 Tissue expression pattern for hGLUT7..... 91

3.2 GLUT7 I314V..... 98

3.3 IDENTIFICATION OF A FRUCTOSE SELECTIVITY COMPONENT IN CLASS II GLUTS..... 111

3.4 IMPORTANCE OF THE AMPHIPATHIC MOTIF NXI/V IN SUBSTRATE SELECTIVITY..... 125

3.7 THREE-DIMENSIONAL MOLECULAR MODELING OF THE FRUCTOSE SELECTIVITY FILTER..... 139

Chapter 4 Discussion..... 142

4.1 CLONING AND CHARACTERIZATION OF HUMAN GLUT7..... 143

4.2 STRUCTURAL AND FUNCTIONAL ROLE OF GLUT7 I314 RESIDUE..... 148

4.2.1 Folded structure of membrane proteins..... 149

4.2.2 Structure-substrate interaction..... 151

4.2.3 Evolutionary and theoretical considerations regarding Ile/Val phenotype in GLUTs members..... 153

4.2.4 Examples of natural mutations of hydrophobic residues in GLUTs members..... 162

4.3 PHYSIOLOGICAL AND PHYLOGENETIC CLASSES OF SLC2A PROTEINS ... 164

4.4 SELECTIVITY FILTER CONCEPT APPLIED TO THE FUNCTION OF SLC2A PROTEINS..... 167

4.5 SUMMARY AND CONCLUSIONS..... 177

APPENDIX..... 181

List of Figures

1.1 STRUCTURE OF MAIN SUGARS TRANSPORTED BY SLC2A TRANSPORTERS..... 4

1.1.1 STRUCTURE OF GLUCOSE AND FRUCTOSE..... 4

1.1.2 STRUCTURE OF CYTOCHALASIN B, FORSKOLIN, GALACTOSE AND 2- DEOXY GLUCOSE..... 5

1.1.3 STRUCTURE OF XYLOSE AND GLUCOSE 6 PHOSPHATE..... 6

1.2 GLUT NOMENCLATURE..... 19

1.3 UNROOTED PHYLOGENETIC TREE OF HUMAN GLUT FAMILY MEMBERS..... 20

1.4 PUTATIVE TOPOLOGY MODEL FOR SLC2A TRASNPORTERS..... 41

2.1 DAYHOFF MATRIX..... 67

3.1. HUMAN GLUT7 STRUCTURE..... 88

3.1. A. OPEN READING FRAME FOR NUCLEOTIDE SEQUENCE OF HUMAN GLUT7..... 88

3.1. B AMINO ACID SEQUENCE OF HUMAN GLUT7 PROTEIN..... 88

3.1. C SEQUENCE ALIGNMENTS OF THE HUMAN GLUT5 AND 7 PROTEINS..... 89

3.2 GLUT7 MEDIATED HEXOSE FLUXES IN *XENOPUS OOCYTES*..... 90

3.3 KINETICS OF GLUT7-MEDIATED GLUCOSE UPTAKE INTO *XENOPUS* OOCYTES..... 92

3.4 KINETICS OF HGLUT7 –MEDIATED FRUCTOSE UPTAKE IN *XENOPUS OOCYTES*...93

3.5. TISSUE DISTRIBUTION OF GLUT7 mRNA BY NORTHERN BLOTTING..... 94

3. 6. *A*: WESTERN BLOT OF OOCYTES MEMBRANES..... 96

3.7. IMMUNOHISTOCHEMISTRY OF RAT ILEUM (*A*) AND COLON (*C*)..... 97

3. 8. COMPARISON OF GLUT5, 7 AND 9 PRIMARY SEQUENCES TO THE CLASS I MEMBERS ONES..... 99

3.9. EXPRESSION OF WILD TYPE AND MUTANT GLUT TRANSPORTERS IN *XENOPUS OOCYTES.* 101

3.10. HEXOSE FLUXES IN *XENOPUS LAEVIS*..... 102

3.11 INHIBITION OF GLUT7-MEDIATED GLUCOSE UPTAKE BY FRUCTOSE..... 103

3.12. INHIBITION OF GLUT7-MEDIATED FRUCTOSE UPTAKE BY GLUCOSE.....105

3.13 KINETICS OF GLUCOSE TRANSPORT IN I314V MUTANT GLUT7.....106

3.14. EFFECT OF THE ADDITION OF 10MM FRUCTOSE UPON I314V GLUT7 MEDIATED D-GLUCOSE UPTAKE..... 107

3.15 HEXOSE TRANSPORT MEDIATED BY HUMAN GLUT7 WILD TYPE AND I314S MUTANT..... 108

3.16 KINETICS OF GLUCOSE TRANSPORT IN I314S MUTANT GLUT7..... 109

3.17 KINETICS OF FRUCTOSE TRANSPORT IN I314S MUTANT GLUT7. 110

3.18. IDENTITY AND SIMILARITY PERCENTAGE AMONG GLUT 2, 5, 7 AND 9..... 113

3.19 HEXOSE FLUXES IN *XENOPUS LAEVIS* OOCYTES EXPRESSING HUMAN GLUT5 WILD TYPE.....114

3.20 KINETICS OF GLUCOSE TRANSPORT IN HUMAN GLUT5..... 115

3.21 HEXOSE FLUXES IN *XENOPUS LAEVIS* OOCYTES EXPRESSING HUMAN GLUT9 WILD TYPE..... 116

3.22 KINETICS OF FRUCTOSE TRANSPORT IN HUMAN GLUT9..... 118

3.23 KINETICS OF GLUCOSE TRANSPORT IN HUMAN GLUT9 119

3.24 EXPRESSION OF WILD TYPE AND MUTANT GLUT TRANSPORTERS IN *XENOPUS* OOCYTES..... 120

3.25 EXPRESSION OF WILD TYPE AND MUTANT GLUT TRANSPORTERS IN *XENOPUS* OOCYTES..... 121

3.26 GLUCOSE AND FRUCTOSE TRANSPORT MEDIATED BY HGLUT2 WILD TYPE AND THE I322V MUTANT..... 122

3.27 GLUCOSE AND FRUCTOSE TRANSPORT MEDIATED BY HGLUT5 WILD TYPE AND THE I296V MUTANT..... 123

3.28 GLUCOSE AND FRUCTOSE TRANSPORT MEDIATED BY HGLUT9 WILD TYPE AND THE I335V MUTANT..... 124

3.29 KINETICS OF GLUCOSE TRANSPORT IN GLUT5 I296V MUTANT. 126

3.30 KINETICS OF GLUCOSE TRANSPORT IN GLUT2 I322V MUTANT..... 127

3.31 KINETICS OF GLUCOSE TRANSPORT IN GLUT9 I335V MUTANT..... 128

3.32 CLASS I AND II ALIGNMENTS. 130

3.33 GLUT11 ISOFORMS A, B AND C MEDIATED HEXOSE FLUXES IN *XENOPUS* OOCYTES. 131

3.34 KINETICS OF GLUCOSE TRANSPORT IN GLUT11 WILD TYPE..... 132

3.35 KINETICS OF FRUCTOSE TRANSPORT IN HUMAN GLUT11 WILD TYPE..... 133

3.36 GLUCOSE AND FRUCTOSE TRANSPORT MEDIATED BY GLUT11 WILD TYPE AND D297N MUTANT..... 134

3.37 GLUCOSE AND FRUCTOSE TRANSPORT MEDIATED BY GLUT11 WILD TYPE AND S298A MUTANT..... 135

3.38 GLUCOSE AND FRUCTOSE TRANSPORT MEDIATED BY GLUT11 WILD TYPE AND V299I MUTANT..... 137

3.39 GLUCOSE AND FRUCTOSE TRANSPORT MEDIATED BY GLUT11 WILD TYPE AND NAI AND NAV MUTANTS..... 138

3.40 PUTATIVE 3D STRUCTURAL MODEL OF HGLUT7 PROTEIN..... 140

3.41 DOCKING MODEL OF GLUCOSE AND FRUCTOSE IN GLUT1 AND GLUT7..... 141

Abbreviations

ATB-BMPA, (1azi-2,2,2-trifluorethyl)benzoyl-1,3bis-(D-mannosyloxy)-2-propylamine

bp, base pairs

BAC, bacterial artificial chrosmosome

cDNA, complementary deoxyribonucleic acid

CB, cytochalasin B

DIG, digoxigenin

2DOG, 2 deoxy-glucose

E. coli, *Escherichia coli*

HEPES, N-(2-hydroxyethyl)-piperazine-N'-2-ethanesulfonic acid

HMIT, human myoinositol trasnporter

FTIR, Fourier-transforming infrared method

GLUT, glucose facilitative transporter

G6P, glucose 6 phosphate

GlpF, glycerol phosphate facilitator (*E.coli*)

GlpT, glycerol phosphate transporter (*E.coli*)

kDa, kilo Dalton

K_m, Michaelis Menten constant

LacY, lactose permease (*E.coli*)

LB, Luria broth

MBM, modified Barth's media

MscL, lactose mechano- sensitive channel

MFS, major facilitator superfamily

MW, molecular weight

NCBI, national center for biotechnology information

NEM, *N*-ethylmaleimide

NIDDM, non insulin depended diabetes mellitus

3OMG, 3-ortho metyl glucose

PAM, percent accepted mutation

PBS, Phosphate-buffered saline

pCMBS, p-chlormercuribenzenesulfonate

PCR, polymerase chain reaction

RACE-PCR, **R**apid **A**mplification of **c**DNA **E**nds-polymerase chain reaction

SCAM- substituted cysteine acessability method

SDS, sodium dodecyl sulphate

SEM, standard error of mean

SGLT, sodium dependent glucose transporter

SLC2A, solute carrier family member

TM, transmembrane spanning domain

V_{max}, maximum transport rate

Structural determinants of transport function in the facilitated hexose transporter family (SLC2A) proteins.

"Mens agitat molem "

Chapter 1.

Introduction.

1.1 Evolution of the "carrier" concept.

The ability to transport glucose across the plasma membrane is a feature almost ubiquitously encountered in all living cells, from the most primordial bacterium to the highly specialized mammalian neurons. The majority of cells require glucose as a primary substrate for oxidative and anaerobic ATP production and for anabolic reactions that have, as an end point, the production of hexose-containing macromolecules[1]. The universal use of glucose as the currency of metabolism is directly linked to the extreme natural abundance of glucose units in the form of cellulose and starch synthesized by the means of photosynthesis in plants and algae.

In mammalian cells, glucose occupies a central role in homeostasis and metabolism. Translocation of glucose across the plasma membrane could be argued to represent perhaps the most important of all nutrient transport systems. Conversely, most of the major categories of membrane transport systems have members involved in the transport of different sugars or their analogues[2]. (Figs 1.1.1-3)

The cell membrane was once considered a static and rigid structure, protecting the cell against loss of essential constituents and allowing specific molecules to exchange according to their lipid solubility[3,4,5], molecular size[6], and electric charge[7]. Soon it became obvious that this concept should be revised and the cell membrane had been identified as an active part of the cell machinery. Early studies[8] of sugar permeability through the erythrocyte membrane showed that there were different rates of penetration

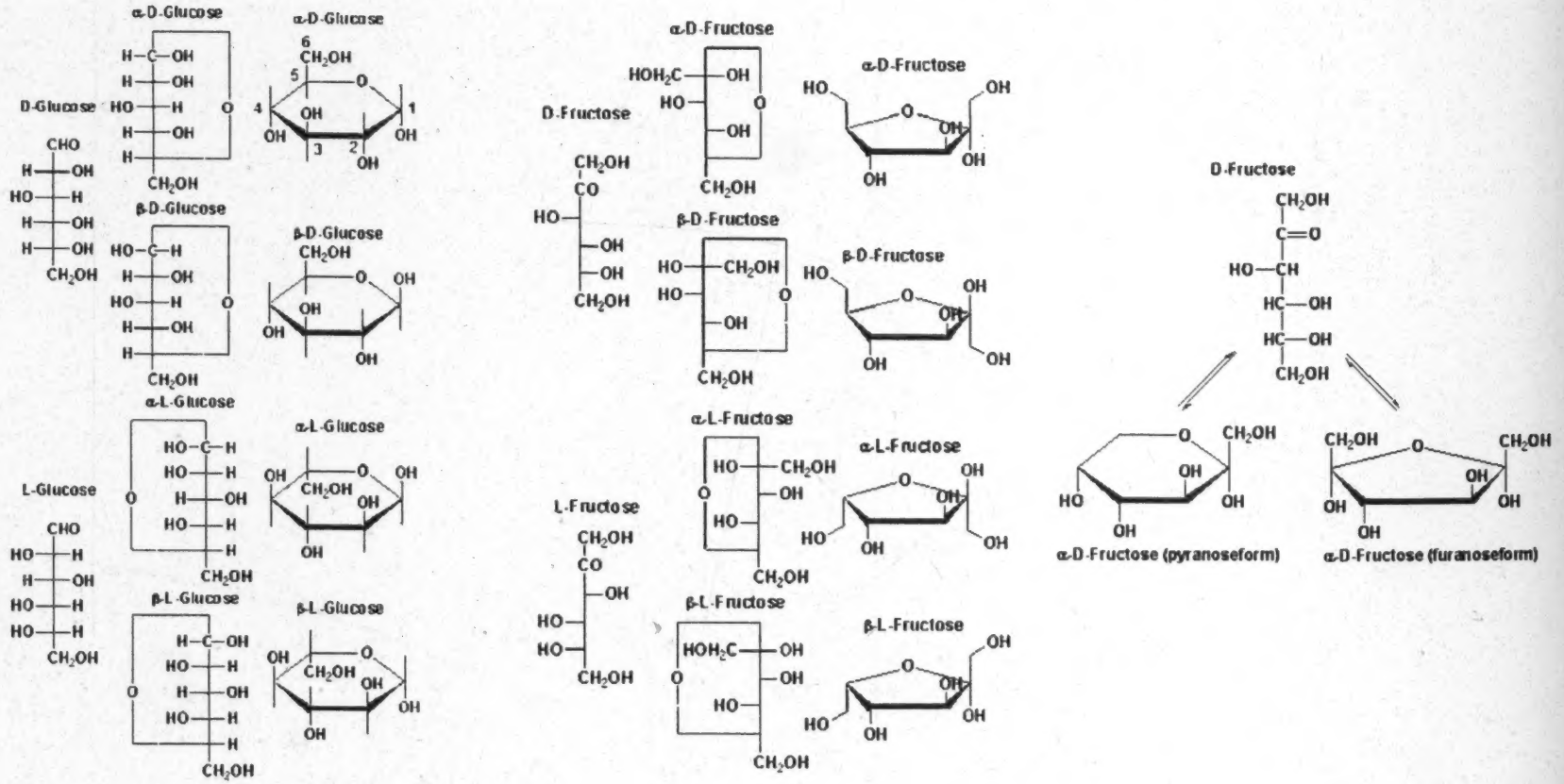

Fig. 1.1.1 Glucose and Fructose chemical structures

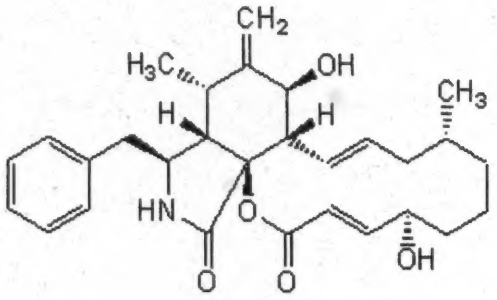

Cytochalasin B

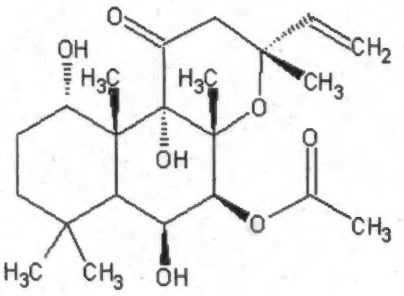

Forskolin A

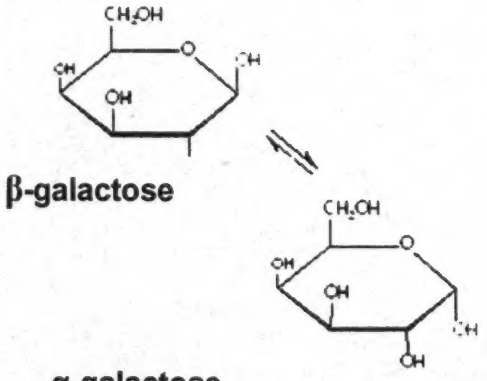

β-galactose

α-galactose

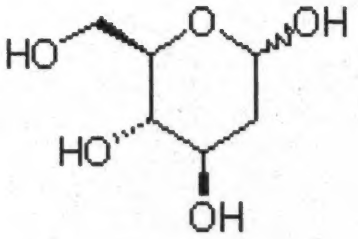

2 DOG

Fig. 1.1.2 Chemical structures of cytochalasin B, forskolin A, galactose, and 2 deoxy - glucose (2DOG),

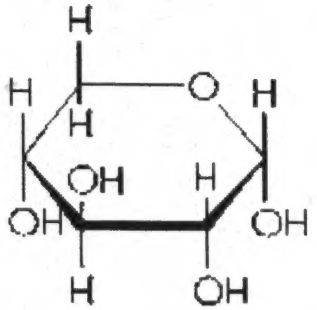

xylose

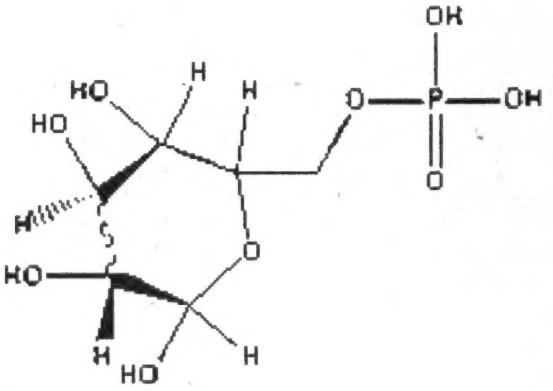

Glucose 6 phosphate

Fig.1.1.3. Chemical structures of xylose and glucose 6- phosphate (G6P)

for some isomeric sugars whereas other did not penetrate at all. It has become obvious, that in these transport systems the mode of passage across the membrane could not be restricted to simple diffusion through aqueous "pores" or through continuous lipid layers. In many cases it proved necessary to assume a closer association between different membrane constituents and the translocating substrate, allowing higher specificity, efficacy and wider possibilities of modification and regulation. As early as 1930, Osterhout[9] suggested that the transmembranous passage of sugars may involve temporary binding to parts of the membrane and Lundegardh[10] was probably the first to suggest that molecular components of the membrane may be involved in such transfers.

These general principles were applied for the first time to the transfer of sugars by Widdas[11] in 1952 who postulated that "carriers" are ultimately responsible for passing sugars forward and backward across the membrane. The starting point of this hypothesis was represented by the finding that simple diffusion fails to explain both the quantitative and qualitative evidence regarding sugar transfer. Quantitative data recorded at the level of the sheep placental barrier did not match the qualitative circumstances associated with the different placental behavior with respect to glucose and fructose. A carrier system was therefore postulated to explain the qualitative requirements based on three main assumptions. Firstly, it was assumed that carriers can transport only glucose but not fructose and secondly, and more importantly, that they are in adsorption equilibrium at their interface with the substrate. Subsequently, it was postulated that carriers pass backwards and forwards across the membrane due to thermal agitation, irrespective of whether they are saturated or not. The logical conclusion of these three assumptions was

that the net rate of transport will be proportional to the difference in the fraction of saturated versus unsaturated carriers on both sides of the membrane. This process was originally thought to be related only to the thermal agitation and not necessarily linked to metabolic processes. At this point, it is worth noting that Widdas[11] was the first to suggest that, the kinetics of sugar carriers might follow Michaelis-Menten kinetics. Later on, Ussing[12] used the term "ferry boats" to describe such carriers offering an oversimplified guide to both the behavior of the molecules and the function they serve. The strength of the concept lay in the fact that it was offering a physically plausible and intuitively reliable qualitative explanation of specific transfers but, unfortunately, the weakness was the lack of quantitative corroboration between the observed phenomena.

The first attempts to more accurately define the kinetics of glucose transport were made on the assumption that permeation of hexose molecules into erythrocytes depended on the difference between the internal cell concentration and the external limiting concentration[13]. This assumption introduced more objective mathematical variables in the study of glucose transport offering a more meaningful interpretation of the experimental data. Only six years later, in 1954, Wilbrandt and Rosenberg[14] defined the characteristics of the "carrier concept" by stating that the essential mechanisms underlying the phenomena are the reaction of the transported substrate with a membrane protein to form a complex and the movement of the complex from one side of the membrane to the other, where the substrate is subsequently released to the aqueous medium. In their paper, Wildbrandt and Rosenberg[14] accurately define and apply

Michaelis-Menten kinetics to the sugar carrier concept. Interestingly, the suggested key elements responsible for the binding reaction were covalent, ionic, and hydrogen bonds.

In defining the carrier concept, Danielli's hypothesis regarding the "propelled shuttle" transport model, occupies a central role[15]. Probably this body of work was the first to introduce the idea of a dynamic carrier, which assumes that during the transport process, the "carrier" molecule undergoes important conformational changes. The hypothesis postulated the existence of an adsorption center on a contractile protein, which is on one side of the membrane when the protein is contracted, and on the other side of the membrane when the protein is extended. At the same time, the concept of a transmembranous passage involving binding to fixed constituents had also started to appear in the literature[16], but at that time was not supported by significant evidence. Thus, the common view was one of a system like an "expanded lattice" in which diffusion is modified by a stretching action on a porous complex, or the hydrogen bonding pore ("polar pore") and did not involve a mobile carrier, but rather a static structure.

Particularly, in regard to the movement of simple sugars, the criteria of a carrier mediated transfer had been noted in a wide range of tissues[17], such as skeletal and cardiac muscle, placenta, adipose tissue, crystalline lens, several types of ascites tumor cells, blood-brain and blood-aqueous barriers, and of course, in red blood cells. One remarkable observation cited the fact that in muscle, adipose and ocular tissues this carrier would require insulin for a full and complete activation[18,19]. Although carrier mediated uptake of sugars had been detected in a diverse variety of tissues, most of the

early kinetic studies were performed on human erythrocytes since these could be obtained easily and in great quantity, thus providing a simple experimental system. The peculiar ease of sugar penetration into human and macaque red blood cells, as compared with erythrocytes of a variety of rodents, carnivores and ungulates had been described since the very beginning of the definition of the concept[8]. Erythrocytes proved to be a very convenient system to study facilitated glucose transport, not only because they were easily and readily accessible, but the high transporter protein content of primate and human red blood cells (~5% of the total plasma membrane proteins) made them an ideal system for identification of the glucose transporters.

Subsequently, functional purification of the erythrocyte glucose transporter was achieved and published by two groups that used independent isolation and reconstitution techniques. The first group[20] used the ability of the of reconstituted fractionated erythrocyte membrane proteins to transport glucose as a primary method of purification. The method was based on the fact that a non-ionic detergent could disrupt and solubilize the membrane and the solubilized fraction could be integrated into liposomes to recreate specific D-glucose permeability. Specific glucose uptake was quantified by performing the experiments under physiological condition (temperature, pH, etc) and using radiolabelled glucose stereoisomers. The extent of the diffusion component was estimated by quantifying the magnitude of L-glucose penetration into reconstituted liposomes. The second group[21] used specific binding of the transport inhibitor, cytochalasin B, as a starting point for the purification process. In principle, their approach was also started by disruption and solubilization of the erythrocyte membrane by the

means of an ether derived detergent. Subsequently the lipids were extracted from the membrane and the purified transporter protein reconstituted into small unilamellar vesicles. In both cases the results were similar, identification of a heterologously glycosylated integral membrane protein, which migrated on a SDS-PAGE as a broad band with an approximate molecular mass of 55kDa, which was reduced to a mass of 46 kDa upon deglycosylation.

Reconstitution of the erythrocyte glucose transporter into liposomes marked an important corner stone in the evolution of the characterization of hexose transporters as both the immunologic and kinetic properties of the newly discovered protein were revealed[22]. Trypsin, which inhibits erythrocyte glucose transport only from the cytoplasmic side, inhibited reconstituted transport activity about 40% when added externally. However, when the trypsin was applied on both sides of liposomes membrane the inhibition was about 80%. This suggested that the reconstituted transporter was oriented about equally in both directions. Antibody prepared against the purified transporter inhibited transport to a maximum of about 50%, also indicating a scrambled orientation. The initial hypothesis of having a "mobile" transporter that undergoes important conformational changes during the translocation process was verified by the kinetic properties exhibited in the liposome and erythrocyte membranes. This was possible by recording the extent of the uptake and efflux of the sugar before and after the membrane was treated with trypsin. The trypsin treatment, at least theoretically, should have inactivated the outward oriented conformations in the liposomes. Recording of the K_m and V_{max} values of the uptake and the efflux revealed that the transporter is

asymmetric with regards to the membrane plane. According to the asymmetric carrier concept, the ratio between K_m and V_{max} should be constant for both directions of translocation, uptake or efflux. The liposomes studies were consistent with this condition and supported the view that the physical model for glucose transporter involves a flexible structure. This predicted that the substrate binding site, initially accessible from one side of the membrane becomes available from the other side only after specific conformational and energetic changes[23]. The conformation of the substrate binding site would, very likely, be different in the two transporter conformations and the conformations were likely to differ in their energy level.

1.2 Kinetic models.

Regarding the kinetic model of hexose transporters there are still a few conceptual controversies regarding issues such as the number of substrate binding sites and the number of the monomers within the functional polymeric unit that are debated between different groups. The simplest kinetic model predicts the existence of a single substrate binding site within the transporter structure, which could be exposed either to the extracellular space or the intracellular one, but not simultaneously to both. This model is known as the "alternating–conformation model" and the protein is proposed to exist in two mutually exclusive conformations such that the single binding site is oriented either toward the outside or the inside of the cell. One of the key predictions of this model is that one single molecule of transporter cannot simultaneously exist in both conformations.

NMR studies[24] have clearly shown that the rate of sugar binding to the transporter and its subsequent dissociation is much faster than the rate of re-orientation of the sugar binding site across the membrane. A model was presented for the transport machinery in which a glucose molecule binds in a cleft between channel-forming transmembrane helices, and during the transport event, a sliding barrier moves past the transport site, thereby exposing the site to the opposite side of the membrane. This study, by revealing individual rate constants for the loaded and unloaded transporter, provided strong support for the single binding site theory.

Conversely, another model predicted a dimeric or tetrameric organization of the transport molecules in the membrane, a fact that would enable the transporter to be structurally more "dynamic" and occupied either from the inward or outward direction, hence presenting more binding sites[25]. Earlier studies[25,26] had suggested that both inward and outward facing substrate binding sites could be occupied simultaneously. The fact that the functional and kinetic experiments performed in erythrocytes could not be replicated with purified GLUT1 (facilitative glucose transporter 1-SLC2A1) created more confusion[27,28]. However, there is evidence both from Western blotting and hydrodynamic studies that GLUT1 can exist as a monomer, a dimer or possible even a tetramer and the kinetic behaviour of all this different forms might be different[29,30]. Detergent extraction of erythrocyte GLUT1 also revealed that the native structure of the protein binds a single molecule of the transport inhibitor cytochalasin B per 2 molecules of GLUT1 and presents at least two binding sites for glucose[31]. In contrast, when reducing agent is added to the purification /extraction buffers, a single molecule of GLUT1 protein binds 1 molecule of cytochalasin B. The proposed explanation considered the possibility that GLUT1 was expressed either as a dimer or a tetramer. Each monomer in these higher order structures would be completely functional and exist in one of two conformations, as predicted by the alternating conformational model. The difference between tetrameric and dimeric transporter consists of the way in which the monomers interact. In dimeric GLUT1, it is proposed that there are no conformational restraints, so each monomer can isomerize between the inward and outward facing sites independently of the other. Since cytochalasin B binds to an inward-facing site, in the dimeric conformation each monomer

could bind this reagent giving rise to the observed 1:1 binding ratio. In contrast, tetrameric GLUT1 is comprised of two dimers of GLUT1 in a pseudo-D2 symmetrical arrangement[31]. They are proposed to have the conformationally active regions constrained such that there is coupled isomerization between the inward and outward facing binding sites in these dimers which results in an antiparallel arrangement of the binding sites[31]. This arrangement would allow for the tetramer to have, at any given time, one subunit folded in the inward facing conformation and the other in the outward facing one. This model fits most of the available data for substrate binding and provides strong support for the functional oligomerization of GLUT1[32]. However, whether or not oligomerization as dimers or tetramers carries any physiological advantage still remains to be established.

Widdas was the first to clearly define how the Michaelis-Menten kinetic properties of a transporter could be defined experimentally, including equilibrium exchange, zero-*trans* and infinite *cis*/*trans* measurements[11] to measure the K_m and V_{max} constants. Equilibrium exchange experiments have been suggested to be of the most powerful type of assay employed in the kinetic study of a transport protein. Cells are preincubated with various concentrations of substrate and the uptake of tracer is measured from the external media with the same concentration of substrate as inside the cells. A modification of this method can be also used to determine the exit of the tracer which would give the K_m and V_{max} values of the substrates' exit. Zero-*trans* entry experiments are the simplest studies to perform, involving the measurement of the uptake of trace amounts of radio-actively labeled D-glucose into cells which have been stored in

a medium without glucose for a certain period of time so that the cytosolic sugar concentration is as low as possible. The external sugar concentration is varied for each measurement. This type of assay measures the sugar binding affinity of the exofacial binding site and the maximum velocity of sugar entry under infinitely high substrate concentrations. Infinite-*cis* experiments determine the K_m of the internal binding site and the V_{max} for exit by preincubating the cells in variable concentrations of hexose plus tracer until equilibration is reached. The experiment is started by the addition of a saturating concentration of sugar plus tracer. Interestingly, in the case of GLUT1, the recorded values of K_m and V_{max} for each of the above mentioned conditions were different. This could only be explained by the existence of different conformations of the transporter during the uptake or efflux processes. Hence, the transporter is said to be asymmetric in regards to the membrane plane.

One other important feature of facilitative sugar transporters is *trans*-acceleration, which is the ability of unlabelled substrate on one side of the membrane to stimulate the transport of radiolabeled substrate from the other side. This phenomenon is most marked at lower temperatures because it is directly linked to the thermodynamics of the conformation changes within the protein. Thermodynamic analysis of GLUT1 had shown that the differences in zero-*trans* Michaelis constants seen at low temperatures arise not as a consequence of different affinities of the transporter for the substrate, but rather from asymmetry in the rate constants for transporter reorientation[33]. At 0°C it was argued that the loaded and unloaded conformations of the transporter are highly asymmetrically distributed across the membrane. It was postulated that, in the absence of

glucose, only ~6% of the transporter would be in the outward-facing conformation. This percentage could be changed by increasing the reaction temperature to 37°C, when almost 40% of the unloaded transporter could be in the outward-facing conformation. Similar asymmetry was predicted for the loaded transporter. This observation was explained on the base of large endothermic enthalpy and positive entropy changes associated with the reorientation of the transporter from inward to outward-facing conformation[34]. Gibbs free energy changes associated with reaching the transition state through which the glucose transporter translocates the substrate could be calculated by applying transition state theory to the kinetics of the transporter[33,34]. These values are strongly endothermic and associated with a large increase in entropy consistent with the dissociation of water molecules from the transporter in the process of moving into the biologically active conformation.

1.3 History of molecular cloning and characterization of GLUT proteins:

In the past 20 years, following the immense progress of molecular biology, human genome mapping and data mining, the sugar transporter family evolved from a single and ubiquitously expressed member (GLUT1) to a phylogenetic family with up to 14 members. However, only during the last 7-8 years, have the last two thirds of the genes that encode glucose transporter-like proteins been identified and characterized. Because of their sequence similarity with GLUT1, these genes appear to belong to the family of solute carriers 2A (*SLC2A*, protein symbol GLUT) (Figs 1.2.). Sequence comparisons of all 14 family members allow the definition of characteristic sugar/polyol transporter signatures[35]: ***(1) the presence of 12 membrane spanning helices, (2) seven conserved glycine residues in the helices, (3) several basic and acidic residues at the intracellular surface of the proteins, (4) two conserved tryptophan residues, and (5) two conserved tyrosine residues***. On the basis of sequence similarities and characteristic elements, the extended GLUT family can be divided into three subfamilies, namely class I (the previously known glucose transporters GLUT1-4), class II (the previously known fructose transporter GLUT5, 7, 9 and 11), and class III (GLUT6, 8, 10, 12, and the myoinositol transporter HMIT1), Fig 1.3.

Protein	alias	Gene name	Chromos. localization	Acc. Nos. cDNA	Gene (ensemble)	Expression
GLUT1[1]		SLC2A1	1p35–31.3 (47.7 MB)	K03195	AC023331	erythrocytes, brain (vascular)
GLUT2[2]		SLC2A2	3q26.2–27 (186.9 MB)	J03810	AC068853	liver, islets
GLUT3[3]		SLC2A3	12p13.3(8.1 MB)	J04069	AC007536	brain (neuronal)
GLUT4[4]		SLC2A4	17p13 (8.4)	M20747	AC0003688	muscle, fat, heart
GLUT5[5]		SLC2A5	1p36.2 (8.3 MB)	J05461	AC041046	intestine, testis, kidney
GLUT6[6,7]	GLUT9[6]	SLC2A6	9q34 (136.5 MB)	Y17803	AC002355	spleen, leukocytes, brain
GLUT7		SLC2A7	1p36.2 (8.2 MB)		AL356306	unknown
GLUT8[8,9]	GLUTX1[10]	SLC2A8	9 (129.9 MB)	Y17801	AL445222	testis, blastocyst, brain
GLUT9[11]	GLUTX[12]	SLC2A9	4p15.3–16 (10.2 MB)	AF210317	AC005674	liver, kidney
GLUT10[13]		SLC2A10	20q12–13.1 (47.3 MB)	AF321240	AC031055	liver, pancreas
GLUT11[14]	GLUT10[15]	SLC2A11	22q11.2 (20.8 MB)	AJ271290	AP000350	heart, muscle
GLUT12	GLUT8[16]	SLC2A12	6q23.2 (145.5 MB)		AL449363, AL35699	heart, prostate

Fig. 1.2 GLUTs nomenclature adapted from H. Joost and B Thorens in 2003[35].

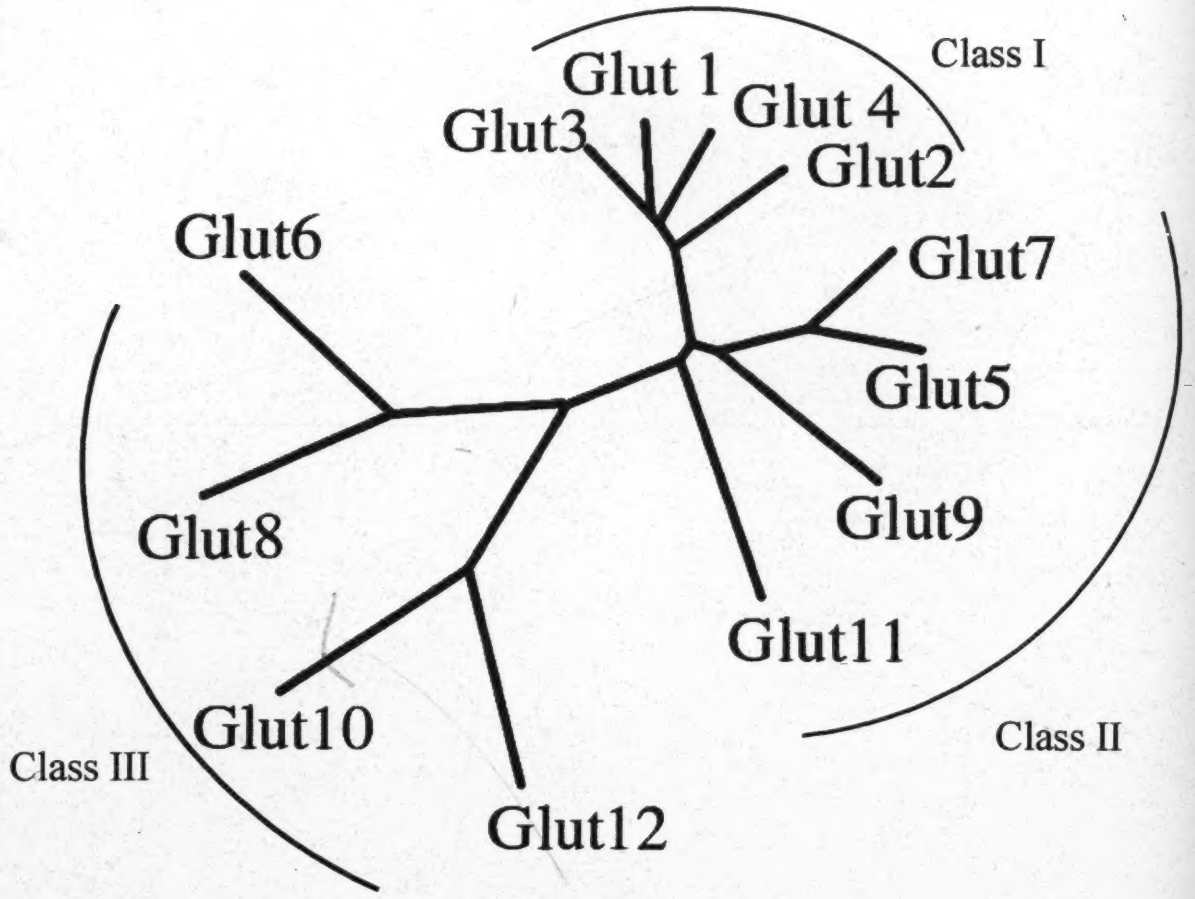

Fig. 1.3. Unrooted phylogenetic tree of the human GLUTs family members.

1.3.1 Phylogenetic class I SLC2A proteins.

1.3.1.1 GLUT1

In 1985, the GLUT1 cDNA sequence had been isolated from HepG2 hepatoma cells[36]. Structural analysis of the purified human erythrocyte glucose transporter by fast atom bombardment mapping and gas phase Edman degradation confirmed the identity of the clone and demonstrated that the HepG2 and erythrocyte transporters were highly homologous. The protein has 492 amino acids and there is a significant homology among the isoforms from different species such as rabbit, rat, mouse and pig. Based on the predicted amino acid sequence coupled to hydropathy analysis, the protein was expected to consist of 12 TM (transmembrane spanning domain) helices with the N- and C-termini and a large loop between helices 6 and 7 located cytoplasmically. Tissue distribution of this transporter revealed a ubiquitous expression among numerous human tissues[37,38]. In humans, GLUT1 is expressed at highest levels in the brain and erythrocytes, but is also enriched in the cells of the blood-tissue barriers, placenta and retina. The commonly accepted role of GLUT1 in peripheral tissues most likely involves a house keeping function, in which GLUT1 provides a constant supply of glucose required for resting cellular homeostasis. The substrate specificity of GLUT1 includes glucose, galactose, 2-deoxy-glucose and 3-O-methyl-glucose. The zero *trans* influx K_m for glucose is 1.6 mM, which indicates that this transporter has a relatively high affinity.

1.3.1.2 GLUT2

This isoform was cloned and characterized based on the observation that the glucose uptake by hepatocytes was significantly different from that in erythrocytes[39]. The substrate affinity of the transport seemed to be lower than that observed in erythrocytes and, in an effort to solve this discrepancy, two different laboratories developed strategies for isolating transporter cDNA from tissues/cells[40,41]. Their strategy employed the use the of GLUT1 cDNA to probe libraries from hepatocytes under conditions of low stringency. The results revealed a protein of 524 amino acids that shared an 80% similarity and 55% identity with GLUT1 which was called GLUT2. Furthermore, hydropathy plots of GLUT1 and GLUT2 proteins are almost super-imposable. The substrate specificity of GLUT2 was different from GLUT1, the transporter being able to translocate not only glucose and its direct analogues 2DOG (2-deoxy-glucose) and 3OMG (3-ortho-methyl glucose), but D-fructose as well. GLUT2 proved to be a high capacity low affinity transporter exhibiting an equal K_m for glucose and fructose of about 66 mM. Thus, GLUT2 is expressed in the hepatocyte membrane where is very likely to be the principal route for the import and export of the sugars at the site of the "metabolic brain" of the body. Another interesting expression site is that of human pancreatic β-cells, which was identified by Thorens[42]. This observation is still debated by other groups, but by analogy with other species rat[43], mouse[44] and pig (personal unpublished results) there is a high likelihood that this finding is correct. The

other two interesting tissues which express GLUT2 are the small intestine and kidney. Initially, either in intestine or kidney the presence of GLUT2 was considered to be confined to the basolateral membrane[45]. This finding correlated with the kinetic properties of a high capacity transporter and a function in translocating of absorbed sugars from the gut or renal epithelium into the blood stream. More recent studies have shown that under special conditions, when the need for the uptake of sugars at the apical pole is increased, GLUT2 could be inserted into the brush border membrane of the renal proximal tubules[46] or small intestine[47].

1.3.1.3 GLUT3

Low stringency hybridization screening of a human fetal muscle library isolated the cDNA encoding the 496 amino acid residue protein - GLUT3[48]. This member of class I GLUTs, has a prevalent expression in the brain, but the protein is also expressed in other tissues such as fat cells, certain skeletal muscles, placenta and kidney[49]. The kinetic studies of this transporter revealed a K_m for 2 deoxy-glucose and 3-O-methyl-D-glucose of 10.6 mM and 1.4 mM, respectively. These relatively high affinity properties suggested that GLUT3 functions under conditions either of high glucose demand or hypoglycemia. In the brain and nervous tissue, the expression of GLUT3 may be required to successfully utilize low concentrations of blood glucose.

1.3.1.4 GLUT4

Exposure of resting adipocytes to insulin results in a rapid and large increase in the rate of glucose transport into the cell. In isolated rat adipocytes this increase may be as much as 30-fold, and the stimulation of transport is achieved within 10 minutes of treatment of cells with insulin. In human adipose tissue, the response to insulin is much smaller, with approximately a 2-4 fold increase in transport[50]. Kinetic studies showed the major effect of insulin is to increase the V_{max} of glucose uptake. The molecular basis of this observation was demonstrated by the finding of a large pool of glucose transporters present inside the adipocytes under resting conditions[51]. By virtue of this sequestration in the intracellular compartment, this population of transporters does not contribute to basal glucose transport. Upon exposure to insulin, these transporters are rapidly inserted into the adipocytes membrane, through a process called 'translocation'. The clear differentiation between the components of glucose uptake in the adipocytes was possible with the production of a monoclonal antibody which recognized a protein of 509 amino acid residues and a molecular weight of ~50 kDa that was capable of binding cytochalasin B and was recruited from the intercellular compartment to the cell surface in response to insulin in adipocytes[52]. This transporter termed GLUT4 or the insulin-responsive transporter, and was subsequently shown to be expressed in adipocytes and muscle. A more recent study also showed the presence of GLUT4 in human and rat pancreatic β-cells, where it could be part of the insulin signaling system[53]. The functional properties of this transporter revealed a K_m for 2 DOG and 3-OMG ranging from 2 to 5

mM. This relatively low K_m will ensure that the protein operates close to the V_{max} over the normal range of blood glucose concentrations, thus allowing the rapid removal of blood glucose into the body's energy stores.

1.3.2 Phylogenetic class II of SLC2A proteins

Class II is comprised of the fructose-specific transporter GLUT5 and three related proteins, GLUT7, GLUT9 and GLUT11. The most striking sequence characteristic of class II transporters is the lack of the tryptophan following the conserved ***GPXXXP*** motif in helix 10 corresponding to tryptophan 388 in GLUT1. This tryptophan was shown to be important for the binding of the ligands cytochalasin B and forskolin, but not for glucose transport activity[54,55] .

1.3.2.1 GLUT5

Application of the low stringency hybridization led to identification of GLUT5[56], whose cDNA encoded a 501 amino acids protein. This protein proved from the outset to be quite different from the other GLUT family members. Firstly, it shared only ~40% identity with the other isoforms and secondly, when initially expressed in *X. laevis* oocytes[57] the transporter exhibited little or no glucose transport, but rather was found to be a D-fructose transporter (K_m ~ 6 mM). This was of great interest due to the physiological implications for such transporter in the context of tissue specific metabolism. However, the substrate specificity of this transporter was determined primarily on the basis of 2-DOG and 3-OMG uptake and not of D-glucose and this resulted in an incomplete characterization of the protein. Also, GLUT5 transport function is not cytochalasin B inhibitable[57], which appears to be a common feature of all

the class II GLUTs, but was a unique observation at the time. Northern blot and immunoblot analysis revealed that the protein is encoded for and expressed in a variety of tissues such as muscle, brain, adipose tissue, kidney and testis. The protein was found to be abundantly expressed in rat small intestine with less expression in the colon. The presence of the protein was primarily identified in the proximal segments of the small intestine at the apical pole of the enterocytes. Expression at this site initially indicated that it formed the major and unique fructose absorption route from the intestinal lumen to the blood stream. However, it appears that GLUT5 could perform the uptake of fructose in conjunction with the GLUT2 for which insertion in the apical pole of the enterocytes could be induced by special conditions.

1.3.2.2 GLUT7

W. Becker and H. Joost indicated that GLUT7 was an uncharacterized gene (*SLC2A7*) which they had identified in a genome wide homology search[58]. The gene was identified on a locus adjacent to the GLUT5 gene (*SLC2A5*) on chromosome1p36.2 suggesting a possible gene duplication event. The deduced amino acid sequence of a cDNA that was assembled on the basis of the genomic sequence exhibited a high degree of similarity with the fructose-specific GLUT5 (58% amino acid identity). The pattern of gene expression and the substrate specificity of the putative protein were unknown at the time its identification.

1.3.2.3 GLUT9

In an attempt[59] to identify glucose transporter 9, the known transporter protein sequences were used to search the expressed sequence tag (EST) database using a Basic Local Alignment Search Tool. The EST clone F00548, derived from a normal human muscle library, was found to have significant homology to GLUT 1 and 5 when its insert was translated. The corresponding genomic sequence is available in the high-throughput genome sequence database (Accession No. AC005674 from chromosome 4 BAC). The cloned human GLUT9 gene, which maps to chromosome 4p15.3-p16, consists of 12 exons coding for a 540 amino acid protein. Based on a sequence entry (NCBI accession number BC018897) and screening of expressed sequence tags an alternative splice variant of GLUT9 was cloned from a human kidney cDNA[60]. The RNA of this splice variant consists of 13 exons and codes for a putative protein of 512 amino acids (GLUT9DeltaN). The two proteins differ only in their N termini, suggesting a different subcellular localization and possible different physiological roles. Screening human tissue RNA by reverse transcription-PCR showed that GLUT9 is expressed mainly in kidney, liver, placenta, and leukocytes, whereas GLUT9DeltaN was detected only in kidney and placenta. (These two proteins are now being referred to as GLUT9a and GLUT9b – personal communication from Dr. Kelle Moley, Washington University). The GLUT9 protein was localized with immunohistochemistry to human kidney proximal tubules. Subcellular fractionation of human kidney revealed the GLUT9 protein in plasma membranes and high density microsomal membranes. Original oocyte expression

studies of GLUT9 revealed a small level of 2DOG uptake and cytochalasin B insensitivity.

1.3.2.4 GLUT11

Human GLUT11 is a novel sugar transporter, which exhibits significant sequence similarity with the members of the GLUT class II members[61]. The amino acid sequence deduced from its cDNA, produced by RT-PCR (reverse transcriptase polymerase chain reaction) with RNA from human heart, predicts 12 putative membrane-spanning helices and all the motifs (sugar-transporter signatures) that have previously been shown to be essential for sugar-transport activity. The closest relative of GLUT11 is the fructose transporter GLUT5 (sharing 41.7% amino acid identity with GLUT11). The human GLUT11 gene (SLC2A11) consists of 12 exons and is located on chromosome 22q11.2. In human tissues, a 7.2 kb transcript of GLUT11 was detected exclusively in heart and skeletal muscle. Transfection of COS-7 cells with GLUT11 cDNA significantly increased the glucose-transport activity reconstituted from membrane extracts as well as the specific binding of the sugar-transporter ligand cytochalasin B. In contrast to that of GLUT4, the glucose-transport activity of GLUT11 was markedly inhibited by fructose. It is concluded that GLUT11 is a novel, muscle-specific transport facilitator that is a member of the extended GLUT family of sugar/polyol-transport facilitators. There had been identified three distinct isoforms which encode three similar proteins of 496, 503 and 499 amino acids respectively have been identified.

1.3.3 Phylogenetic class III of SLC2A proteins.

Class III comprises five isotypes: GLUT6, GLUT8, GLUT10, GLUT12, and HMIT1. Sugar/polyol transport activity has been shown for GLUT6, GLUT8 and HMIT1. Class III GLUT's are characterized by a shorter extracellular loop 1 that lacks a glycosylation site, and by the presence of such a site in the larger loop 9.

1.3.3.1 GLUT6

The human GLUT6 cDNA (formerly designated GLUT9) was cloned by PCR and RACE-PCR amplification[62] on the basis of sequence information obtained from murine expressed sequence tags and a human genomic sequence (BAC clone ASAC1644). The deduced amino acid sequence of GLUT6 presents 507 amino acids and all elements (glucose transporter signatures) that are characteristic for the GLUT family and are required for their function as sugar transporters. Specifically, the sequence predicts a tertiary structure that includes 12 membrane-spanning helices like all the other members of the SLC2A family. Human GLUT6 mRNA is predominantly expressed in brain, spleen and peripheral leukocytes. However, the presence of a GLUT6 protein in these tissues has not been demonstrated so far. Glucose transport activity of GLUT6 has been shown in a system of reconstituted membranes, but is as yet poorly characterized. The transporter appears to be a low-affinity facilitator, since transport activity was found only at high substrate concentrations (5 mM). Thus, it cannot be excluded that GLUT6

facilitates the transport of yet unknown substrates with higher affinity. Corresponding with its low affinity for glucose, GLUT6 exhibits low affinity binding of cytochalasin B.

1.3.3.2 GLUT8

GLUT8 (formerly designated GLUTX1) was the first of the novel GLUT-isoforms that was identified[63]. The human and mouse cDNA were independently cloned by two groups[63,64] on the basis of sequence information obtained in searches of the EST databases. Like GLUT6, GLUT8 belongs to the class III sugar transport facilitators, which are characterized by the lack of a glycosylation motif in loop 1, and by the presence of such a motif in the larger loop 9. The deduced sequence of GLUT8 exhibits 477 amino acids and all the motifs that are associated with sugar transport activity. Apparently this protein is targeted to intracellular compartments by dileucine motifs in a dynamin dependent manner. The genes of GLUT8 and GLUT9 show a strikingly similar organization and are both located on chromosome 9 within a distance of ~ 5 MB. Sugar transport activity of GLUT8 has been shown with two different methods. Expression of the protein in *Xenopus* oocytes produced high-affinity glucose transport activity (K_m ~ 2 mM)[63]. Interestingly, this activity was specifically inhibited by fructose. Transfection of COS-7 cells with GLUT8 cDNA produced the expression of reconstitutable glucose transport activity and of high-affinity cytochalasin B binding[64]. Human GLUT8 mRNA was predominantly found in testis; lower amounts were detected in most other tissues including insulin sensitive tissues, e.g brain, muscle, adipocytes [63,64]. In addition, GLUT8

mRNA and protein was detected in pre-implantation embryos (blastocysts)[65]. Expression in testis appeared to be germ cell-associated and gonadotrop-independent, since GLUT8 mRNA was not found in testicular carcinoma and testis from patients treated with estrogen and cyproterone acetate[64]. Furthermore, GLUT8 was not found in testes from pre-pubertal rats or mice. In brain, GLUT8 mRNA was detected in hippocampal pyramidal neurons and granule neurons of the dentate gyrus; experimental diabetes induced by treatment of rats with streptozotocin produced a modest increase of GLUT8 mRNA and protein in these structures[66].

1.3.3.3 GLUT10

Human GLUT10 cDNA (*SLC2A10*) was isolated[67] by 3' and 5' RACE-PCR, with sequence information from an EST and from its genomic sequence (BAC clone HS28H20). According to the multiple alignment of the deduced amino acid sequence, GLUT10 is a class III sugar transporter with highest sequence similarity to GLUT8. The deduced amino acid sequence of GLUT10 predicts all sugar transporter signatures with the exception of the PESPR motif after helix 6. The lack of this motif is very surprising, because it is conserved not only in all other members of the GLUT family but also in the organic cation transport facilitators.

So far, no information as to the transport activity and selectivity of GLUT10 is available. GLUT10 contains 541 amino acids with several glucose transporter sequence motifs and amino acids essential for glucose transport function. In addition, secondary

structure analysis of GLUT10 predicts 12 putative transmembrane domains, a hallmark structure of the GLUT family. The tissue distribution of GLUT10 was determined by Northern and Western blot analysis, which revealed the highest levels of expression in the liver and pancreas.

1.3.3.4 GLUT12

The cDNA of GLUT12 has been detected in breast cancer cells and was cloned from a human embryonic cDNA library and then characterized in *Xenopus laevis* oocytes[68]. GLUT12 (617 amino acid residues) possesses the structural features critical to facilitative transport of glucose, but the key to understanding the possible physiological roles of this novel protein requires analysis of functional glucose transport. In the above mentioned study, *Xenopus laevis* oocyte expression system was used to assay transport of the glucose analog 2-deoxy-D-glucose and characterize the glucose transport properties and hexose affinities of GLUT12. The results demonstrated that GLUT12 facilitates transport of glucose with an apparent preferential substrate affinity for glucose over other hexoses assayed. These results shed some insights upon the potential role and importance of GLUT12 in insulin-sensitive tissues and also cells with high glucose utilization such as cancer cells.

1.3.4 Other sugar transport proteins related to the GLUT family

1.3.4.1 GLUT14

Probably not a true GLUT isoform, but more likely a pseudogene of GLUT3, it has been identified on chromosome 12p13.3 (17.1M), about 10 Mb upstream of GLUT3, with which it shares remarkable identity[69]. It would consist of 11 exons with a genomic organization similar to that of *GLUT3* and likely resulted from a duplication of *GLUT3.* GLUT14 has two alternatively spliced forms; the shorter form of GLUT14 (GLUT14-S) consists of 10 exons and produces a 497-amino-acid protein that is 94.5% identical to GLUT3. The long form (GLUT14-L) has an additional exon and codes for a protein with 520 amino acids that differs from GLUT14-S only at the N-terminus. In contrast to the expression of GLUT3 in many tissues, both isoforms of GLUT14 are putatively expressed in testis. The mRNA level of GLUT14 in testis is about four times higher than that of GLUT3.

1.3.4.2 HMIT

HMIT was identified[70] by screening EST databases with the sequence of rat GLUT8. Full-length cDNAs were isolated from rat hypothalamus and human frontal cortex cDNA libraries. The deduced amino acid sequences of rat and human HMIT are 618 and 629 amino acids long, respectively, with 90% identical and 93% similar residues.

The rat HMIT sequence is 36% identical and 44% similar to that of rat GLUT8. It contains 12 predicted transmembrane domains (TM) with a long cytoplasmic loop between TM6 and TM7 and several of the glucose transporter signature sequences. The N-terminal region contains an ER retention signal (RRR, position 4 to 6) and a dileucine internalization signal (position 22 to 23) and the C-terminal tail contains a tyrosine-based internalization motif (YIRV, position 599 to 602). An extracellular loop of 95 amino acids, which contains 3 N glycosylation sites, is present between TM9 and TM10. HMIT shows highest similarity with five non-mammalian proteins of unknown function; three are from *Caenorhabditis elegans* and two from *Arabidopsis thaliana*. These five proteins contain an extracellular loop between TM9 and TM10, which shows an average of 33% similarity and 30% identity with the corresponding HMIT loop. The loops of these six proteins all contain eight cysteines and a CGFC motif and 2 to 4 N glycosylation sites. Other closely related proteins include the bacterial H^+/galactose and H^+/xylose symporters, H^+/myoinositol symporter of *Leishmania donovani* (MIT) and two yeast inositol transporters (ITR1 and ITR2). HMIT has a MW of 67 kDa when expressed in reticulocyte lysates. HMIT is expressed predominantly in brain, where it is found as a glycosylated protein of MW 83 kDa. It is present both with astrocytes and some neurons. Electron microscopy revealed the presence of HMIT in intracellular compartments and on the plasma membrane. Expression on the cell surface may require the presence of an accessory protein.

1.4 Topology model and three dimensional modeling

Since the first member of the GLUT family was cloned, numerous attempts have been made to determine the 3D structure of the protein with the goal of understanding how these facilitative hexose transporters move their substrate from one side of the membrane to the other[71,72,73,74]. Kinetic analyses in the human red blood cells are mostly consistent with an alternating conformation mechanism, however, kinetic anomalies have been observed that appear to be inconsistent with this simple mechanism[75,76]. This contradiction may be the result of difficulties in accurately measuring the real steady state kinetic properties of these transporters.

The isolation of GLUT1 in a functionally active state has allowed some interesting biophysical analysis of this polytopic membrane protein. Infrared spectroscopy is a valuable method for investigating protein secondary structure, and enables the relative proportions of α-helical, β-strand and random coil formation to be determined from the frequency of the amide I and II bands. Fourier-transforming infrared methods (FTIR) allow the analysis of protein structure in dilute aqueous media, producing spectra which can be deconvoluted to analyze the overlapping amide absorptions caused by various secondary structures which might be present within the protein. FTIR studies[77] of GLUT1 protein in lipid bilayers have shown that the glucose transporter contains, in addition to the predominant α -helical structure, an appreciable amount of β-structure and random coil conformation. The study of the time dependency

of H-2H exchange revealed that more than 80% of the polypeptide backbone is readily accessible to the solvent. This result indicates that a portion of the intramembrane-spanning region of the membrane protein is exposed to the solvent, suggesting the existence of an intraprotein aqueous channel. The residual (10-20%) portion of the protein, which exchanges slowly, includes some α -helical structure, probably situated in a hydrophobic environment inside the membrane. Compared with the spectra recorded under conditions in which the "inward-facing" form predominates, a small but reproducible shift in the bands assigned to α-helical and β-strand structures is observed after incubation with 4,6-O-ethylidene-D-glucose, which largely fixes the transporter in the "outward-facing" conformation. An increase of temperature, which is known to increase the proportion of transporter in the outward-facing conformation, results in a similar shift in this α-helical absorption band. Polarized FTIR spectroscopy[78] has detected the presence of α-helices and random coil conformation in GLUT1, but not β-sheet structures and has further indicated that the α-helices are preferentially oriented perpendicular to the lipid bilayer plane forming an effective tilt of less than 38 degrees from the membrane normal. Such a preferential orientation was further supported by ultraviolet circular dichroism spectra which revealed that the 208 nm Moffit band, found in the detergent-solubilized preparation, was absent in the film preparation. Linear dichroism data further indicated that D-glucose, a typical substrate, further reduces this effective tilt angle slightly. The results of this study revealed that the folding of the GLUT1 comprises of 82% α-helices, 10% β-turns and 8% random coil structure but not β-sheet structure. Furthermore, studies[79] with hydrogen-deuterium supported the FTIR

results by showing that the same 80% of the polypeptide backbone of the GLUT1 is readily accessible to solvent water. Hydrogen exchange kinetic behavior of human erythrocyte glucose transporter protein in vesicles was studied in the absence and in the presence of D-glucose or the inhibitor, cytochalasin B. This approach was chosen to detect a proposed channel of water penetrating into the protein through which the sugar molecule passes and to monitor any conformational changes induced by the substrate or inhibitor. Analyses of the kinetic data revealed several classes of hydrogens which exchange with readily distinguishable rates. Of 660 hydrogens detected per transporter, approximately 30% exchanged with rates generally characterized as those of free amide hydrogens indicating they interface with solvent water. Since the transporter is known to be embedded deep in the hydrophobic area of the membrane with minimum exposure to the outside of the membrane lipid bilayer, a significant portion of these free amide hydrogens must be at the purported channel rather than outside of the membrane. The remaining 70% of the labeled hydrogens exchanged with much slower rates which vary 10 to 10,000-fold, indicating that they are internally structured peptide amide and side chain hydrogens. These findings suggested the presence of a hydrophilic pore like structure, surrounded by amphipathic transmembrane helices, through which the substrate is transported across the membrane. The first putative topology model was produced[80] employing a technique based on tryptic digestion of GLUT1, which revealed a 12 transmembrane (TM) spanning helices model.

The cytoplasmic orientation of the C-terminus and of the large loop connecting TM's 6 and 7 has been confirmed by proteolytic cleavage and epitope mapping experiments. Cleavage of the GLUT1 within erythrocyte membrane by exposure of the transporter from the cytoplasmic side produced peptide fragments corresponding to residues 213-269 and 457-492 within the TM segment 6-7 loop and C-terminus, respectively[81]. The loop connecting putative TM 1 and 2, which is predicted to be extracellular[82], contains the only site of the N- linked glycosylation in the primary sequence, Asn 45 (Fig 1.4). The glycosylation of GLUT1 exclusively at this site has been confirmed by mutagenic studies in which perturbation of this asparagine residue resulted in abolition of all glycosylation[83].

In the absence of a crystallographic structure, a few models had been advanced. The first three-dimensional model[84] of GLUT1, was based on a hypothetical arrangement of the two 6-helical TM domains, while a second approach used a cluster of 4 TMs surrounding a central water accessible channel for the substrate[85]. A GLUT3 model[86] was developed based on the crystallographic structure of MscL (*Mycobacterium tuberculosis* lactose mechano sensitive channel), and included general insights from aquaporin1 and a model for GLUT1 was developed based on a prior scheme for LacY (*E. coli* lactose permease) helical packing[87].

It is clear that to fully understand how these membrane proteins translocate their substrates, an accurate and detailed 3D structure is required. Recently, two bacterial MFS transport proteins (GlpT and LacY) have been crystallized[88,89] and their structures

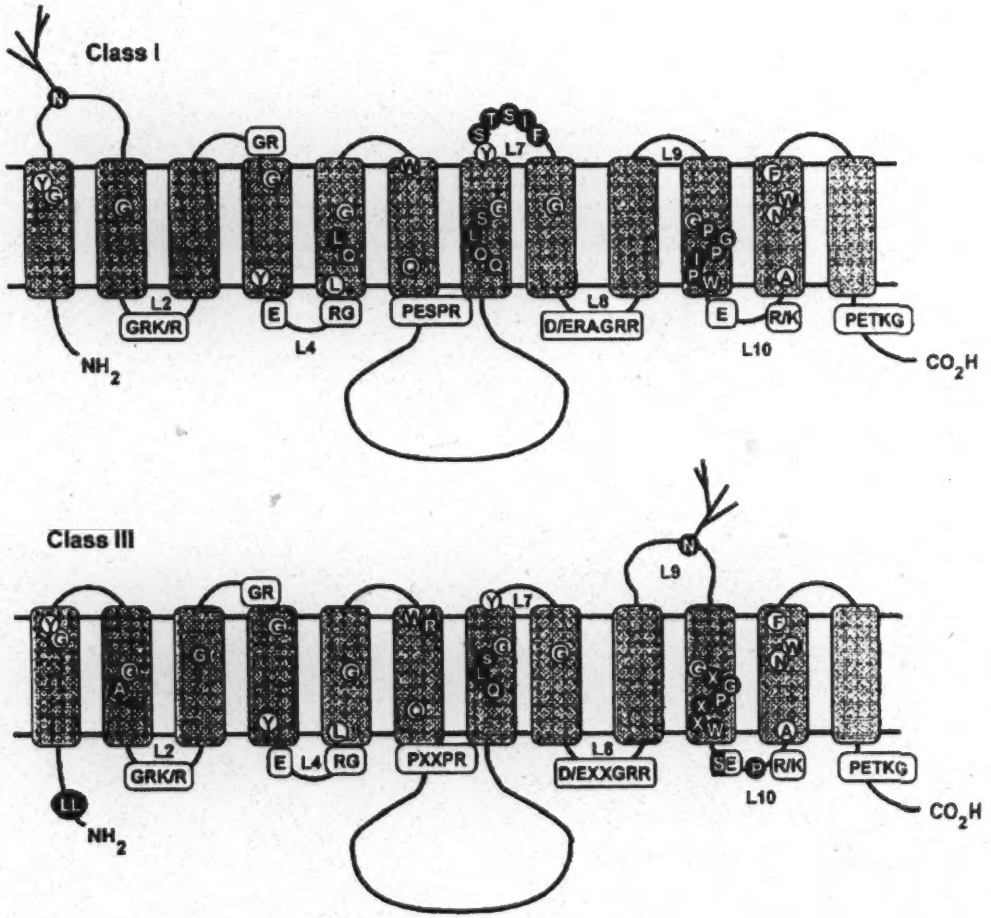

Fig.1.4. Putative topology model for SLC2A transporters[35].

resolved to 3.3Å for their cytoplasmic-facing conformations. In this inward facing conformation, both proteins exhibit a very similar pattern with a pseudo-two-fold axis of symmetry and this data is consistent with the 12-transmembrane helical model of GLUTs that was first proposed by Mueckler in 1985[90]. The pseudo symmetry also supports the notion that the 12 TM transporter genes are descended from a common 6 TM encoding ancestral gene that underwent a duplication event. Based on published crystallographic data, eight out of the 12 TM helices form a central cavity containing the cytoplasmic substrate-binding site. The structural conformation of these transporters suggests an analogous mechanism for co-transport and antiport and, by extension, simple uniport, involving tilting of the helices such that substrate binding sites are alternately exposed to either the cytoplasm or exoplasm. An alternating conformation mechanism of this type was postulated originally by Vidaver[91], based purely on kinetic considerations. This model suggested that membrane transport proteins undergo a series of important conformational transitions such that the ligand binding sites are alternatively presented to one side of the membrane, and then the other. However, it is likely, that GLUTs share the same basic helical packing arrangement with these two bacterial transporters and given this homology their structural coordinates are very useful starting point for modeling the exofacial substrate binding site.

1.5 Structural determinants of facilitative hexose transport.

1.5.1 Particular positions of hexose ring structures necessary for binding and or transport.

The use of D-glucose analogues[92,93] as inhibitors of substrate transport by GLUT1 and 4 proved to be a powerful approach to study the putative exofacial binding site/s. Firstly, it was concluded that the D-glucose, in the pyranose ring form, accesses the GLUT binding site at a specific orientation with the C-1 position entering first (*i.e.* the front of the molecule relative to the binding site) while interacting with the transporter through hydrogen bond forming at C-1, C-3 and C-6 [93,94,95]. The C-2 position hydroxyl has been shown not to play a role in substrate recognition by any of GLUT isoforms[94]. Secondly, substitutions into the C-4 and C-5 positions of D-glucose are well tolerated[93,94] at the exofacial site. This observation enabled the creation of specific C-4 and C-5 photolabelled glucose analogues which were then used in the study of the intracellular trafficking of different GLUT isoforms[96,97]. Interestingly C-6 aliphatic substitutions on the glucose ring, could enable formation of hydrophobic interactions with the transporter that produces an increased affinity of transport process[93].

In the case of fructose, accessibility to the exofacial binding site was studied using analogues of both the D-fructo-furanose and pyranose anomers[98]. Comparison of the common features of D-fructofuranose and D-fructopyranose suggest that the arrangement of hydroxyl groups at C-1, C-2, C-3 and C-4 and the ring oxygen are essentially the same

in both anomers. The two fructose isoforms differ only around the C-5 and C-6 positions and the specificity of fructose transporting GLUTs might have evolved in such a way as to make use of D-fructose in all its ring formations. The tolerance of GLUT5 for D-fructose C-3, C-4 and C-5 epimers is very poor, suggesting that each of these hydroxyl groups in the fructo-configuration may be involved in the H-bonding. However, there is a chance that the epimerized hydroxyls sterically reduce the binding. Interestingly, the fact that the affinity for C-2 methyl versus C-2 allyl β-D-fructofuranoside is almost two fold higher suggests that the additional size of the allyl group reduces interaction with GLUT5 around the C-2 position. Similarly, the affinity for methyl β-D-fructopyranoside versus allyl β-D-fructopyranoside was almost double. Clearly, these data are consistent with the postulates that GLUT5 accepts both furanose and pyranose ring compounds, preferring the β configuration and having a limited capacity to accept bulky groups at the C-2 position (particularly in an α conformation). The allyl substitution at the C-1 position revealed a very poor tolerance too, suggesting that the anomeric half of fructose is preferentially recognized by the fructose transporter. This observation makes sense given that the first half of the fructose molecule is similar in both the furanose and pyranose forms of D-fructose. The anomeric centre can therefore be considered as the front of the molecule relative to the binding site and the C-5 and C-6 positions are less important in the translocation process and during the transport are probably positioned relatively far from the components of the binding sites. This again makes sense, considering that these are the positions where the hydroxyl groups of the furanose and pyranose forms differ and the fructose transporters are able to transport both of them with

similar affinities. Data presented by Holman, suggested that GLUT5 transporter is highly specific for the fructo-hydroxyls and will not accept D-fructose epimers[98]. Consistent with this, it was found that the allyl substitution is not well tolerated at positions C-1, C-2, C-3, C-4 and C-5. However, the bulky allyl group is tolerated at position C-6 of D-fructofurnaose (Fig 1.2.1).

1.5.2 Key amino acids for GLUT structure/ function.

1.5.2.1 Hydrophilic residues with functional importance.

In GLUT1 the exofacial facing substrate binding site appears to involve Gln 161 within helix 5[99] and Gln 282 within helix 7[100]. A comparison of TM7 in GLUT2 and 3 revealed that the QLS (277-279) motif originally identified in GLUT1 and implicated as part of the substrate binding site[101] is present in both isoforms. Conversely, in the case of fructose, the presence of the methanol radical group at the C-1 position of D-fructose[100] would sterically preclude the interaction with exofacial substrate binding site components – Gln 277 or 282 in GLUT3 or 1, respectively. These findings support the hypothesis that the QLS motif in GLUTs 1, 3 and 4 could act as a selective binding site that discriminates between hexoses at the exofacial pole of the transporter.

Several approaches have been used to identify amino acid residues which line the aqueous pore of GLUT proteins and might be involved in substrate binding. These include site-directed mutagenesis of native cysteine residues[102], glycosylation scanning

mutagenesis[103] and cysteine scanning mutagenesis[104]. This has resulted in the determination that TM7 has a number of key residues which face the "pore" and play a role in glucose permeation through GLUT1[105]. Mutation of six resiudes, Gln 282, Gln 283, Ile 287, Ala 289, Val 290, and Phe 291, all located close to the exofacial side of the cell membrane, produced transporters that were inhibited by incubation with extracellular *p-chlormercuribenzenesulfoante* (pCMBS). pCMBS sensitivity implies that either the residue is positioned close enough to the glucose permeation pathway for the reaction to inhibit glucose binding and transport or lies within a critical area of the protein such that modifications results in a significant conformational change in the protein. Not surprisingly, when the highly conserved residues that are present in all the mammalian glucose transporters (Leu 278, Gln 282, Gln 283, Gly 286, Asn 288, and Tyr 292) were mutated to cysteine, the resulting proteins had significantly diminished transport activities. In agreement with the proposed role of Gln 282 as a component of the exofacial binding site[100], mutation of this residue to cysteine resulted in a greater than 75% reduction in 2-DOG transport activity. On the other hand mutation of the Asn 288 to cysteine had a dramatic effect on the relative transport activity, while substitution with Ile had almost no effect[100]. Interestingly, the adjacent hydrophobic neutral residue, Ala 289, was reported by Mueckler[105] to be pCMBS sensitive when mutated to a cysteine, whereas Oslowski[20] showed that this residue was pCMBS insensitive

Within the extracellular loop between the TM's 7 and 8 an STS motif[106] (Ser 294-Thr 295-Ser 296) has been identified which is highly conserved in the Class I mammalian

hexose transporters. Mutation of Ser 294 to Ala or Thr suppressed transport activity and cytochalasin B (specific endofacial ligand for some GLUT isoforms) binding. Interestingly, the binding of ATB-BMPA [*2N^4-(1azi-2,2,2-trifluorethyl)benzoyl-1,3bis-(D-mannosyloxy)-2-propylamine*], a photolabeled compound which is very selective for the exofacial site, was unaffected by these mutations. Replacement of Thr 295 with Ala presented the same effect by abolishing glucose transport and cytochalasin B binding and leaving the ATB-BMPA binding unaffected. Finally, the mutation of Ser 296 did not modify the transport properties. Based on these observations it was concluded that Ser 294 and Thr 295 are involved in conformational changes in GLUT1 during the transport process and that their mutation may arrest the transporter in an outward-facing conformation.

Another study, conducted by Mueckler[107] used cysteine scanning to identify functionally important amino acid residues in TM8. 2-DOG transport in GLUT1 Thr310Cys, Asn317Cys and Thr318Cys mutants was significantly lower than the wild type. The side chains of Thr 310 and Asn 317 are were also predicted to lie within the aqueous translocation pathway based on the presumed orientation of the helix. However, while the pCMBS reaction at position 310 did inhibit the transport of 2 DOG, there was no effect seen with C317. This was interpreted to be inconsistent with hydrogen bonding between glucose and the side chain of Asn 317 and suggested that this might be explained by Asn 317 lying closer to the cytoplasmic face of the membrane than any of the amino acid positions that were sensitive to pCMBS reactivity. Thus, it is possible

that helix 8 twists as it passes through the membrane such that the Asn 317 actually lies alongside TM 5 or 10 and is being "protected" from the inhibitory activity of pCMBS. The serine chain of this residue may be involved in stabilizing helical packing via hydrogen bonding to a residue in an adjacent helix (TM5 or 10). Similarly, cysteine substitution at Thr 318 may disrupt the hydrogen bonding between the hydroxyl group of the threonine side chain and a side chain from an abutting helix.

Within the intracellular loop between TM 8 and TM9 there is a highly conserved motif Gly332-R333-R334 *(GRR)* which has been shown to have a role in achieving the inward-facing conformation during the transport process[108]. The mutations R333L and R334A produced a marked decrease in glucose transport but failed to affect the binding of the endofacial ligands IAPS-forskolin and cytochalasin B. These data suggested that positive charges in the GRR motif at the cytoplasmic surface of the transporter participate in the conformational changes of the carrier protein during transport.

Another four residues within TM10 were identified, by the means of cysteine scanning mutagenesis and pCMBS sensitivity, that appear to be in direct contact with the aqueous environment of the pore and all of them are located toward the extracellular side of the transporter[109]. Only one of them, Glu 380, is hydrophilic and the rest V376, F379 and P383 are hydrophobic and may have a role in stabilizing helix-helix interactions.

In helix 11 of GLUT1, mutation of Ala 407 and Trp 412 produced a significant decrease in 2DOG uptake, but both mutants were largely retained intracellularly suggesting that these mutations may affect the intracellular processing and transport of

the proteins to the plasma membrane[110]. Moreover, the transport activity of four other mutants (A411C, T412C, A415C & Phe422C) was significantly reduced when compared with the C-less mutant. Remarkably, all of these residues cluster along a single face of TM11.

Thr 30 is a hydrophilic residue positioned at the exofacial pole of the pore within TM1, the last remaining helix proposed to form the aqueous pore of GLUT proteins. Its mutation to cysteine reduces the transport function of GLUT1 and also is accessible to pCMBS reagent. This suggests that it is contact with the pore and maybe able to form hydrogen bonds with the substrate molecule during the transport process[111].

1.5.2.2 The role of aromatic residues in non hydrophilic substrate-transporter interactions.

In GLUT proteins both the endofacial and exofacial entrances to the pore are lined by a number of hydrophobic aromatic residues. GLUT1 F26, F28, F291, F297, W412 and F422 are on the exofacial side and W388, Y389, F395 and F460 on the intracellular face of the protein (positions are numbered accordingly to the GLUT1 sequence). These residues form a ring around the pore in a series of steps that form layers of π electrons along the channel. A similar arrangement of aromatic amino acids residues has been noted in the bacterial maltose and sucrose porins[112,113] and has been termed the "greasy slide"[112]. Although the porins assume a β-barrel structure, the same general strategy for facilitating transport of polar carbohydrate moieties might have been adopted by mammalian GLUT proteins. By analogy, it could be suggested that the mobility of the glucose in the pore may be enhanced by alternating hydrogen bonds and π interactions along the surface of the pore[112]. The relative contribution of π interactions to glucose transport could be evaluated by substituting polar amino acids for aromatic residues with important consequences on the overall functionality of the transporter[114,115].

1.5.2.3 The role of proline residues in conformational changes.

Conformational flexibility of GLUT protein structure is believed to be necessary for functional activity. The classic model of a "pipe-like" structure of a transporter which is more or less rigid has become obsolete and cannot explain all the molecular, biochemical, kinetic and modeling data described above. The major change in the transporter's conformation that occurs after substrate binding and during transport catalysis appears to be greater than can be accounted for by a limited and localized movement of the side chains of a few amino acids. Molecular dynamic simulation suggested that an important role in the structural flexibility of the GLUT proteins is played by the TM10[116]. Interestingly, the pivotal role in the conformational changes induced by the flexibility of TM10 appears to be played by the one of the smallest amino acid residues, namely proline. The role of Pro 385, a highly conserved residue among the members of MSF, has been proposed to be critical in permitting the alternation of the hexose binding site(s) towards one side or the other of the membrane. Apparently, proline residues in transmembrane helices have a dual role, functional and structural[117]. Evidence for the dynamic transport catalytic role came from mutagenesis studies on membrane transporters such as the Ca^{2+}- ATP-ase[118], *E. coli* mellibiose[119] transporter and the *E. coli* lac permease[120], in which perturbation of transport occur as a result of mutating this proline residue. Proline is chemically unique with its side chain bound to form a pyrrolidine ring, allowing the ψ angle to adopt a range of positions and cause kinks in α helices. The dual structural and dynamic property of prolines may account for

their high frequency in transmembrane helices[121], despite their obvious tendency to be less favoured in the helical regions of cytosolic proteins[122]. The low dielectric constant of the membrane environment may account for this difference. The proline nitrogen lacks a proton so that the proline peptide bond cannot participate in hydrogen bonding to a neighboring carbonyl group. The ability to break the intramolecular hydrogen bonding pattern of the helix in the low dielectric constant environment of the membrane is the property that is the most useful in producing flexible kinks in membrane proteins[123]. The structural role of the prolines was identified by the X-ray crystallography structure of the photosynthetic center[124] and the high resolution electron microscopy structure of bacteriorhodopsin. In both these structures prolines form helix bows. The structural role appears to consist in producing a pocket that can bury a charged residue[125]. The packing has a convex surface that contacts lipid and a concave surface that buries the transmembrane charge. It has been noted that this type of structure is opposite to that occurring when proline residues are present in helices of cytosolic proteins[125] and in which the convex surface of the kinked helix project into the bulk water phase. In GLUT1 there are six membrane-buried proline residues, three in TM6 and three in TM10. In TM10, the three proline residues at positions 383, 385, and 387 are part of the unique proline rich domain *G382-PGPIP-W382* which is conserved in all mammalian glucose transporters. The strong conservation of this sequence suggests that this region has an important role in allowing the transport catalytic function by allowing sequential and alternating opening and closing of the external and internal hexose binding sites. In this regard, it seems likely that the kinking in helix 10 due to prolines at residues 383,

385 and 387 of GLUT1, can bury the charged residue Glu 380. Mutation of Pro 385 to Ile was found to reduce significantly the transport activity of 2 DOG[116] raising the possibility that this residue may be involved in the conformational changes necessary for the interconversion between the inward- and outward -facing presentation of the substrate binding. Within TM6 there are three proline residues, Pro187, Pro 196 and Pro 205 that are conserved in all the mammalian hexose transporters except GLUT2[126] where they are replaced by His, Arg, and Phe. Successive mutation of those three prolines in GLUT1 to the homologous amino acids from GLUT2 produced two mutants displaying similar transport activity relative to wild type while only Pro196Arg induced a marked decrease in transport activity.

1.5.2.4 Hydrophobic residues with structural-functional importance.

Based on the results of Holman and Barnett[92-94], it was concluded that substitution into the C-1 position of D-glucose has a dramatic effect on the interaction at the exofacial binding site, suggesting that the front of glucose molecule interacts with the outer facing binding site. By contrast, hexose analogues with hydrophobic alkyl substitutions into C-4 and C-6 positions were found to have high affinity for the transporter, in some cases exceeding that of D-glucose. The high affinity of the hydrophobic C-6 substituted analogues suggested that there is a hydrophobic pocket on the transporter, which is close to the C-6 of the sugar as it accesses the exofacial site. This hypothesis was supported by the fact that C-4 and C-6 substituted analogues were able to bind well to the exofacial site, but were not transported. Therefore, it was proposed that on initial binding of the sugar, there was not close contact with the C-4 and C-6 positions, but in the absence of a bulky substitution at C-6, the transporter could close the hydrophobic patch around the rear end of the hexose molecule and so facilitate the transport catalysis.

Despite the lack of capacity to establish hydrogen bonds with the substrate the hydrophobic residues play an important role in the functionality of hexose transporters. GLUT1 Leu 279 lies within the highly conserved motif 'QLS', which is adjacent to the proposed 'bottle-neck' region of the GLUT1 translocation pathway[101]. Val 277, Ile-Asn 287-288 and Val 290 also are cited as being part of the pore lining surface in GLUT1. The conserved "QLS" motif which is part of the *L278-QLSQQLSGGINAVFYY-293* region in TM7 might participate in both hydrogen bonding to the substrate and also in

closing the exofacial site during the transport catalysis[127]. Glu279Cys and Ile274Cys mutants proved to be exclusively and extremely sensitive to NEM (*N*-ethylmaleimide) and not to respond to pCMBS treatment. As a result of its membrane buried location, Glu 279 is very likely excluded from the interaction with the aqueous phase of the pore. Interestingly, Ile 274 is positioned on the opposite face of the helix relative to Asn 288 and should be accessible by pCMBS, but is not. This might be explained by the orientation of TM7 within and along the translocation pore by forming an exofacial side cleft that might prevent pCMBS from reaching further down the endofacial pore. Mutation of Glu 282, Glu 283, Ile 287, Val 290 and Phe 291 to cysteine produced mutants that displayed extremely low basal transport activities and also pCMBS sensitivity. Glu 282 and Glu 283 are both accessible to the extracellular application of pCMBS and putatively they can form hydrogen bonds with sugar moieties. On the other hand the Glu279Cys mutant displayed only a limited pCMBS sensitivity, but a marked NEM sensitivity, raising the possibility that this residue is more likely to have a structural role. At this point it is worthy to note that the glutamine residues in this region may participate in the so called "glutamine phase" involved in the putative GLUT1 functional dimerization[73]. This concept was initially described in regards to the homo-dimerization of the major histocompatibility complex class I proteins[128], which displays a high homology in helix α1 with the TM7. The crystal structure of this protein contains a homodimer and it is hypothesized that the glutamine residue homologous to Gln 282 in GLUT1 mainly participates in forming the homodimer by mutual glutamine interaction, known as "glutamine finger". Even if there is no functional correlation between these

two proteins, dimerization of GLUT1 via "a glutamine phase" is an interesting hypothesis. The indicated structure at least demonstrates that the "glutamine phase" of TM7 has the potential of forming hydrophilic helix-helix interactions.

Another interesting finding regarding the capacity of TM7 of GLUT7, to establish helix-helix bonds was described in relation to the interaction with TM2[73]. Apparently, these two helices form a "cleft-like structure" at the exofacial side of the GLUT1 aqueous pore. Interaction between TM7 and 2 might be responsible for shaping the functional conformation of the exofacial face of the vestibule which consequently, might influence the transporting properties of GLUT1. Cysteine scanning mutagenesis of TM2 revealed that the mutation of Gly 75, 76 and 79 as well as Phe 72 and Ser 80 produced mutants with diminished transport function. Interestingly, all of these residues are located on the same face of the helix, which is not accessible to either intracellular or extracellular pCMBS suggesting they lie on the opposite side of the helix from the aqueous pore of the transporter. The direct consequence of this finding is that these mutations could interfere with a transport competent folding and therefore affecting the overall function of the protein. The cluster of the three glycine residues could provide space for a complementary bulky or hydrophobic partner from another helix segment (helix-helix interactions) or lipid tail (helix lipid interaction). Further down, on the same face of the helix 2 there are three NEM sensitive valine residues 69, 83, and 87 and it seems that volume equivalent substitution of cysteine for valine is tolerated, but addition of the

bulky NEM disturbs the biologically active conformation. These results support the notion of a very tight hydrophobic packing at this particular region of helix 2.

Within the extracellular loop between TM7 and TM8 of GLUT1, lie three hydrophobic aromatic residues[127] Phe 291, Tyr 292 and Tyr 293 that putatively are part of the hydrophobic pocket at the exofacial side of the aqueous pore. Mutation of Tyr293 to Ile abolishes cytochalasin B binding, suggesting that this mutation locks the transporter in the outward facing conformation. Interestingly the mutation of Thy293 to Phe maintains the cytochalasin B binding, indicating that both the size and the hydrophobicity of Tyr are important in the normal transition of the transporter from one conformational state to another. It has been conjectured that the hydrophobic patch moves around the back of the sugar to separate it from the external solution, occluding the sugar within the center of the protein and strengthening the interaction with hydrogen binding amino acid side chains in this region.

An interesting structural role for some of the hydrophobic residues within TM8 was proposed[129,130]. Initially, substitution of the Ile 311 to cysteine revealed an increase in the transport properties when pCMBS was added to the incubation media. According to the model predicted by the molecular dynamic simulation this residue should have been in contact with the lipid layer or to abut helix 5. This is why it was considered possible that the Ile side chain might create a hydrophobic interaction with a neighboring residue from helix 5, and therefore, create a tight hydrophobic packing of these two helices in such a way in which the conformational mobility during the transport process

would be diminished in comparison to the Cys mutant. Two other important hydrophobic residues within TM8, Leu 325 and Val 328, were identified and predicted to lie in proximity of the exofacial side of the helix. These residues were proven by the means of substituted cysteine accessibility method (SCAM) and molecular modeling to be in near proximity to another two hydrophilic residues positioned in TM4 and located on the antiposing face relative to the aqueous pore and TM8. The putative three dimensional model placed Leu 325 and Val 328 (both in TM8) and Gly 145 and Ser 148 (both in TM4) within 6-16 Å from each other and on the same face of the TM4 and 8 facing the aqueous pore which would allow the formation of cross link interaction between this four residues. Moreover the analysis of other residues within these two TMs revealed that towards the cytoplasmic end the two helices are tilting ad twisting placing themselves further apart than 16 Å distance. This fact suggested that towards the inner face of the membrane these two helices diverge whereas the orientation of their exofacial halves is convergent.

Two amino acid residues were identified in TM5[131] that face the pore and which when mutated markedly influences the transport properties. One of them is Glu 161, which putative function was presented in the previous paragraphs and the second amino acid residue, is Val 165 and, accordingly to Mueckler[132], this residue is placed in within the sugar translocation pathway and when mutated to isoleucine or even leucine, the glucose transport properties are almost lost. This was a highly surprising result given the nature of the conserved substitution, especially in a hydrophobic environment where the

possibility of creating direct interaction with the substrate is unlikely. The only plausible alternative was postulated to be either that larger aliphatic side chains at the position inhibit the direct interaction of the substrate with Glu 161 or sterically inhibit the normal conformation changes during the transport process resulting in a more "rigid" structure that does not meet the molecular flexibility requirements of a physiological transport.

The role of Val 165 in the anatomy of transport process is quite interesting, as it is placed one helical turn above the putative sugar binding site and lining the aquous pore. Another possibility would be that the interaction of valine with a different hydrophobic residue from another helix to create a "hydrophobic selectivity filter" based on steric considerations. Even more interestingly the opposite face of TM5 is presumably in direct contact with the fatty acyl core of the lipid bilayer and is composed mainly of highly hydrophobic amino acid residues (four leucines, two valines and one isoleucine). These data were the first experimental evidence for the existence of an amphipathic transmembrane helix in human glucose transporters. This particular amphipathic character was further postulated, to be a common feature of those helices that are capable to cluster together in the membrane to form the walls of water filled channel through which glucose can permeate the lipid bi-layer of cellular membrane.

Within TM5 on the face that is in direct contact with the aqueous pore it had been communicated that five[131] residues (Gly 175, Glu 172, Ala 171, Ile 168 and Gly 167) displayed reduced function when mutated to cysteine. Very interestingly, all these residues located in the exofacial extremity of the aqueous pore are solvent accessible only

when pCMBS is placed extracellularly whereas injection of pCMBS into oocytes did not influence the transport. This data indicates that, during the transport cycle, these residues are accessible from the external solvent but not from the cytoplasmic compartment.

Conversely, other five residues (Leu 156, Gly 157, Thr 158, Leu 159 and His 160) within TM5[131] lining the aqueous pore and predicted to lie closest to the cytoplasmic surface of the membrane did not show reduction of transport properties when pCMBS was applied extracellularly. This particular disposition is consistent with a simple alternating conformation model for the GLUTs mechanism of transport. Such evidence had been previously communicated[133,134] in regards to the *E. coli* lac permease and glucose-6-P antiporter and this evidence predicted before the publication of the crystal structures the alternating transport mechanism of these related proteins.

Within TM10 three amino acids residues[109] have been shown to interact with the exofacial pCMBS. Thus, Val 376, Phe 379, and Gln 380 were postulated to be accessible by the exofacial solvent. However, in the case of Val and Phe is very likely that this disposition to favor the formation of cross link or hydrophobic interactions with other residues from the adjacent helices in order to maintain a biologically active conformation of the transporter. Another interesting characteristic of TM10 is the unique pattern of sensitivity to pCMBS, wherein residues within the extracellular half of the helix tend to be inhibited by the cysteine substitution and residues within the cytoplasmic half of the helix are stimulated by this substitution. However the structural or functional implications of this unusual result are not immediately apparent, but they can be related

to the tighter hydrophobic packing at the cytoplasmic end of the outward-facing biological active conformation. One of the most interesting cytoplasmic residues is Trp 388 within TM10 which was initially showed by Mueckler[109] that did not display pCMBS sensitivity but which mutation to glycine or to isoleucine significantly reduced the transport function. In apposition with it there is another tryptophan residue, Trp 412, situated in TM11[110]. Initially, it was postulated that this two residues, out of total of the six tryptophan residues within GLUT1, would be involved in cytochalasin B binding. On the other hand the indol nitrogen of the tryptophan can act as a hydrogen bond donor and therefore could establish interaction with the substrate. Thus, Trp 388 and 412 could contribute to the inner substrate binding site. Alternatively, these residues might be involved in maintaining and stabilizing the biologically active conformation of the protein near the binding site during the transport process. This hypothesis is supported by the fact that region 379-388 is a very dynamic segment[123] of the transporter, which after substrate binding, undergoes significant structural movements from an aqueous environment to a less accessible position, maybe in the proximity of the membrane. Also, this residue might be involved in stabilizing the substrate molecule during the passage through the aqueous pore via direct interaction with the alkyl groups of the C-6 as described in the previous paragraphs.

Studies with sulfhydryl reagents have shown that TM11 contains only two residues pCMBS accessible, which are positioned at the extracellular end of the pore, predicting that a large portion of this helix is inaccessible from the exofacial side of the

membrane[110]. However, mutation to cysteine revealed the importance of five hydrophobic residues revealing either a reduction in transport activity as for Trp 412, Phe 422, and Ile 404 or an increase as for Val 406 or Met 420. Very interestingly, all these residues are clustered on the same helical face of the TM11 and they are predicted to be in the proximity of the aqueous pore.

Cysteine scanning mutagenesis of TM1[111] revealed two hydrophobic residues (Tyr 30 and Val 32) placed at the exofacial side of the helix as pCMBS sensitive and six hydrophobic residues sensitive to the administration of the membrane permeable NEM reagent (Met 13, Val 16, Val 20, Phe 26, Tyr 28, and Val 32). Surprisingly, one hydrophobic residue (Ile 33) was stimulated by both NEM and pCMBS administration.

1.6 Summary

Over the last 60 years the investigation of the GLUT led to the recognition of some important common characteristics that apply to their structure and function:

1) The kinetic and functional behavior of GLUT (SLC2A) proteins is best described by the Michaelis-Menten kinetic curve.

2) The structural model that explains the functionality of the GLUTs is represented by the "ping-pong" or "alternating conformation" model. This model predicts that during the transport process, the transporter molecule is capable of passing through different state transitions from an outward to an inward facing conformation. This mobile and dynamic conformation exposes the substrate binding site(s) to the either outer or inner environment.

3) Based on this model, it was predicted that the transporter is asymmetric in regards to the membrane plane, namely the kinetics of the influx and efflux processes are not identical.

4) The predicted membrane topology of GLUTs follows a recurrent pattern of Major Facilitator Superfamily proteins, namely 12 putative transmembrane spanning domains. These 12 TMs fold in the membrane in two clusters of 6 helices which are connected through a long intracellular loop. This arrangement could provide the flexibility required by the conformational changes during the transport process.

5) The biologically active conformation of GLUTs is predicted to form a translocation pore bounded by 8 TMs. These TMs are in direct contact with the aqueous solvent that contains the substrate and so can influence its permeation from one side to another of the membrane. Therefore, some of the hydrophilic amino acid residues in these TMs have the potential of establishing hydrogen bonds with the substrate molecule and hence to participate in the transport process. Hydrophobic and neutral amino acid residues within these helices also have an important role in transport by influencing the substrate specificity of the pore.

6) These proteins are predicted to function as monomers, dimers or tetramers given depending on the tissue of expression.

Chapter 2.

Methods

2.1 Multiple Sequence Alignments of Protein Primary Structures.

The selected 12 sequences of the SLC2A family were analyzed by CLUSTALX, a multiple sequence alignment and analysis workbench. The latest freeware version of CLUSTALX can be obtained from a public directory at the FTP site:

http://inn-prot.weizmann.ac.il/software/ClustalX.html.

Multiple alignments were evaluated using the PAM 250. The PAM (percent accepted mutation) values provide a scale to measure the relatedness of two sequences as a function of evolutionary similarity (based on frequencies of mutational conversions). For non identical residues, the PAM scale ranges from negative values (residues unlikely to be substituted by mutations) to positive values for residues frequently found to be interconverted by mutation. By trial and error Dayhoff[135] found that for weighting purposes a 250 PAM matrix works well. At this evolutionary distance (250 substitutions per hundred residues) only one amino acid in five remains unchanged and the percent divergence has increased to roughly 80%. However, the amino acids vary greatly in their mutability. According to Dayhoff roughly 55% of the tryptophans, 52% of the cysteines and 27% of the glycines would still be unchanged, but only 6% of the highly mutable asparagines would remain.

Residue pairs with scores above 1 replace each other more often as alternatives in related sequences than in random sequences. This is an indication that both residues can carry out similar functions. A score exactly equal to one indicates amino acid pairs that are found as alternatives at exactly the frequency predicted by chance. Residue pairs with

scores less than 1 replace each other less often than in random sequences and would be an indication that these residues are not functionally equivalent. Some of the properties that are visible from this matrix and go into its makeup are - size, shape, local concentrations of electric charge, conformation of van der Waals surface, ability to form salt bonds, hydrophobic bonds, and hydrogen bonds. Interestingly, these patterns are imposed principally by natural selection and only secondarily by the constraints of the genetic code. This tends to indicate that coming up with your own matrix of weights based on some logical features may not be very successful because your logical features may have been over-written by other more important considerations.

One of the problems with this measure of distance is that it assumes that all sites are equally mutable. But this is clearly false. Another problem is that by examining proteins with few differences, the highly mutable amino acids have been stressed. Lastly, due to the collection of proteins known at that time, the matrix is biased because it is based mainly on small globular proteins. Amino acids are grouped according to the chemistry of the side group: C-sulfhydryl, STPAG-small hydrophilic, NDEQ-acid, acid amide and hydrophilic, HRK-basic, MILV-small hydrophobic and FYW-aromatic.

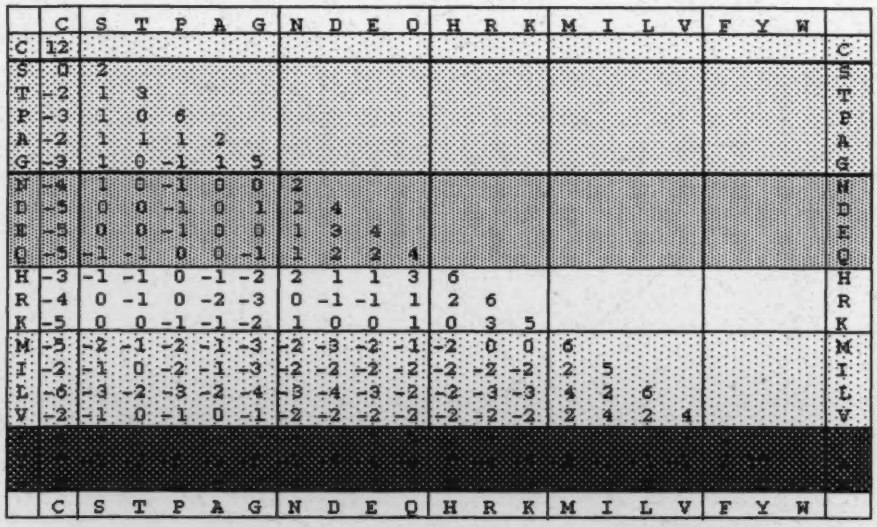

	C	S	T	P	A	G	N	D	E	Q	H	R	K	M	I	L	V	F	Y	W	
C	12																				C
S	0	2																			S
T	-2	1	3																		T
P	-3	1	0	6																	P
A	-2	1	1	1	2																A
G	-3	1	0	-1	1	5															G
N	-4	1	0	-1	0	0	2														N
D	-5	0	0	-1	0	1	2	4													D
E	-5	0	0	-1	0	0	1	3	4												E
Q	-5	-1	-1	0	0	-1	1	2	2	4											Q
H	-3	-1	-1	0	-1	-2	2	1	1	3	6										H
R	-4	0	-1	0	-2	-3	0	-1	-1	1	2	6									R
K	-5	0	0	-1	-1	-2	1	0	0	1	0	3	5								K
M	-5	-2	-1	-2	-1	-3	-2	-3	-2	-1	-2	0	0	6							M
I	-2	-1	0	-2	-1	-3	-2	-2	-2	-2	-2	-2	-2	2	5						I
L	-6	-3	-2	-3	-2	-4	-3	-4	-3	-2	-2	-3	-3	4	2	6					L
V	-2	-1	0	-1	0	-1	-2	-2	-2	-2	-2	-2	-2	2	4	2	4				V
	C	S	T	P	A	G	N	D	E	Q	H	R	K	M	I	L	V	F	Y	W	

Fig. 2.1 Example of a Dayhoff 250 PAM matrix used to calculate evolutionary distance scores.

Each matrix value is calculated by first dividing the frequency of change, for each amino acid pair, in related proteins separated by one step in an evolutionary tree by the probability of a chance alignment based on the frequency of the amino acids. The ratios are expressed as logarithms to the base 10 (approx. 1/3 bit values). The approach used in ClustalX is a modified version of the method of Feng and Doolittle[136] who aligned the sequences in larger and larger groups according to the branching order in an initial phylogenetic tree. This approach allows a very useful combination of computational tractability and sensitivity.

The positions of gaps that are generated in early alignments remain through later stages. This can be justified because gaps that arise from the comparison of closely related sequences should not be moved because of later alignment with more distantly related sequences. At each alignment stage, it aligns two groups of already aligned sequences. This is done using a dynamic programming algorithm where one allows the residues that occur in every sequence at each alignment position to contribute to the alignment score.

The details of the algorithm used in ClustalX have been published [137], which was an improved version of an earlier algorithm [138]. First, a crude similarity measure between every pair of sequence is calculated. This is done using the fast, approximate alignment algorithm of Wilbur and Lipman[139]. Then, these scores are used to calculate a "guide tree" or dendrogram, which will tell the multiple alignment stage in which order to align the sequences for the final multiple alignments.

2.2 Phylogenetic Tree Construction.

To study the evolutionary relationships between the members of GLUTs family members the PHYLIP version 3.6 software was used which is one of the most recent applications consisting of a series of executable programs. The latest freeware version of PHYLIP can be obtained from the Washington State University website: http://evolution.genetics.washington.edu/phylip.html.The strategy employed for constructing the phylogenetic trees in this study consists of several steps. First, the results of multiple alignment analysis of 112 sequences saved in a PHYLIP format were input in PRODIST, a program that calculates evolutionary distance measurements for protein sequences based on the PAM 001 of Dayoff. This program, like many other of the PHYLIP software package, depends primarily on the input order of the sequences to generate distance measurements. In this program each individual data set was randomly ordered and sampled 50 times to reduce the possibility of bias. An additional feature, termed "global rearrangements", also optimized the regional placements of one or more protein sequences on a tree .In other words, subtrees from the tree were removed and added back in all possible places until no further improvements could be achieved. The output file from PRODIST generated a distance matrix data set and contained information that expressed the best overall evolutionary distances of all species in the data set.

The information gathered by the PRODIST program was inputted into one of distance matrix programs available into the PHYLIP package. For the present study I

chose the KITSCH program to generate the phylogenetic tree. This software estimates phylogenies from distance matrix data under the "ultrametric" model which is the same as the additive tree model except that an evolutionary clock is assumed. The Fitch-Margoliash criterion and other least squares criteria are assumed. The output data generated an out tree file which was used as an input data set for the phylogenetic tree drawing software.

Finally, the information from the distance matrix program was entered into DRAWTREE program which effectively converts the textual information from KITSCH into an unrooted phylogenic tree.

2.3 Homology building

We developed one model of human GLUT7 protein by homology with the predicted GLUT1 1SUK[161] model coordinates and the crystal structures of GlpT from *E. coli* (PDB No. 1PW4) and similarly, of the structure of LacY from *E. coli* (PDB No. 1PV6). This template structure was subject to 10 ns molecular dynamics simulation in water/octane and ions. This run was NPT, with Berendsen coupling for temperature and pressure. All bonds were constrained using the LINCS[140] algorithm for the protein and SETTLE[141] (36) for water in the GROMACS[142] suite. The Glut7 structure was deposited in PDB, code 1YG7.

The alignments were done with Clustal X and BLOSUM62[143], with gap penalties of 10 for insertion and 0.1 for extension. As constraints, we used residues experimentally

determined to be in loops, namely the glycosylation site N45, the conserved motifs of loops 2–3 and loop 8–9 (89/330RXGRR93/334), loop 6–7 residues 213–269, loop 7–8 K300[144] , and loop 11–12 C429. The homology modeling was done with *Nest*, a program inside the JACKAL suite[145] and refinement with MODELLER[146]. For validation we used PROCHECK[147] , WHATCHECK[148] , and molecular docking experiments. For the correct assignments of residues to transmembrane helices 1 and 2 we used evolutionary modeling; we aligned the templates (Swiss-Prot No. P08194) with a homologous human protein obtained searching with PSIBLAST[149] glucose 6-phosphate translocase from *Homo sapiens* (Swiss-Prot No. O43826), with a homology difference of 40.2%.

2.4 Molecular dynamics simulations (MDS).

We used the force-field GROMOS43a and the protein was placed in a water box (solvation layer of ~7 Å thicknesses). All runs were at 300 K with a time step of 2 fs. All bonds were constrained using the LINCS algorithm for the protein and SETTLE for water. We performed runs for 400 ps and for 2 ns. We used Berendsen's scheme for temperature and pressure coupling for both protein and solvent (water). Electrostatic forces were calculated with the particle-mesh Ewald algorithm. Initial energy minimization was done with the steep descent algorithm (1000 steps) followed by conjugate gradient to a maximum force of 0.1 kJ mol^{-1} nm^{-1}. All simulations were performed with the MDS package GROMACS v3.. For trajectory analysis we used the

tools included in GROMACS and VMD v1.82, the first 100 ps (equilibration) were neglected.

2.5 Transport channel prediction.

To determine the passageway and cavities graphically we used VOIDOO[150] to generate the protein surface with a probe radius of 1.2 Å and grid spacing of 0.5 Å. Subsequently, MAPMAN[151] was used to convert between the *.ezd* and *.mask* formats, and the passageway surface was calculated using the script *cavities.mamac* in the program MAMA[152] . We used VMD[153] to display graphical images.

2.6 Substrate Docking

The ligand coordinates for β-D-glucose and forskolin were obtained from the PDB sum database (http://www.biochem.ucl.ac.uk/bsm/pdbsum); phloretin and Cytochalasin B were built manually and optimized with the MM+ force field in HYPERCHEM. A GROMACS-compatible file for dihedrals and topology was generated for each with the server PRODGR using the total-charge option, and not minimized. We prepared the initial GLUT7 model for docking by running the 400-ps MDS in water referred to above. Docking for each ligand was explored separately using ZDOCK 2.3 in its default global-scanning mode, so that the program found the docking sites without intervention of the

operator. The setting for "densities" (angular steps) was 6°, and for clusters of docking results we selected the 100 best. Promising docking results were subject to a further test by solvating with a water layer of ~7 Å and running MDS for 100 ps with particle-mesh Ewald for electrostatic interactions (GROMACS force field). Analysis of binding site results was done with SPDBV 3.7 and the tools from GROMACS . Docking of of D-glucose and D-fructose was explored using Autodock and Autodock Tools[154].

This computer modelling was done in collaboration with Jorge Fischbarg at Columbia University.

2.7 Isolation of a cDNA encoding human GLUT7 gene.

Based on the alignment of human GLUT5 cDNA (accession No: NM_003039) and human genomic contig AL356306 (replaced by AL035703 in the NCBI database presently), three forward and three reverse primers were designed based on conserved regions of both DNA sequences. One specific band of approximately 0.8 kb was amplified using a human intestinal cDNA library (Clontech, Palo Alto, CA) which was different from the GLUT5 sequence. This new product was then used to search the database for a unique coding region and we found a putative full-length sequence already deposited in the database (accession No: XM_060424) annotated by the International Human Genome Sequencing Consortium using automated computational analysis.

Therefore, we designed primers based on the unique regions of the putative gene and attempted to amplify the full-length cDNA from a human intestinal cDNA library.

The PCR reaction (30 μL) contained 50 ng of cDNA library, 2.5 units of *Taq*-Deep vent DNA polymerase (100:1) and 10 pmol each of the 5' and 3'-oligonucleotide primers 5'-TACGGGATCC CGATGGAGAA CAAAGAGGCG GGAACCCCT- 3' (*Bam*HI site underlined) and 5'-CGGAATTCCG CAGGGCCGCT AAAAGGAAGT TTC- 3' (*Eco*RI site underlined). Amplification for one cycle at 94°C for 5 min, 57°C for 55 sec, 72°C for 100 secs, thirty two cycles at 94°C for 55 s, 57°C for 55 s, 72°C for 100secs (Robocycler™ 40 Temperature Cycler, Statagene, La Jolla, CA) generated visible PCR products of the predicted size,

The PCR reaction mixture was resolved on a 1% agarose gel and a band at 1.7 kb was isolated and purified (QIAEX II Gel Extraction kit, Qiagen). This product was firstly ligated into pGEM-T (Promega, Madison, WI) and then subcloned into the enhanced *Xenopus* expression vector pGEM-HE (32) using *Bam*HI and *Eco*RI. By providing additional 5' and 3'-untranslated sequences from a *Xenopus* β-globin gene the pGEM-HE construct gave significant functional activity, which was used in the subsequent characterization of the human protein. The authenticity of the construct was confirmed by sequencing. The open reading frame (ORF) of this putative cDNA is 1575 bp long and could encode a 524 amino acid protein which we have assigned as GLUT7 *(SLC2A7)*.

2.8 Site directed mutagenesis.

A 4597 bp human wild type GLUT7- pGEM-HE construct was used as a template for creating a GLUT7 mutant in which we substituted isoleucine for valine 314 (I314V). Site directed mutagenesis was performed using a Quick Change II Site-Directed Mutagenesis Kit. Unlike PCR-based mutagenesis, the QuikChange II method relies on linear amplification of template DNA by mutagenesis-grade *PfuUltra*™ high fidelity DNA polymerase. Mutagenic primers are extended during temperature cycling, incorporating the mutation of interest into the newly synthesized strands.[1] The unique primer design allows replication of only the parental strand to take place in each successive round. Because *PfuUltra* DNA polymerase is able to replicate DNA with the highest accuracy compared to other thermostable enzymes, it virtually eliminates the possibility of producing undesirable random errors. Final treatment with Dpn I ensures the digestion of only the dam-methylated parental strands. My approach was slightly different from the protocol provided by the manufacturer. I optimized the conditions of the amplification using the following program : segment1 – 1 cycle at 95°C for 30 s, segment 2 – 30 cycles with denaturation 95°C for 30s, annealing 55°C for 1 min and extension 68°C for 9 min .This modified version of the mutagenesis enabled me to use only one primer significantly reducing the cost of each reaction. The resulting nicked circular mutagenic strands are transformed through electroporation into the DH-α-electrocompetent cells, where bacterial ligase repairs the nick and allows normal replication to occur. Greater than 80% of the colonies contain the desired insert. The

forward primer was 5'- CGG GCA TCA ATG CGT TCA ACT ACT ATG CGG AC-3'. A second mutant was created using the same strategy but replacing Val with Ser, using a forward primer 5'-TCG GGC ATC AAT GCC AGC AAC TAC TAT GCG GAC ACC-3'. The new constructs used the recombinant pGEMHE vector which contained the mutants of interest inserted between EcoRI and BamHI restriction sites. Both mutants were then cloned using an incubation of 16-18 hours on agar plates enriched with ampicillin. The following day one six colonies of each mutant were selected and incubated in liquid LB – ampicillin enriched media for 16-18 hours and then the plasmid was isolated using a modified version of the QIAGEN miniprep kit.

The resulting plasmids were sent for sequencing to Macrogen (http://www.macrogen.com/eng/sequencing/sequence_main.jsp). Resulting sequences were analyzed with BLAST software available on the NCBI website at (http://www.ncbi.nlm.nih.gov/blast/bl2seq/wblast2.cgi) in regards to the human GLUT7 protein sequence to verify the insertion of the desired mutations.

Two constructs containing a pcDNA3.1 vector and two isoforms of human GLUT9, wild type and the N-truncated one (GLUT9 ΔN) had been sent to us by Dr. Kelly Molly (Washington University, St L.) in order to characterize and express them in oocytes. The two clones had been extracted with KpnI and XbaI restriction enzymes and subcloned into our pGEMHE vector between the same sites. A similar approach was used regarding the human GLUT11 isoforms (A, B and C). Drs. Hans Joost and Annette Schurmann sent us the three isoforms subcloned in to a pUC18 vector between HindIII

and KpnI binding sites. These isoforms were subsequently cloned in our vector pGEMHE as well. We bought a commercial isoform of GLUT2 from ATCC, which was already inserted into a pGEM4Z vector and restricted for subcloning with BamHI and SphI enzymes. GLUT5 was available in our laboratory cloned in a pcDNA3 vector and was then subcloned into the pGEMHE vector using XmaI and XbaI restriction sites.

Three sets of plasmids were created using human isoforms of GLUTs 2, 5, 9 and a pGEMHE vector producing constructs of 4597kb, 4527kb and respectively 4558kb. The constructs were used as templates for creating GLUTs 2, 5, 9 mutants in which we substituted isoleucine for valine at the homologue positions 316,321 and respectively 306 (I316V/ I321V / I306V). Site directed mutagenesis was performed using an adapted version of the Quick Change II Site-Directed Mutagenesis Kit described previously. For GLUT2 mutants we used the forward and reverse primers 5'-CCG GAA TCA ATG GCG TTT TTT ACT ACT CAA CCA GC-3' and 5'-GCT GGT TGA GTA GTA AAA AAC GCC ATT GAT TCC GG-3'. For the corresponding GLUT5 mutant we used the forward primer 5'-CGG GCG TCA ACG CTG TCT ACT ACT ACG C-3' and the reverse primer 5'-GCG TAG TAG TAG ACA GCG TTG ACG CCC G-3' . GLUT9 mutant was created using the forward primer 5'- GTG GCC TCA ATG CAG TTT GGT TCT ATA CCA ACA GC-3' and the reverse primer 5'- GCT GTT GGT ATA GAA CCA AAC TGC ATT GAG GCC AC-3'.

In the case of human GLUT11, five mutants were created in order to check the importance of the homologous valine residue in the context of the DSV motif that

corresponds in class II and I members, to the NAI and NAV motif, respectively. I switched firstly D280 to an N residue, then S281 to A, and ultimately V282 to I, and used for creating these mutants a pGEMHE- GLUT11 wild type template. Then using a pGEMHE-GLUT11 D280N template I created the double mutant GLUT11 D280N, S281A which contained at position 282 a V residue. To re-create the NAI motif as in the other class to members I used the double mutant template and a primer that contained all the three mutations so I created the triple mutant NAI.

The primers used were D280N 5'- GAG CTC TGC GGG AAT GAC TCG GTG TAC GCC TAC-3', S281A 5'- CTC TGC GGG AAT GAC TCG GTG TAC GCC TAC-3'and D280NS281AV282I 5'- GAG CTC TGC GGG AAT GAC GCG ATA TAC GCC TAC-3'. The resulting plasmids were transformed into *E. coli* DH-α5 electro competent cells using an Eppendorf Electroporator 2510 machine that used a 1,800 V voltage for the electroporation procedure. The transformed cells were then plated and incubated for 16-18 hours on agar plates enriched with ampicillin (1 in 10,000).

2.9 Preparation of the oocytes.

Xenopus laevis oocytes represent a very simple and powerful system for transient expression of the heterologous membrane proteins. The main advantages are represented by the high translational capacity and the huge cellular volume, which directly reflects into a bigger membrane surface and therefore more membrane protein. High accessibility of the mRNA microinjection technique and of the radioisotope flux measurements are

other significant factors that recommend the *X. laevis* oocytes as a good and reliable expression system. The first publication of the results obtained in this system goes back as far as 1971[155].

In the hexose transporters field the first use[156] of this system was related to the expression of the sodium dependent glucose transporter 1. Mature laboratory bred oocytes positive female *X. laevis* are available from Nasco and there are kept in covered tanks in chlorine free water under controlled lighting conditions (light dark cycle , 12 h each) and constant temperature of 16-18^{0}C. Multiple small batches of oocytes can be harvested from a single frog by surgical removal of a single ovarian lobe, thus allowing a series of experiments to be performed in oocytes from the same animal. Alternatively, the oocytes were harvested using a technique employed in Dr. Young's laboratory, whereby the animal are sacrificed, making more cells available for large-scale experiments.

The ovaries of adult female *X. laevis* contain mixtures of oocytes at six different stages (I-VI) of development[157]. In my experiments I used only the last two stages (V and VI) which are generally used in expression studies. Oocytes in these stages are large cells (1-1.3 mm in diameter) with a light vegetal pole and a darker animal pole (containing the nucleus) and can be easily differentiated from the other stages. The harvested ovary tissue is first treated with collagenase to release the individual oocytes and detach a surrounding layer of follicle cells. This procedure is followed by hypertonic phosphate treatment to complete the removal of the follicle layer. The oocytes are allowed to 'recover' for 2 - 3 hours and then the manual removal of the last layer of follicle is attempted. Oocytes should be carefully sorted at each stage to remove damaged cells and those showing

visible signs of degradation, such as leakage of egg yolk, changes in coloration or altered sharpness of the vegetal/animal pole boundary. For better results oocytes should be kept in relatively large volumes of medium and should not be crowded especially after microinjection.

2.10 Expression of Recombinant hGLUT7 in Xenopus oocytes.

Plasmids containing hGLUT 2, 5. 7, 9, 11 genes were linearized with Nhe I and in vitro transcribed with T7 polymerase mMESSAGE mMACHINE™ (Ambion). Adult female *Xenopus laevis* were obtained from Nasco Fort Atkinson, WI and housed at 18 °C on the 12 hour light/dark cycle. Stage V/VI oocytes were harvested from anesthetized frogs and placed in Modified Barth's Media (MBM) (88 mM NaCl, 1 mM KCl, 0.33 mM $Ca(NO_3)_2$, 0.41 mM $CaCl_2$, 0.82 mM $MgSO_4$, 2.4 mM $NaHCO_3$, 2.5 mM Na pyruvate, 0.1 mg/ml Penicillin, 0.05 mg/ml Gentamycin sulphate, 10 mM Hepes at pH 7.5). The follicular layer was removed by treatment for two hours with type I collagenase (Sigma) 0.02 g/ml. After selection, hypertonic phosphate treatment was applied to all oocytes subjected to microinjection. Prior to mRNA microinjection the oocytes were incubated in MBM at 16-18 °C for 24 hours to restore their osmolarity. The oocytes were injected with 10-50 nl (~20 ng) GLUT 2, 5, 7, 9, 11 synthetic mRNA transcripts and incubated for 3 – 5 days at 16-18 °C prior to functional uptake assays.

2.11 Northern Blotting.

Northern blot analysis of the possible GLUT7 mRNA expression in spleen, thymus, prostate, testis, ovary, small intestine, colon and leucocytes and heart, brain, placenta, lung, liver, skeletal muscle, kidney and pancreas were performed using a normal tissue mRNA Northern Blots (Clontech catalog # 7759-1, batch 7090547 and #7760-1 lot 9041180). Each lane was normalized against expression of the ß-actin gene. A PCR-based fragment of 813 bp corresponding to the last 271 amino acids of the C-terminal end of the wild type hGLUT7 was generated as a hybridization a probe. The forward primer was 5'-CTGAGAGGCCACACGGACAT-3' and the reverse primer was 5'-CGGAATTCCGCAGGGCCGCTAAAAGGAAGTTTC-3'. Briefly, the probe was subcloned in a pCR II-TOPO vector (Invitrogen) and linearized with restriction endonucleases *Sac*I and *Not*I for the subsequent production of the antisense and sense probes, respectively. Digoxigenin (DIG)-labeled antisense and sense riboprobes were synthesized by *in vitro* transcription with T7 and SP6 RNA polymerase and DIG RNA labeling mix (ROCHE Diagnostic, Mannheim, Germany) according to the manufacturer's instructions. The (DIG) labelled probes were hybridized to the blot under conditions of high stringency (85°C for 5 minutes). After washing the signal was recorded using Kodak-XAR5 film after 5 minutes exposure.

2.12 Preparation of Isolated Plasma Membranes.

Isolated brush-border membranes from rat jejunum and ileum were made using a standard technique routinely employed in our laboratory. Briefly, mucosal scrapings were taken from the jejunum and ileum on ice and the divalent cation precipitation method used to isolate the brush-border membranes from intracellular and basolateral membranes. Sodium potassium ATPase activity, a marker for basolateral membranes was reduced to 30% of the initial homogenate levels and alkaline phosphatase activity was enriched seventeen fold.

Recombinant protein expression in *Xenopus* oocytes can be detected by western blots or immunocytochemistry. For Western blotting the preparation of the oocytes plasma membranes involves approximately 100 oocytes mixed with 1 ml ice-cold lysis buffer containg 0.1 mM PMSF in a 15 ml centrifuge tube. By thorough up and down pipeting the oocytes are broken open while the tube is kept on ice. A first centrifugation at ~500 x g, 5 min at 4°C produces the first supernatant which is going to be transfers into a polycarbonate ultracentrifuge tube and subsequently centrifuged at 16,000 x g for 30 min at 4°C. The remaining pellet contains the membrane fraction of the lysed oocytes and could be further used for western blot analysis.

2.13 Western Blotting and Immunohistochemistry.

Two polyclonal antibodies were raised against the unique 11 amino acid sequence of the C-terminal tail of GLUT7 (PTASPAKETSF) by Alpha Diagnostic International,

San Antonio, TX. Testing of the affinity-purified product in Western blots indicated that antibody 7440 recognized the expression of GLUT7 protein in plasma membranes of mRNA-injected oocytes, but was negative for water-injected oocytes.

Oocytes were embedded in OCT (10% polyvinyl alcohol, 4% polyethylene glycol) embedding media (Shandon) and flash frozen in liquid nitrogen. Ten micrometer thick sections were cut on a cryostat (Leica cryostat, Richmond Hill, Ontario, Canada), placed on slides and stored at -20°C. On the day of use, sections were brought to room temperature and fixed with methanol for 90 s. Following a 5 min wash with PBS (potassium chloride, 76.5%, potassium phosphate monobasic anhydrous, 0.3% ,sodium chloride, 12.2%, sodium phosphate dibasic, 10.7%- note all concentrations are w/v), the sections were treated with 1% SDS for 5 min to increase antigen exposure, and again thoroughly washed in PBS (3 times for 5 min each). The sections were then treated with 10% goat serum (0.1% Tween 20) to decrease nonspecific binding of the secondary antibody, followed by a rapid rinse with PBS and incubation with primary antibody. The primary anti-GLUT7 antibody, was diluted 1:200 in a 25% w/v milk solution (25 g powdered milk in 100 ml PBS with 0.05% Tween 20) and placed on slides for 24 h at 4°C, followed by washes with high salt (3 M NaCl) PBS and then PBS. The slides were then incubated with 1 mg/ml biotinylated goat anti-rabbit secondary antibody (Chemicon) diluted 1:200 in PBS, for 1 h at room temperature. The sections were washed in high salt PBS and PBS and then treated with streptavidin-conjugated FITC (Amersham) for 30 min in the dark. After three 5 min washes with PBS in the dark, the slides were mounted

and sealed with nail polish. They were then viewed and photographed under a confocal microscope (Zeiss LSM510).

2.14 Radiotracer flux assays

The influx experiments were performed at 20 ^{0}C using 10-12 oocytes for each condition and ^{14}C or ^{3}H labelled hexose at a specific activity of 1 μCi/ml. The experiment is initiated by addition of medium containing the appropriate radiolabelled substrate. After the incubation period (determined by the kinetic parameters of each particular clone) the oocytes were washed 5-7 times with ice cold MBM to stop the incubation and then individual oocytes were placed in vials and dissolved in 0.5 ml 5% SDS for 30 min. Finally, scintillation fluid (5 ml) was added to each vial and radio activity measured using a Beckman LS6500. Incubation periods for kinetic and substrate specificity studies were chosen to be within in the linear phase of the uptake curve to approximate zero-*trans* conditions and measure initial rates of transport. All experiments were performed 3-7 times and the results were compared to the influx values obtained with water-injected oocytes to determine the transporter mediated component of uptake, which will be greatest at substrate concentrations equal to or less then the anticipated Km.

2.15 Kinetic analysis.

D-glucose uptake was measured over a range of concentrations from 0.05 – 6 mM using 30 min incubations, which had been determined to be within the linear slope of

uptake. Uptake was corrected for endogenous uptake using water-injected eggs from the same batch of eggs in each experiment. ENZFITTER software was used to determine the transport kinetics for the GLUT7-mediated glucose uptake by non-linear regression analysis. Conventionally, a non-metabolized substrate is used for kinetic measurements to avoid the possibility of the kinetic parameters of a rate limiting intracellular metabolic pathway superceding the kinetic constants of the transporter. In this study 2 deoxy-D-glucose was found not to be a substrate and so the naturally occurring hexoses were focused upon. However, it should be noted that when SGLT1 is expressed in oocytes there is no discernable difference in the rates of transport between D-glucose and α-methyl-D-glucoside. SGLT1 is expressed at very high levels in oocytes and achieves a far greater rate of uptake than we observe with GLUT7, so we conclude that hexokinase cannot be rate limiting under our conditions.

Chapter 3.

Results.

3.1. Cloning of hGLUT7 (SLC2A7).[♣]

Cloning of the hGLUT7 employed a PCR based strategy based on the high percentage similarity between hGLUT5 and hGLUT7 (68%) DNA sequences found in the NCBI database and on the fact that both genes are present on the same chromosome (Chr 1p). PCR employing unique primers for the putative GLUT7 sequence with a human intestinal cDNA library generated a 1.7-kb cDNA (Fig. 3.1A) product that gave codes for a predicted amino acid sequence shown in Fig. 3.1B. This 524-amino acid sequence, when aligned with the one of GLUT5, shows 68% similarity and 53% identity between the two proteins (Fig. 3.1C). Both the nucleotide and amino acid sequence data have been deposited with GenBank (accession no. AY571960). This clone was then used to produce mRNA for injection into oocytes and functional characterization of the protein.

3.1.1 GLUT7 functional studies.

The uptake of a panel of hexoses into mRNA- and water-injected oocytes showed that GLUT7 mediated the transport of glucose and fructose. Figure 3.2A shows a typical experiment. There was no significant GLUT7-mediated flux of D-galactose, 2DG, or D-xylose. The mold metabolite CB, known to inhibit transport activity of many GLUT's, had no significant effect on the uptake of glucose mediated by GLUT7 (Fig. 3.2B). Similarly, 200 μM phloretin had no effect on glucose uptake (Fig. 3.2C).

[♣] Portions of this subchapter have been previously published and are reproduced with permission from : Li Q, **Manolescu A**, Ritzel M, Yao S, Slugoski M, Young JD, Chen XZ, Cheeseman CI. *Cloning and functional characterization of the human GLUT7 isoform SLC2A7 from the small intestine.* Am J Physiol Gastrointest Liver Physiol. 2004;287(1):G236-42.

A.

atggagaacaaagaggcgggaacccctccacccattccatccagggaggggcggctccagccgacgctgttgctggcgaca
ctgagcgcggcctttggctcagccttccagtacggctacaacctctctgtggtcaacacgccgcacaaggtgggcacaagctgt
ggatggggcaatgttttccaggtcttcaagtcattttacaacgaaacctactttgagcgacacgcaacattcatggacgggaagct
catgctgcttctatggtcttgcaccgtctccatgtttcctctgggcggcctgttggggtcattgctcgtgggcctgctggttgatagct
gcggcagaaaggggaccctgctgatcaacaacatctttgccatcatccccgccatcctgatgggagtcagcaaagtggccaag
gcttttgagctgatcgtcttttcccgagtggtgctgggagtctgtgcaggcatctcctacagcgcccttcccatgtacctgggagaa
ctggcccccaagaacctgagaggcatggtgggaacaatgaccgaggttttcgtcatcgttggagtcttcctagcacagatcttca
gcctccaggccatcttgggcaacccggcaggctggccggtgcttctggcgctcacaggggtgcccgccctgctgcagctgctg
accctgcccttcttcccccgaaagcccccgctactccctgattcagaaaggagatgaagccacagcgcgacaagctctgaggag
gctgagaggccacacggacatggaggccgagctggaggacatgcgtgcggaggcccgggccgagcgcgccgagggcca
cctgtctgtgctgcacctctgtgccctgcggtccctgcgctggcagctcctctccatcatcgtgctcatggccggccagcagctgt
cgggcatcaatgcgatcaactactatgcggacaccatctacacatctgcgggcgtggaggccgctcactcccaatatgtaacgg
tgggctctggcgtcgtcaacatagtgatgaccatcacctcggctgtccttgtggagcggctgggacggcggcacctcctgctgg
ccggctacggcatctgcggctctgcctgcctggtgctgacggtggtgctcctattccagaacagggtccccgagctgtcctacct
cggcatcatctgtgtctttgcctacatcgcgggacattccattgggcccagtcctgtcccctcggtggtgaggaccgagatcttcct
gcagtcctcccggcgggcagctttcatggtggacggggcagtgcactggctcaccaacttcatcataggcttcctgttcccatcc
atccaggaggccatcggtgcctacagtttcatcatctttgccggaatctgcctcctcactgcgatttacatctacgtggttattccgg
agaccaagggcaaaacatttgtggagataaaccgcatttttgccaagagaaacagggtgaagcttccagaggagaaagaagaa
accattgatgctgggcctcccacagcctctcctgccaaggaaacttccttttag.

B.

MENKEAGTPPPIPSREGRLQPTLLLATLSAAFGSAFQYGYNLSVVNTPHKVGTSCGWGNVFQVFKSFYNET
YFERHATFMDGKLMLLLWSCTVSMFPLGGLLGSLLVGLLVDSCGRKGTLLINNIFAIIPAILMGVSKVAKA
FELIVFSRVVLGVCAGISYSALPMYLGELAPKNLRGMVGTMTEVFVIVGVFLAQIFSLQAILGNPAGWPVL
LALTGVPALLQLLTLPFFPESPRYSLIQKGDEATARQALRRLRGHTDMEAELEDMRAEARAERAEGHLSVL
HLCALRSLRWQLLSIIVLMAGQQLSGINAINYYADTIYTSAGVEAAHSQYVTVGSGVVNIVMTITSAVLVE
RLGRRHLLLAGYGICGSACLVLTVVLLFQNRVPELSYLGIICVFAYIAGHSIGPSPVPSVVRTEIFLQSSR
RAAFMVDGAVHWLTNFIIGFLFPSIQEAIGAYSFIIFAGICLLTAIYIYVVIPETKGKTFVEINRIFAKRN
RVKLPEEKEETIDAGPPTASPAKETSF

Fig. 3.1 A. Open reading frame nucleotide sequence of human GLUT7 mRNA as published in GeneBank under accession number NM_207420. **B.** Amino acid sequence of the human GLUT7 protein as published in GeneBank under accession number AAS78590.

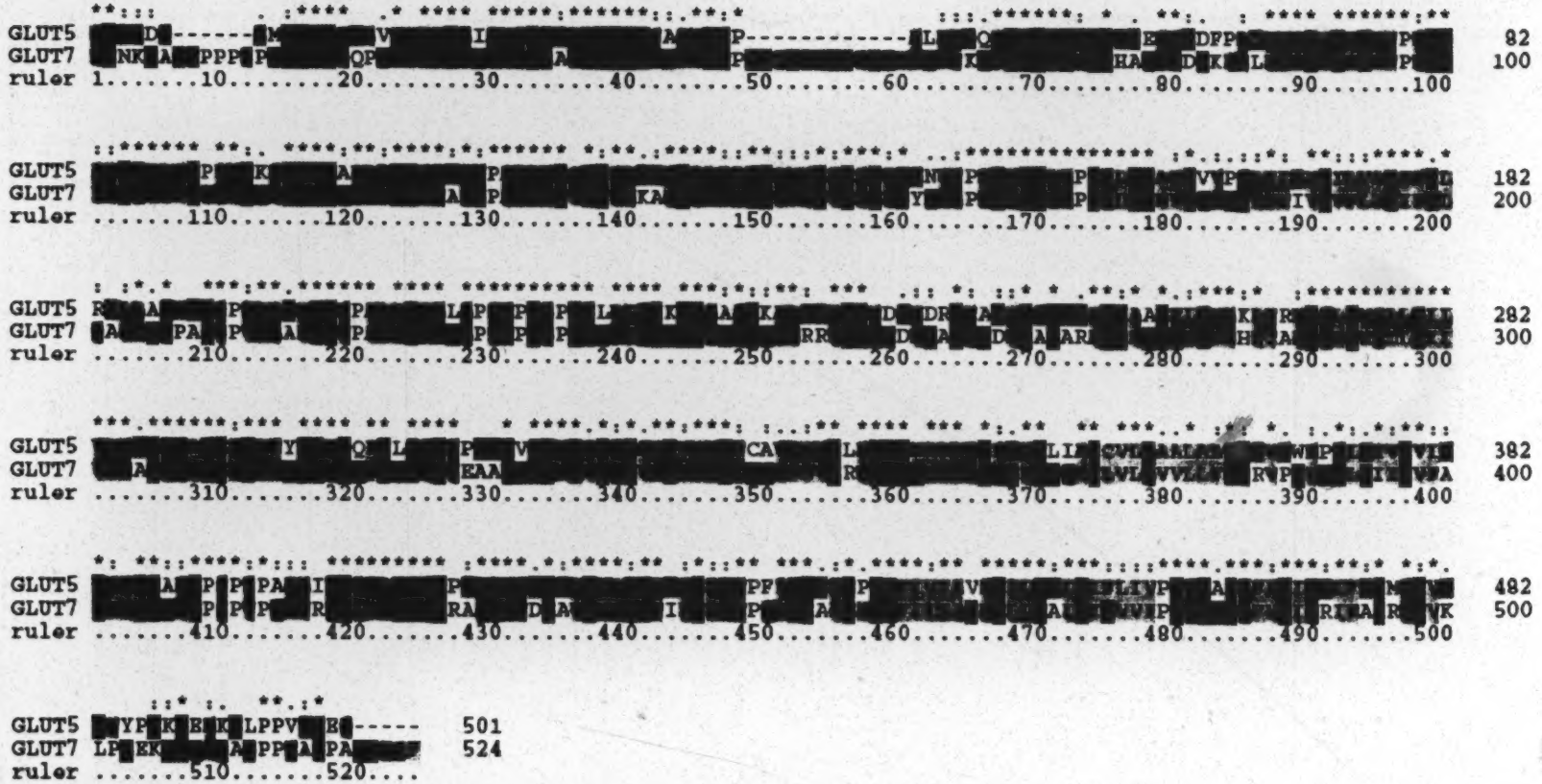

Fig 3.1.C Sequence alignments of the hGLUT5 and 7.

The amino acid sequences had been aligned using a ClustalX software based on the sequences deposited on the NCBI human genome data bank.

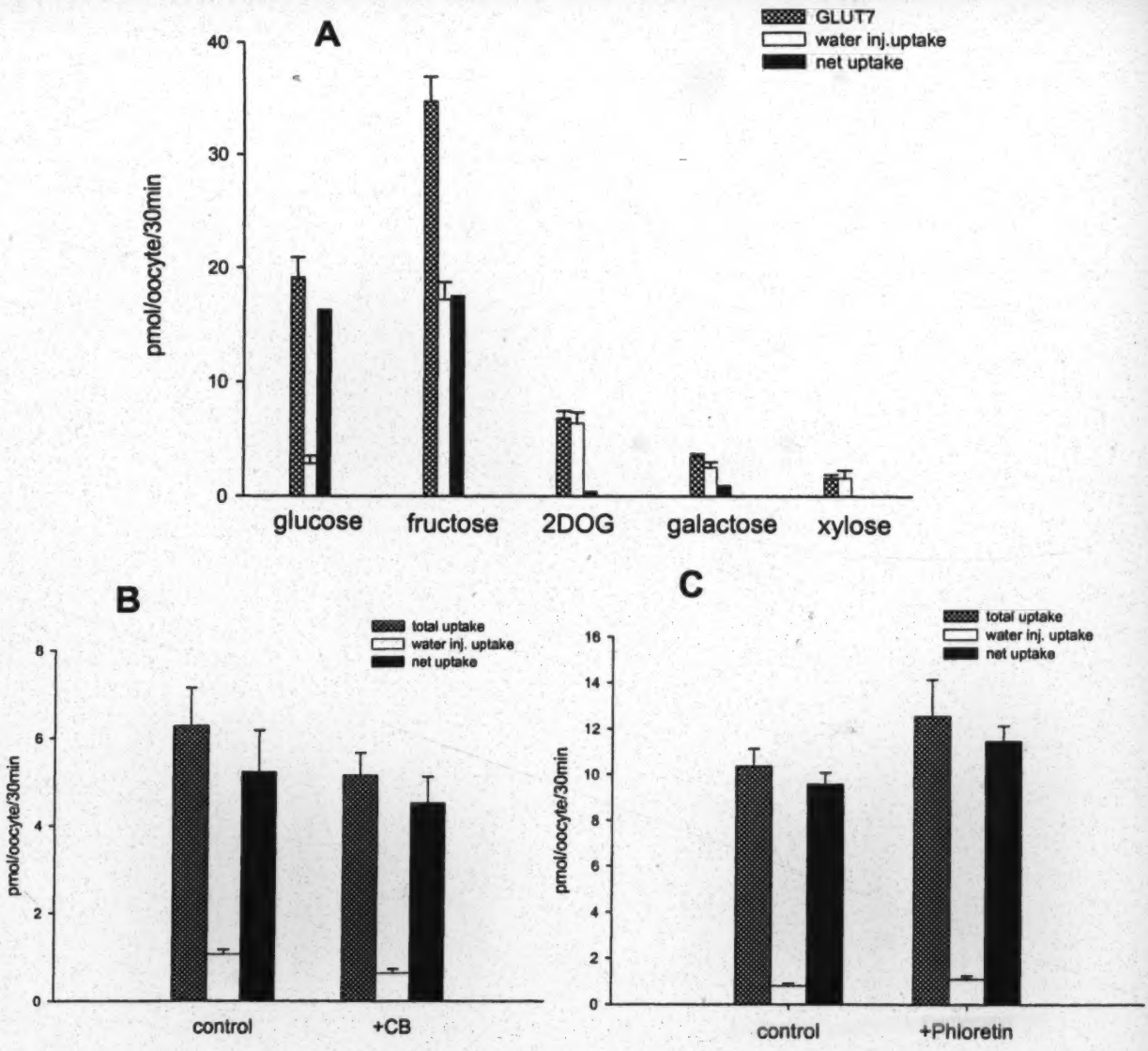

Fig. 3.2 GLUT7 mediated hexose fluxes in *Xenopus oocytes*. Oocytes were injected with GLUT7 mRNA or water 5 days before the measurement of uptake of radiolabelled substrates (100 μM). Bars represent uptake measured over 30 min into 8–10 oocytes injected with mRNA (hatched bars), water (open bars), and net uptake (filled bars). Error bars represent the standard error of the mean. 2DOG, 2-deoxy-D-glucose. *B*: effect of the addition of 100 μM cytochalasin B (CB) on the uptake of 100 μM D-glucose into oocytes injected with GLUT7 mRNA *C*: effect of addition of 200 μM phloretin on 100 μM D-glucose uptake. In these experiments, 18–20 oocytes were used for each condition.

The time course of 100 μM glucose uptake into oocytes expressing GLUT7 was linear for at least 40 min, and so 30-min incubations were chosen for subsequent kinetic experiments. This length of incubation maximized the uptake signal while remaining on the linear portion of the uptake curve. Uptake of glucose over the concentration range 0.05–1.5 mM was curvilinear and, when corrected for uptake into water-injected oocytes, exhibited Michaelis-Menten type kinetics with a K_m of 302 ± 60 μM (Fig. 3.3). Similarly, the fructose uptake was tested and the kinetics also conformed to Michaelis-Menten kinetics with a Km for uptake of 173 ± 98 μM (Fig. 3.4).

3.1.2 Tissue expression pattern for hGLUT7.

Northern blotting of intestinal mRNA with the antisense cDNA DIG-labeled probe corresponding to the COOH-terminal coding sequence for the last 271 amino acids of hGLUT7 gave a band corresponding to a transcript of 1.35 kb. This was detected in the small intestine and colon as well as weaker signals in the testis and prostate. Spleen, thymus, ovary, and leucocytes gave no detectable signal (Fig. 3.5). A second blot showed no signal in the heart, brain, placenta, lung, liver, skeletal muscle, kidney, or pancreas (data not shown).

Protein expression was determined by using a commercially prepared antibody raised against the 11 COOH-terminal amino acids of the hGLUT7 sequence. The

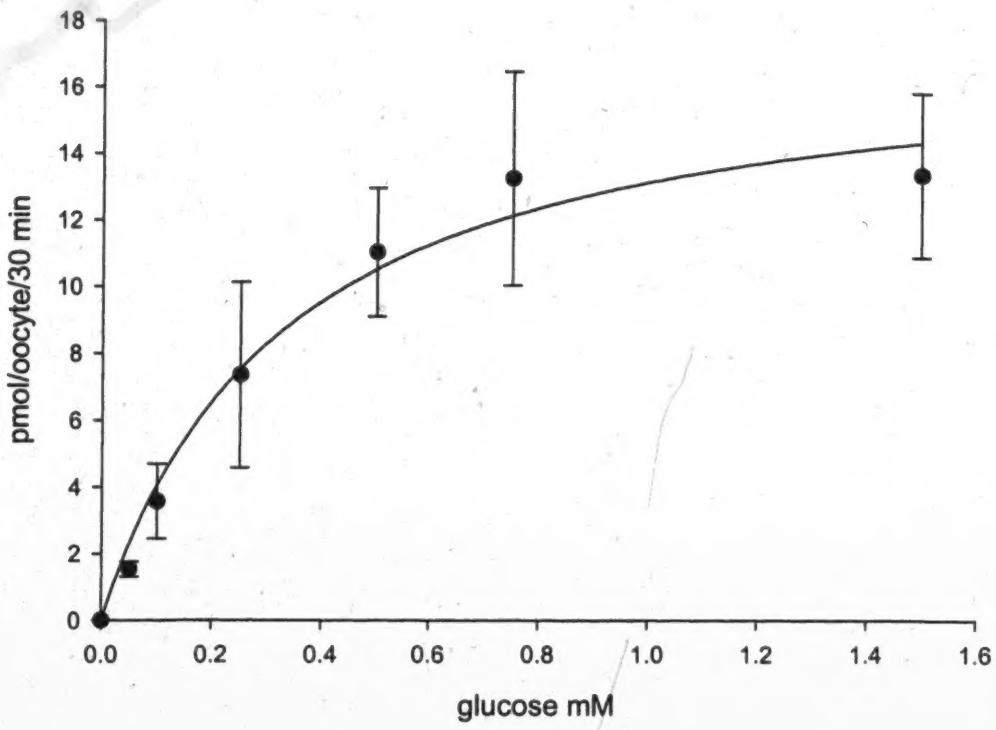

Fig. 3.3 Kinetics of GLUT7-mediated glucose uptake into *Xenopus oocytes*. Glucose uptake using 30-min incubation periods over a range of concentrations (conc) is shown. The uptake is corrected for the uptake measured into the same batch of oocytes injected with water, and the fitted curve is that solved by nonlinear regression for a single Michaelis-Menten component with a K_m of 0.3 mM and a V_{max} of 20 pmol·oocyte^{-1}·30 min^{-1}.

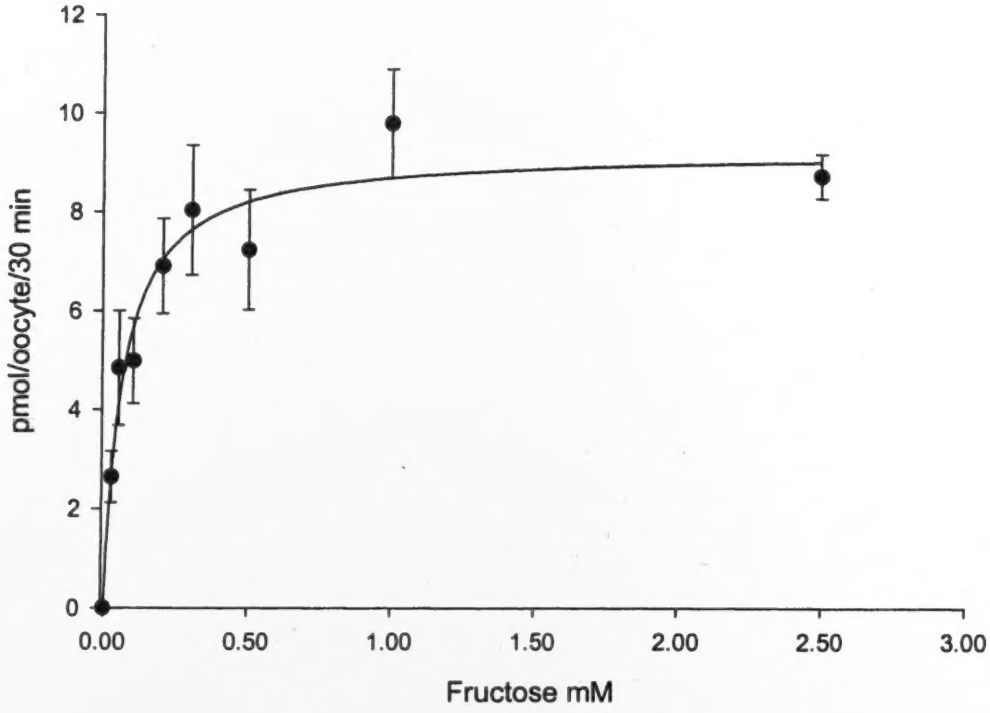

Fig. 3.4 Kinetics of hGLUT7 –mediated fructose uptake in *Xenopus oocytes*. [^{14}C] D-Fructose uptake (30min at 22°C) was measured 3 days after oocyte injection with mRNA (20 ng). The data points represent the mean uptake into 10-12 individual oocytes corrected for the uptake into oocytes injected with water. A curve was fit by non linear regression for a single Michaelis-Menten component with a K_m of 0.09 mM and a V_{max} of ~ 9 pmol, oocytes^{-1}, 30min^{-1}.

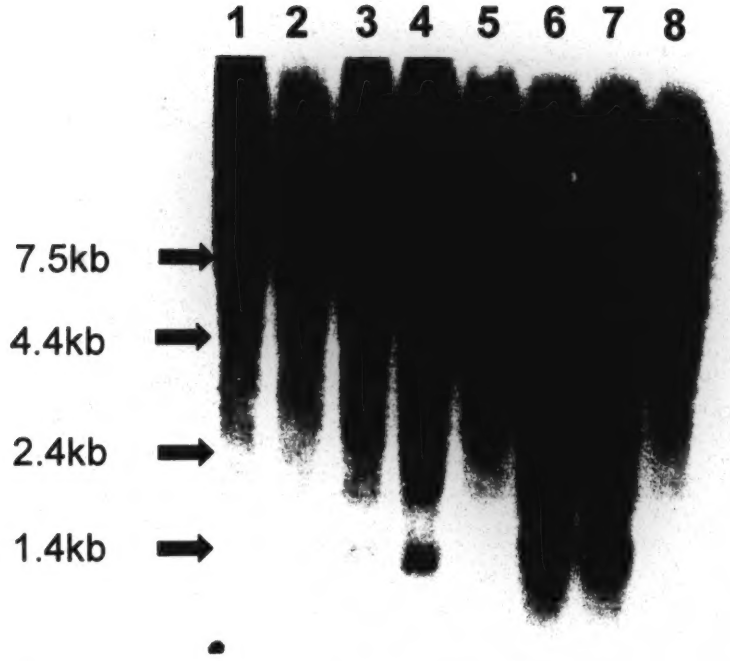

Fig. 3.5. Tissue distribution of GLUT7 mRNA by Northern blotting. The digoxigenin (DIG)-labeled partial GLUT7 cRNA corresponding to amino acids M254–M524 was used as a probe. Lanes were loaded with mRNA normalized to the same β-actin RNA concentration. After hybridization, the blot was exposed to film for 5 min before developing. *Lane 1*, spleen; *lane 2*, thymus; *lane 3*, prostate; *lane 4*, testis; *lane 5*, ovary; *lane 6*, small intestine; *lane 7*, colon; *lane 8*, leucocytes. The bands correspond to a size of 1.35 kb. Marker indicates size in kilobases

specificity of the polyclonal antibody 7440 was clearly demonstrated by comparing the staining pattern of slides prepared from water-injected *Xenopus* oocytes with that of oocytes 5 days after injection with hGLUT7 mRNA. The mRNA injection clearly led to the expression of novel protein in the plasma membrane, which was detected by the antibody using Western blotting, whereas there was no binding of the antibody to membranes from water-injected eggs (Fig. 3.6B). Western blotting of pooled oocyte plasma membranes from oocytes injected with hGLUT7 mRNA showed a single protein band (Fig. 3.6B), whereas in membranes from eggs expressing hGLUT5 no band was observed, supporting the conclusion that antibody 7440 can specifically detect the expression of the hGLUT7 protein. Conversely, the GLUT5 antibody failed to detect hGLUT7 protein (Fig. 3.6A). Western blotting of brush-border membranes prepared from the jejunum and ileum of Sprague-Dawley rats also reacted with the GLUT7 antibody, giving a band at a position equivalent to an apparent molecular weight of 53 kDa. The expression was low in the jejunum and higher in the ileum (Fig. 3.6C).

Immunohistochemistry of hGLUT7 mRNA-injected oocytes, using the same GLUT7 antibody, showed significant expression of protein in the plasma membrane, whereas there was no signal detected in water-injected eggs. This confirmed that the antibody could also be used with tissue slices as well as for Western blots. Immunohistochemistry of rat frozen intestinal tissue with the 7440 antibody showed expression of a hGLUT7-like protein (Fig. 3.7) that corresponded to the Western blotting of rat membranes with strong staining in the ileum. However, although Northern

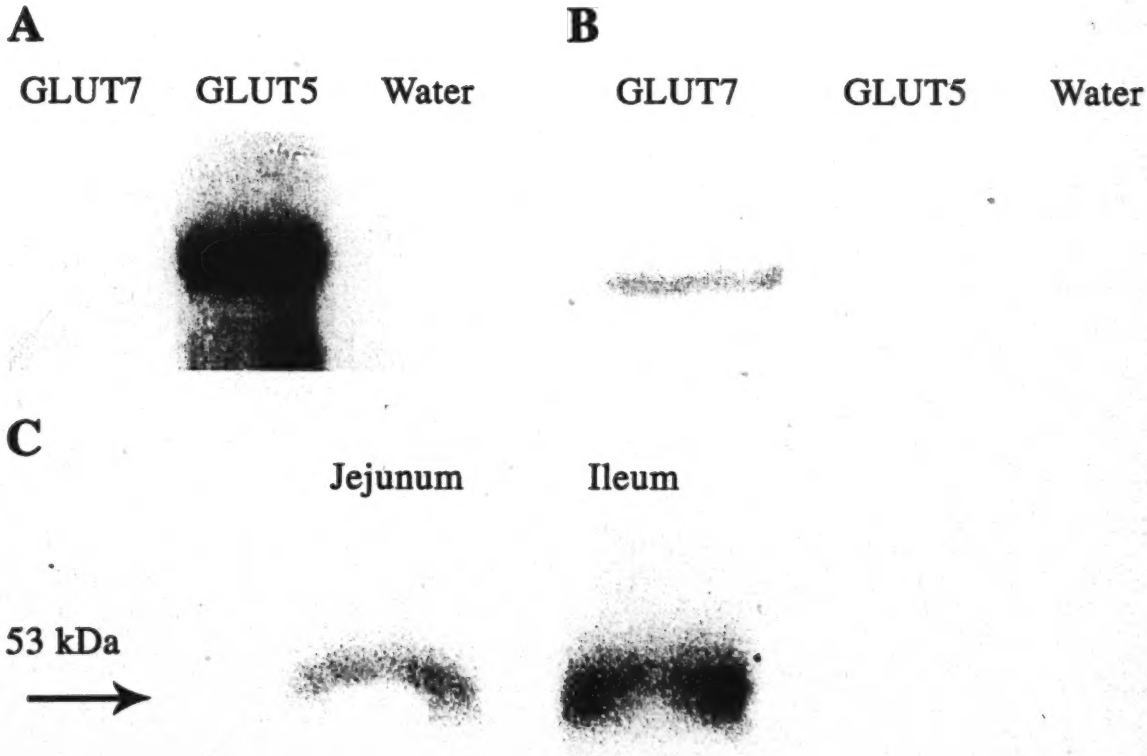

Fig. 3.6. ***A***: Western blot of oocytes (50) membranes prepared from oocytes 5 days after injection with human GLUT7 mRNA (shown to be transporting glucose and fructose) or with GLUT5 mRNA (shown to transport fructose) or injected with water and probed with anti-GLUT5 antibody. **B**: same membranes probed with anti-GLUT7 antibody 7440. **C**: Western blot of rat jejunal and ileal brush-border membranes probed with the anti-GLUT7 antibody 7440.

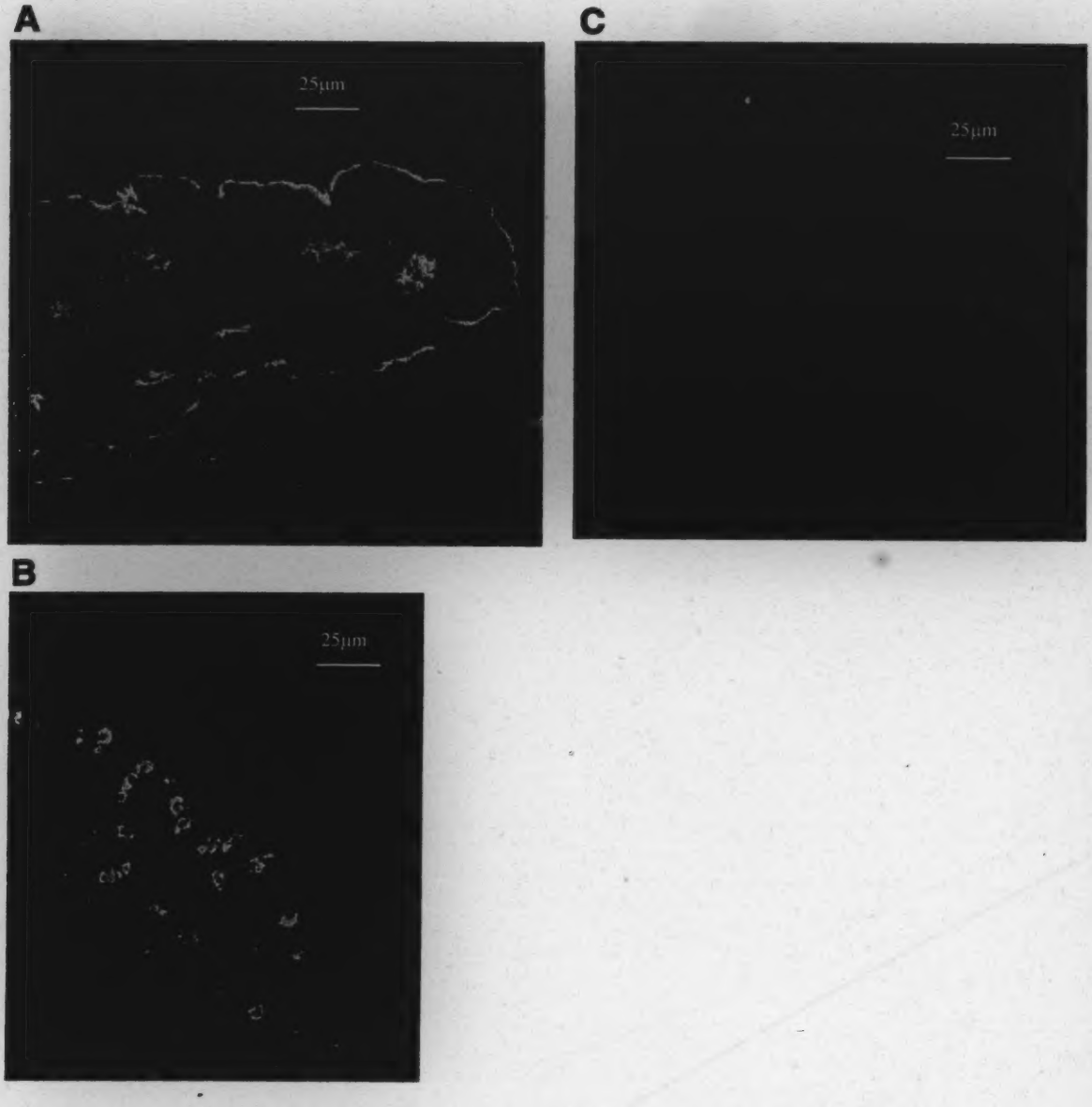

Fig. 3.7. Immunohistochemistry of rat ileum (*A*) and colon (*C*) probed with the primary antibody 7440 raised against the putative last 11 amino acids of human GLUT7 and ileum probed with the antibody preabsorbed with the antigenic synthetic peptide (*B*). Frozen sections (11 µm) of rat intestine were probed with the primary antibody overnight at 4°C. The presence of GLUT7 was visualized with an FITC-tagged secondary antibody. Images were captured with a Zeiss LSM510 confocal microscope.

blotting for human tissues indicated the presence of GLUT7 mRNA in the colon, no staining was detected in rat tissue for this region of the gastrointestinal tract. Examination of the staining patterns in the rat ileum indicated that the protein was predominantly expressed in the brush-border membrane with only a very weak signal in the lateral or basal membranes. The protein was not found in the underlying muscle layers nor within the villus core, indicating that GLUT7 is not expressed in endothelial or muscle cells. Some bright signals evident in both control and test tissues represent autofluorescence of mast cells in the villus core. The specificity of the binding of antibody 7440 was again confirmed by the inability of the preabsorbed primary antibody to bind to proteins in the ileal brush-border membrane (Fig. 3.7B).

3.2 GLUT7 I314V.[♣]

Comparison of the amino acid sequence alignments of GLUT's 1, 2, 5 & 7 revealed that at the homologous position of the V290 in GLUT1, GLUT's 2, 5 and 7 contain an Ile (I306, I321 & I314 respectively), Fig.3.8. Given that GLUTs 2, 5 and 7 transport fructose and all have this conserved Ile while the GLUTs which transport glucose, but not fructose, have a Val at the equivalent site, I focused on the possible role of this residue in relation to the substrate specificity of GLUT7.

Two mutants of human hGLUT7 cDNA encoding a point mutation in position 314 were constructed in which the native Ile was replaced with either with Val or Ser. After

---

[♣] Portions of this subchapter have been previously published and are reproduced with permission from : Manolescu A, Salas-Burgos AM, Fischbarg J, Cheeseman CI. *Identification of a hydrophobic residue as a key determinant of fructose transport by the facilitative hexose transporter SLC2A7(GLUT7).* J Biol Chem. 2005 Sep 26; [Epub ahead of print]

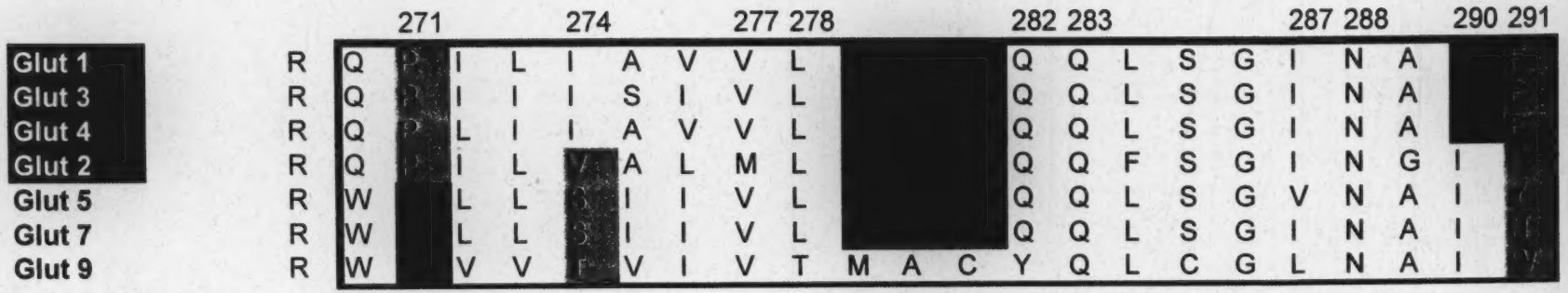
271
274
277 278
282 283
287 288
290 291
Glut 1
Glut 3
Glut 4
Glut 2
Glut 5
Glut 7
Glut 9
R Q P I L I A V V L Q Q L S G I N A
R Q P I I I S I V L Q Q L S G I N A
R Q P L I I A V V L Q Q L S G I N A
R Q P I L V A L M L Q Q F S G I N G I
R W L L G I I V L Q Q L S G V N A I
R W L L G I I V L Q Q L S G I N A I
R W V V F V I V T M A C Y Q L C G L N A I

Fig. 3.8. Comparison of GLUT5, 7 and 9 primary sequences to the class I members ones. Sequences were aligned using Clustal X software and written from N to C-termini. Based on the putative membrane topology of this helix, its C-terminus end faces the extracellular side of the membrane (see figure1). At position 314 of GLUT7 the protein that could transport fructose as well as glucose have an isoleucine residue highlighted in yellow. In the alignment is also presented the position of the putative selectivity binding site motif QLS in GLUT 1-3. As could be seen from the alignment the conserved I 314 is placed in the near proximity of the putative binding site and above it close to the exofacial border of the pore.

injection of the mRNA into oocytes, the subsequent expression of the mutants in the oocyte plasma membrane was assessed by immunohistochemistry and semi-quantitative Western blot analysis of isolated oocyte plasma membranes (Fig 3.9). Both methods employed a commercially prepared antibody raised against the 11 C-terminal amino acids of the wild type human GLUT7. In all cases, these conservative single amino acid substitutions did not affect expression of the proteins in the oocytes and the mutant was present at levels similar to the wild type protein, (Fig. 3.9).

To identify any alterations of substrate specificity for mutant proteins we performed a comparison between the uptake of a series of hexoses by wild type GLUT7, and the I314V mutant. There was a striking difference between the wild type GLUT7 and the I314V mutant functional activity, with the mutant showing a 80% reduction in the transport of fructose, while glucose uptake was similar to the wild type one (Fig. 3.10). Also, wild type GLUT7 does not transport D-galactose or 2-deoxy-D-glucose and in this regard the I314V mutant was no different. 200 μM phloretin had no effect on glucose uptake by either protein, (Fig. 3.10).

Next I investigated whether the loss of fructose transport represented an effect on the binding of the substrates, or blocked translocation in some other way, by comparing the kinetic characteristics of the glucose uptake in both proteins. We previously reported that hGLUT7 has a high affinity for glucose and fructose[158]. This was based upon kinetic analysis of glucose and fructose uptake (Km ~ 300 μM and Km ~ 114 μM, respectively) and the ability of fructose to competitively inhibit glucose transport (IC_{50} 60.3 ± 25.8

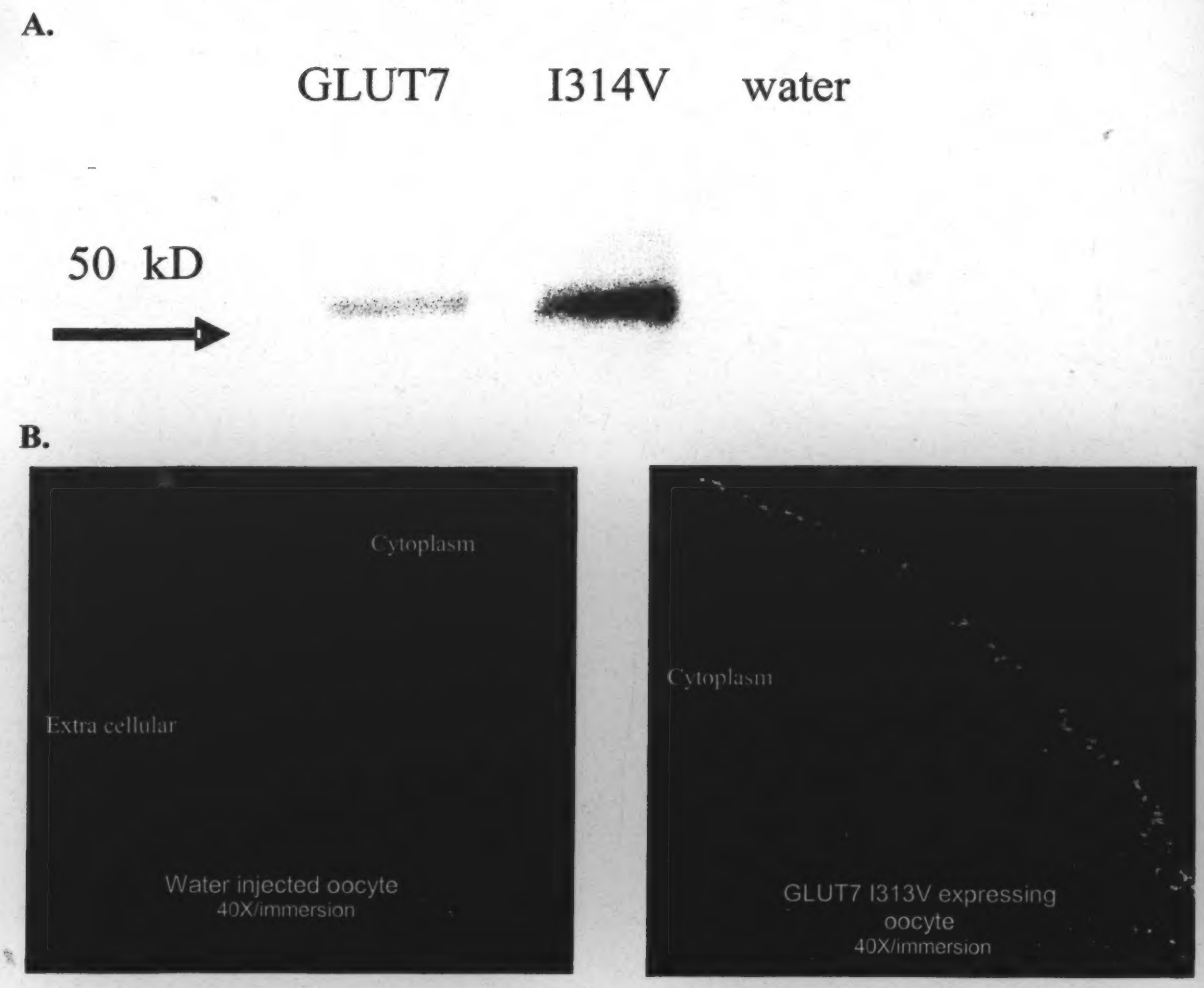

Fig. 3.9. Expression of wild type and mutant GLUT transporters in *Xenopus* oocytes. Three days after injection with wild type or mutant GLUT mRNA, oocytes were used to prepare plasma membranes for Western blot analysis or for GLUT protein visualization using indirect immunofluorescence laser confocal microscopy. **A.** Immunoblot with 20 μg of membrane proteins loaded per lane. The arrow on the left indicates the mobility of prestained 50 KDa molecular weight standard. **B.** Stage 5 *Xenopus* oocytes expressing wild type or mutant GLUT 2, 5 and 7 mRNA (20 ng), or injected with water were frozen, sectioned and stained with 7440 IgG followed by fluorescin-conjugated goat anti rabbit IgG. Sections were visualized with a Zeiss LSM510 confocal microscope.

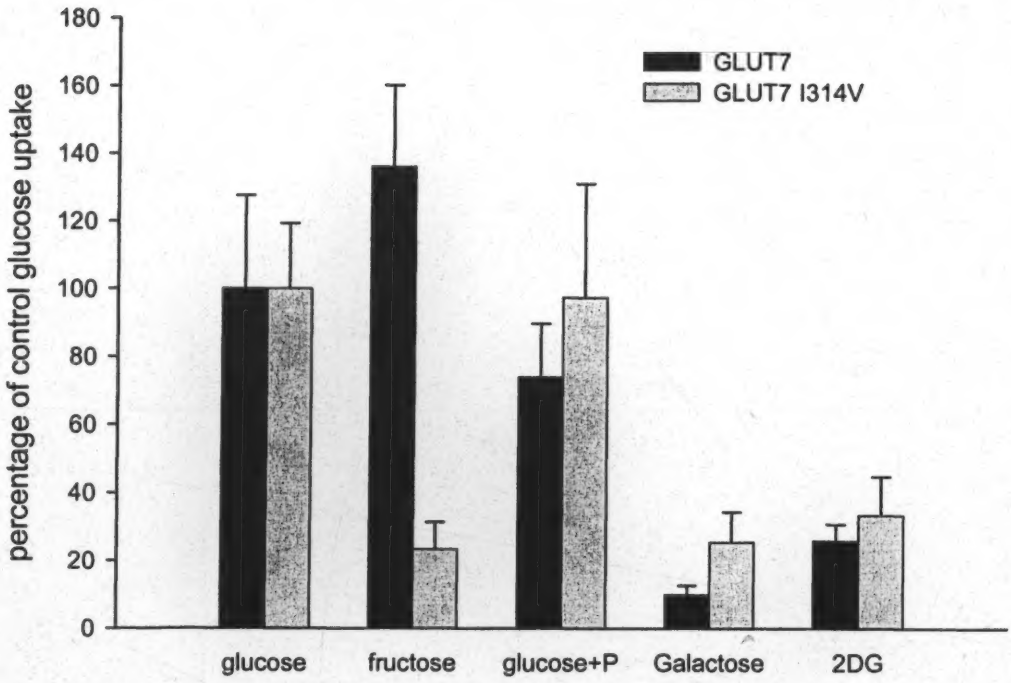

Fig. 3.10. Hexose fluxes in *Xenopus laevis* oocytes expressing GLUT7 wild type and I314V mutant. Stage 5 *Xenopus* oocytes were injected with GLUT7, I314V mRNA (20 ng) or water 3 days prior to the measurement of uptake of 100 μM radiolabelled substrates. Bars represent the mean net uptake measured over 30 minutes into 10-12 oocytes injected with mRNA and corrected for the uptake into water injected oocytes. Error bars represent SEM. (abbreviation P- Phloretin)

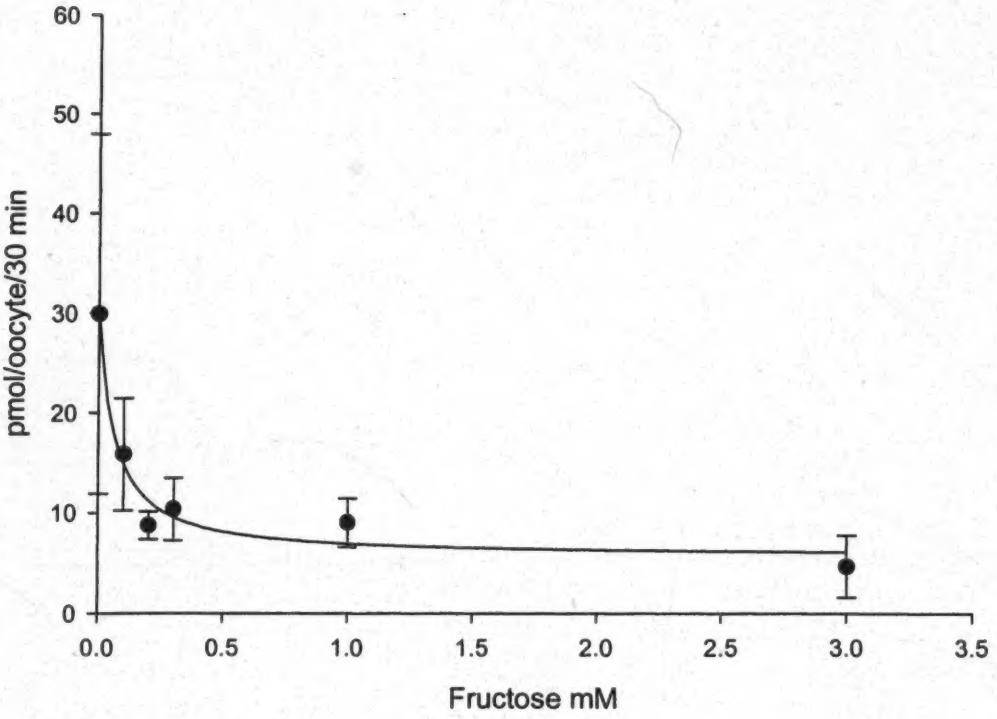

Fig. 3.11. Inhibition of GLUT7-mediated glucose uptake by fructose. The uptake of 100 μM D-glucose was measured in the presence of increasing concentrations of cold D-fructose. Incubations lasted 30 min, and the data points represent the mean uptake into 10-12 individual oocytes corrected for uptake into water-injected oocytes under identical conditions. The curve was fitted by nonlinear regression analysis, which gave an IC_{50} of 60.3 μM.

μM-), Fig. 11). Fructose inhibition of glucose uptake showed an IC_{50} of 60.3 ± 25.8 μM, indicating that GLUT7 also has a high affinity for this hexose (Fig.3.4).

Therefore, to complete this analysis I determined the IC_{50} for glucose inhibition of fructose uptake. Both sets of experiments confirmed that hGLUT7 has a high affinity for these two hexoses. The IC_{50} for glucose inhibition of 100 μM fructose transports was 122 ± 56.0 μM, (Fig. 3.12).

Kinetic analysis of glucose transport in the GLUT7 I314V mutant confirmed the initial uptake measurements, using a single glucose concentration, that this point mutation had no effect on glucose transport, Fig. 3.13. Uptake of glucose over the concentration range 0.05 – 2.5 mM was curvilinear and, when corrected for uptake into water-injected oocytes, exhibited Michaelis-Menten type kinetics with a Km of 127 μM ± 49. Interestingly, glucose (100 μM) transport by this mutant was completely unaffected by the presence of excess cold fructose (10 mM), Fig. 3.14, suggesting that fructose was either unable to access the hexose binding site or was no longer recognized.

It could be argued that even though the substitution of Ile with Val is very conservative it could produce a very significant structural alteration to the conformation of the binding site in the protein. Therefore, the effect of a substitution of isoleucine with serine at position 314 in GLUT7 was also tested. This was found to have no effect on the specificity of the transporter with glucose and fructose transport both being retained, (Fig. 3.15- 17)

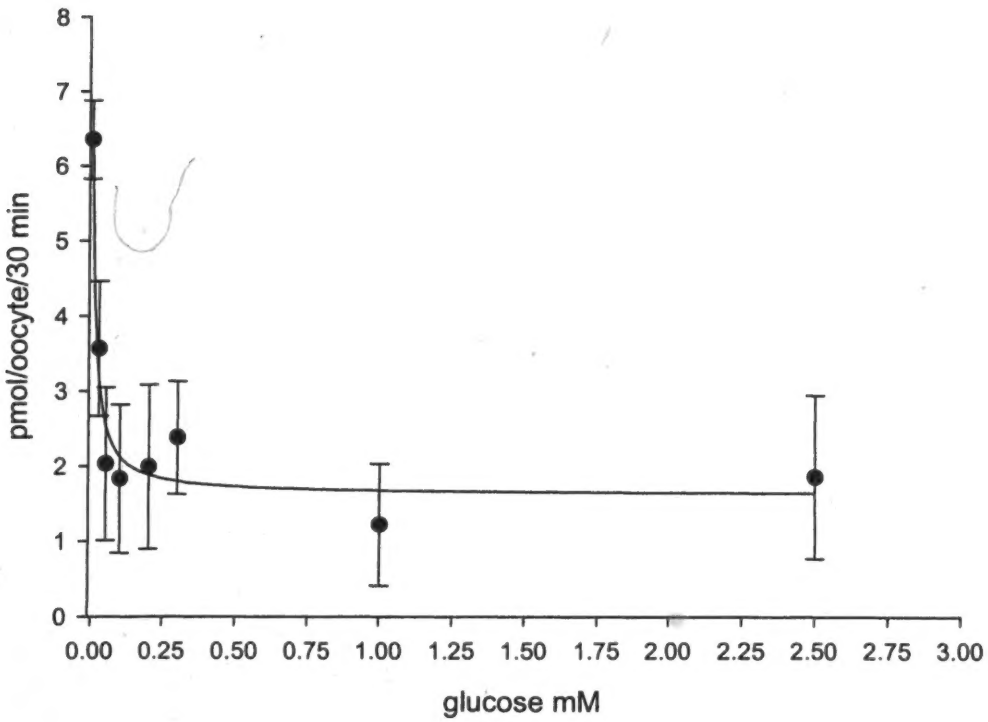

Fig. 3.12. Inhibition of GLUT7-mediated fructose uptake by glucose. The uptake of 100 μM D-fructose was measured in the presence of increasing concentrations of cold D-glucose. Incubations lasted 30 min, and the data points represent the mean uptake into 10-12 individual oocytes corrected for uptake into water-injected oocytes under identical conditions. The curve was fitted by nonlinear regression analysis, which gave an IC_{50} of ~50 μM.

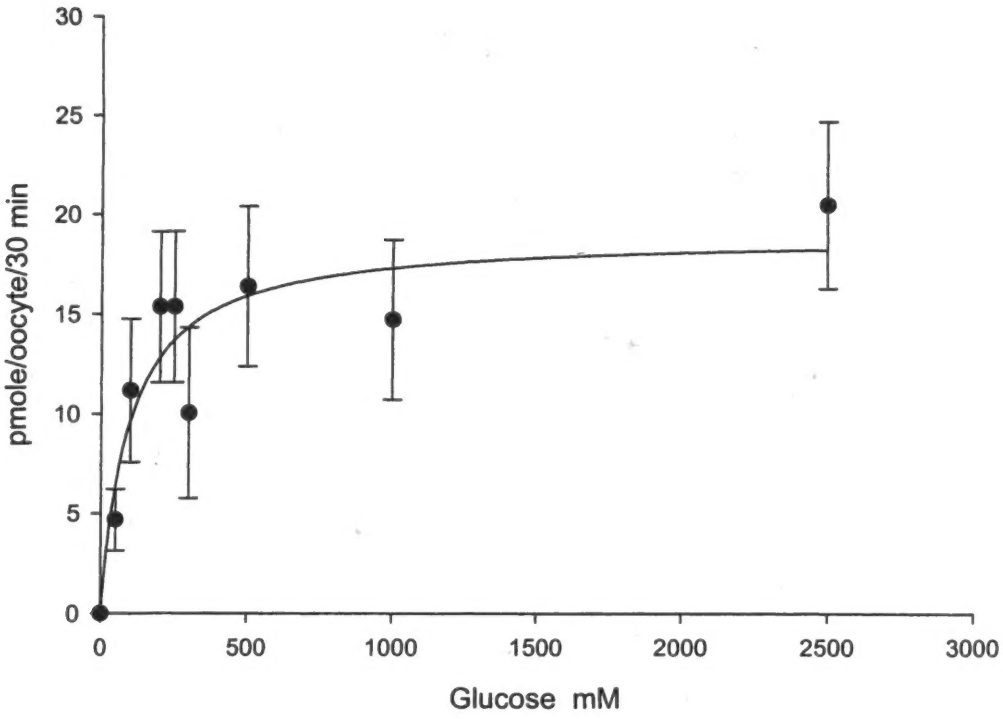

Fig. 3.13 Kinetics of glucose transport in I314V mutant GLUT7. [^{14}C] D-Glucose uptake (30 min at 22°C) was determined 3 days after injection of *Xenopus laevis* oocytes with mRNA (20 ng). Data represent mean uptake into 10-12 individual oocytes corrected for uptake into water-injected oocytes . A curve was fit by non linear regression for a single Michaelis-Menten component with a K_m of 0.12 mM and a V_{max} of 19 pmol, oocytes^{-1}, 30 min^{-1}.

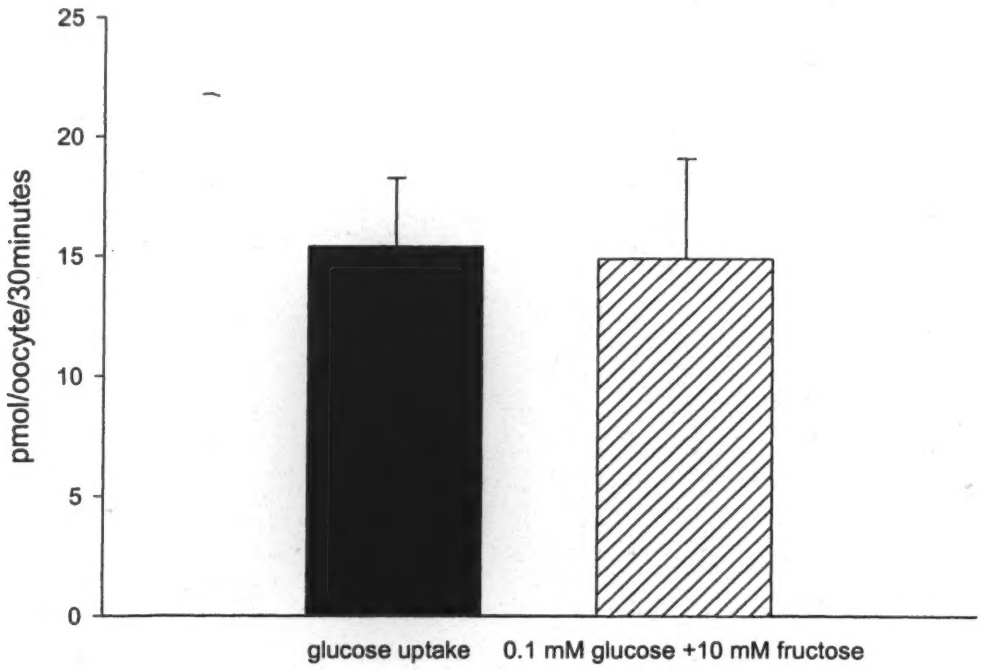

Fig. 3.14. Effect of the addition of 10 mM fructose upon I314V GLUT7 mediated D-glucose uptake. Uptake of 100μM [^{14}C] D-glucose (30 min at 22 °C) was determined in the absence or presence of 10 mM unlabeled D-fructose in 10-12 oocytes injected with I314V GLUT7 mRNA. Uptake for each condition was corrected by subtracting uptake into water-injected oocytes.

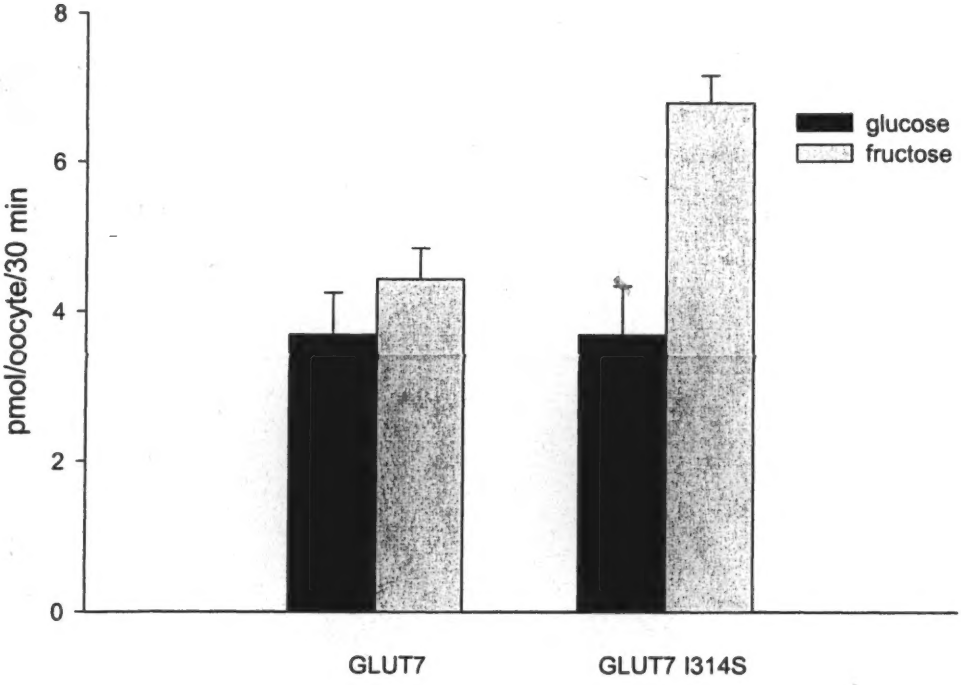

Fig. 3.15 Hexose transport mediated by human GLUT7 wild type and I314S mutant. *Xenopus laevis* oocytes were injected with hGLUT7, GLUT7 I314S mRNA or water 3 days before determinations of uptake of [^{14}C] D-glucose and [^{14}C] D-fructose (100 μM, 30 min at 22 °C). Bars represent the mean net uptake into 10-12 mRNA injected oocytes corrected for the uptake into water injected oocytes under identical conditions.

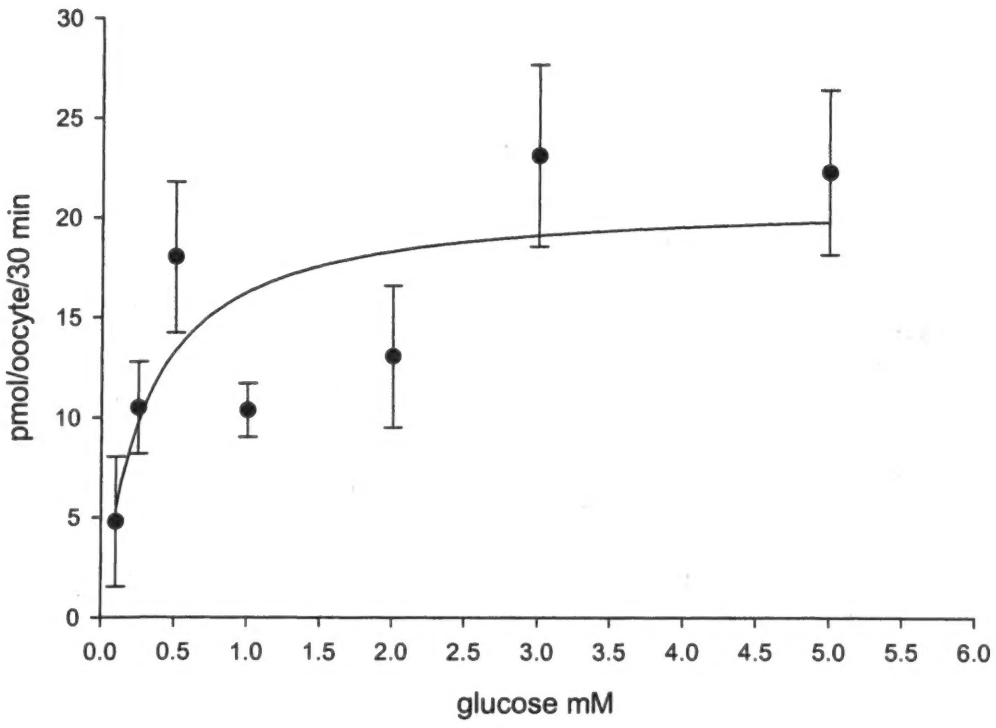

Fig. 3.16 Kinetics of glucose transport in I314S mutant GLUT7. [^{14}C] D-Glucose uptake (30 min at 22°C) was determined 4 days after injection of *Xenopus laevis* oocytes with mRNA (20 ng). Data represent mean uptake into 10-12 individual oocytes corrected for uptake into water-injected oocytes. A curve was fit by non linear regression for a single Michaelis-Menten component with a K_m of 0.29 mM and a V_{max} of 22 pmol·oocytes^{-1}·30min^{-1}.

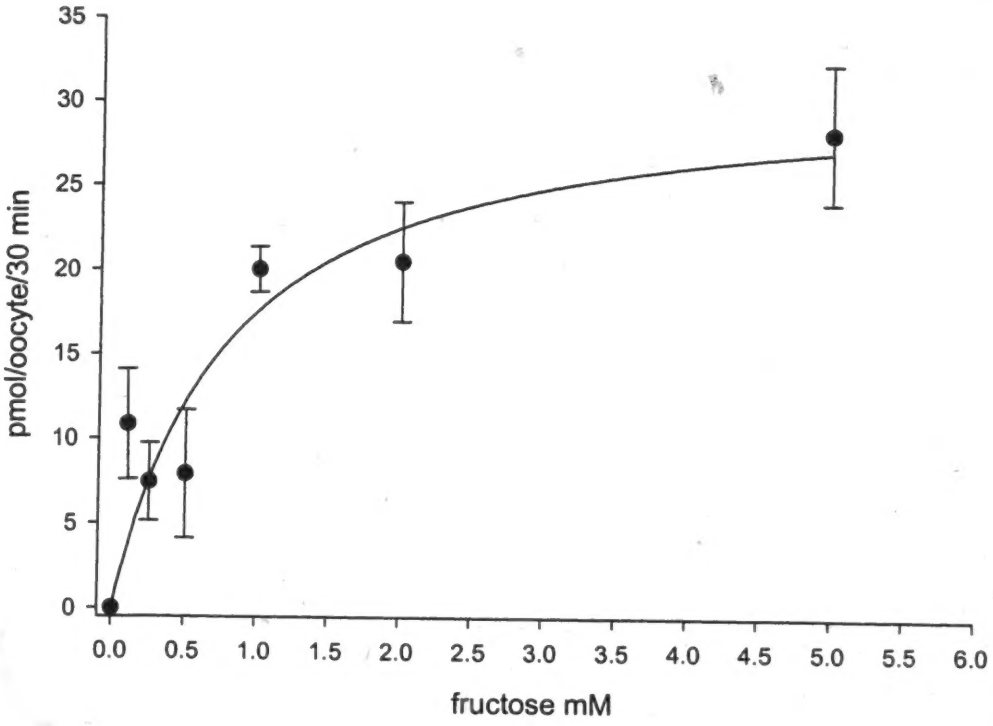

Fig. 3.17 Kinetics of fructose transport in I314S mutant GLUT7 . [^{14}C] D-Glucose uptake (30min at 22°C) was determined 4 days after injection of *Xenopus laevis* oocytes with mRNA (20ng). Data represent mean uptake into 10-12 individual oocytes corrected for uptake into water-injected oocytes. A curve was fit by non linear regression for a single Michaelis-Menten component with a K_m of 0.78 mM and a V_{max} of 31 pmol·oocytes^{-1}·30min^{-1}.

3.3 Identification of a fructose selectivity filter component in class II GLUT's .

Having shown that the Ile 314 in human GLUT7 plays a determinant role in substrate selectivity[159], I extended the analysis to the other members of the class II SLC2A family, in order to investigate the role of the Ile 314 homologous positions in the other glucose/fructose transporters. The study was started by comparing the sequence alignments of GLUTs 2, 5, 7, 9 that share at the position 316, 321, 314 and 306 an Ile residue, (Fig. 3.8). Conversely, GLUT's 1, 3, 4 have a Val residue at the homologous position 290 in GLUT1. Molecular modeling of the 3-D structure of hGLUT1[160,161] and hGLUT7[2] shows that this position faces the transporter's aqueous pore and is in the immediate proximity of the vestibule on the extracellular side of the membrane. When we modelled GLUT1 (1SUK, PDB) and GLUT7 (1GY7), using the glycerol phosphate transporter GlpT (1PW4, PDB) as a template it was found that V290 and I314 appear to face the aqueous pore, possibly forming an inter-helical hydrophobic interaction with W89 in TM2 (Fig 3.40 and 3.41). In addition, the docking results for glucose and fructose within the predicted protein structures was consistent with the binding site being just below these residues (~4 Å) and consistent with the mutagenesis, and kinetics results obtained with GLUT1 and GLUT7.

The phylogenetic arrangement of the first two classes of GLUT's (Fig. 1.3 introduction) clearly shows that GLUT2 is placed at a closer phylogenetic distance to the

class II, which explains why its physiological behavior shows substrate specificity closer to the second class than the first. This observation is furthermore strengthened by the high percentage of similarity and identity shared amongst GLUT2 and GLUT5, 7 and 9 (Fig. 3.18). Thus, GLUT's 1, 3, and 4 transport glucose, 2DOG and 3-OMG and do not transport fructose, whereas GLUTs 2, 5, 7 & 9 transport fructose and glucose but do not transport 2DOG and 3 OMG. The structural "translation" of this observation is represented by the conservation at the position 321 of the Ile and not of the Val like all the other class I members.

The hGLUT2 transports fructose with a Km of 66 mM and glucose with a similar Km. I showed that hGLUT7 has a Km of ~ 100 μM for fructose and ~ 300 μM for glucose[1]. For GLUT5 the literature presents the kinetic pattern of the fructose uptake whereas the kinetic data for glucose transport is very scarce[163]. This is why I expressed hGLUT5 in oocytes and assessed the transport of a panel of substrates (Fig. 3.19). More over, based on the observation that wild type human GLUT5 is able to transport D-glucose I determined the GLUT5 glucose uptake kinetics parameters (Fig. 3.20). From my data, the curvilinear analysis of the kinetic function revealed a Km of 650 ± 181 μM for the glucose uptake.

In regards to GLUT9, the substrate selectivity has been recently communicated[164]. However, in addition to the published data I expressed hGLUT9 in *Xenopus* oocytes and determined the uptake of a wider panel of substrates (Fig. 3.21). Given that both fructose and glucose were transported at similar rates I determined the affinity of hGLUT9 for

	GLUT 2	GLUT 5	GLUT 7	GLUT 9
GLUT 2		53% / 38%	53% / 34%	47% / 29%
GLUT 5			68% / 53%	59% / 41%
GLUT 7				59% / 41%

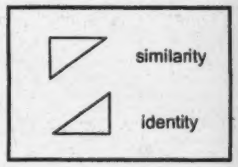

Fig. 3.18. Identity and similarity percentage among GLUT 2, 5, 7 and 9. The percentages were calculated using a BLAST engine for local alignment available at http://www.ncbi.nlm.nih.gov/blast/bl2seq/wblast2.cgi from the NCBI website.

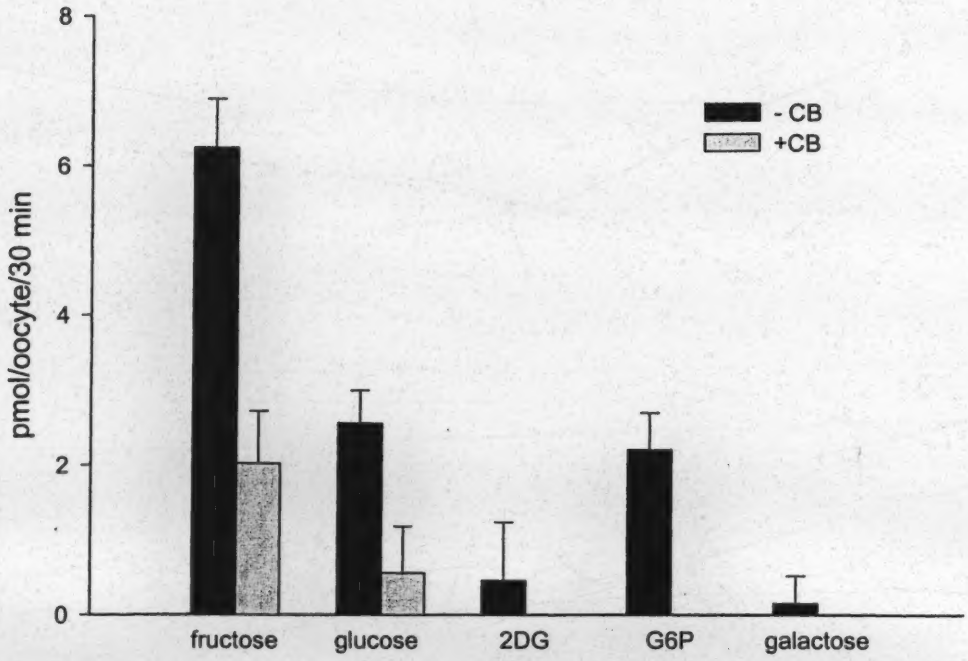

Fig. 3.19 Hexose fluxes in *Xenopus laevis* oocytes expressing human GLUT5 wild type. Stage 5-6 Xenopus oocytes were injected with GLUT 5 mRNA (20 ng) or water 3 days prior to the measurement of uptake of 100 μM radiolabeled substrates. Bars represent the mean net uptake measured over 30 minutes into 10-12 oocytes injected with mRNA and corrected for the uptake into water injected oocytes. Error bars represent SEM. (abbreviation G6P- glucose 6 (six) phosphate).

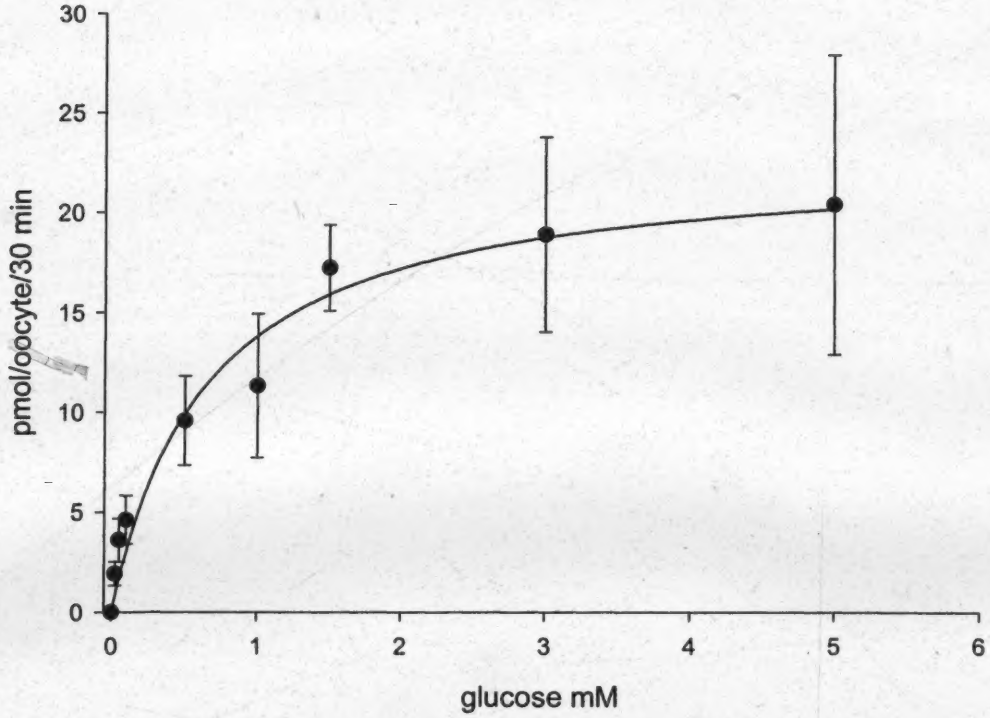

Fig. 3.20 Kinetics of glucose transport in human GLUT5. [^{14}C] D-Glucose uptake (30 min at 22°C) was determined 3 days after injection of *Xenopus laevis* oocytes with mRNA (20 ng). Data represent mean uptake into 10-12 individual oocytes corrected for uptake into water-injected oocytes. A curve was fit by non linear regression for a single Michaelis-Menten component with a K_m of 0.65 mM and a V_{max} of 22 pmol·oocytes^{-1}·30min^{-1}.

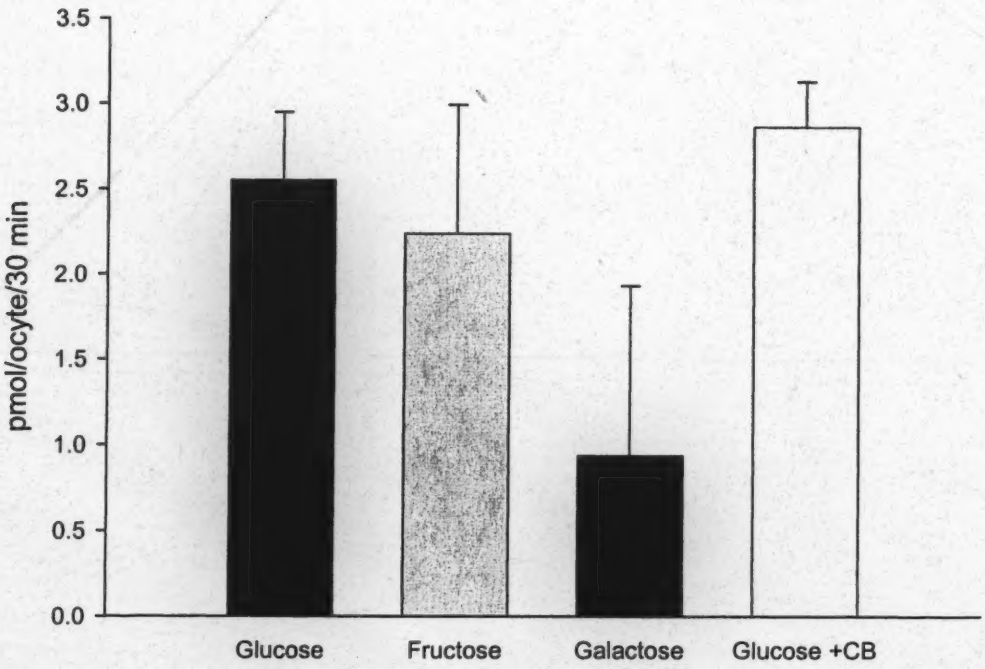

Fig. 3.21 Hexose fluxes in *Xenopus laevis* oocytes expressing human GLUT9 wild type. Stage 5-6 *Xenopus* oocytes were injected with GLUT 9 mRNA (20 ng) or water 3 days prior to the measurement of uptake of 100 μM radiolabelled substrates. Bars represent the mean net uptake measured over 30 minutes into 10-12 oocytes injected with mRNA and corrected for the uptake into water injected oocytes. Error bars represent SEM.

them by measuring the kinetic parameters that indicated a Km of ~1.1 mM for fructose and ~ 400 μM for glucose (Figs. 3.22 &3.23).

Three mutants of human GLUT's 2, 5 and 9 cDNA encoding the mutation of the Ile from position 322/296/335 to Val were constructed. After injection of the mRNA into oocytes, the subsequent expression of the wild type GLUT's 2, 5and 9 and of their mutants in the plasma membrane was assessed by immuno-cytochemistry and semi-quantitative Western-blot analysis. Both methods employed commercially manufactured antibodies raised against the C-terminal end of the wild type proteins (Figs. 3.24 & 3.25).

In all cases, the unique substitution of Val for Ile did not affect the expression of the mutant proteins in the plasma membrane of the oocytes and all the mutants exhibit a similar level of expression to the wild type proteins, as determined by the semi quantitative analysis. However, there was a remarkable difference between the translocation of glucose and fructose by the wild types GLUT's versus their mutants (Fig. 3.26-28). Comparison of the mediated uptake of fructose or glucose by the wild types/homologues mutants GLUT's clearly indicates that the fructose transport is markedly reduced by this conservative substitution. Structurally and chemically Ile differs very little from Val, both having similar hydrophobicity and size. Nonetheless, the putative hydrophobic interaction of Ile/Val with Trp89 in TM2 could dramatically influence the fructose transport process but does not interfere with the glucose permeation in GLUT7. Furthermore, I investigated whether the loss of the fructose transport reflects or not on the translocation of glucose, by comparing the kinetic

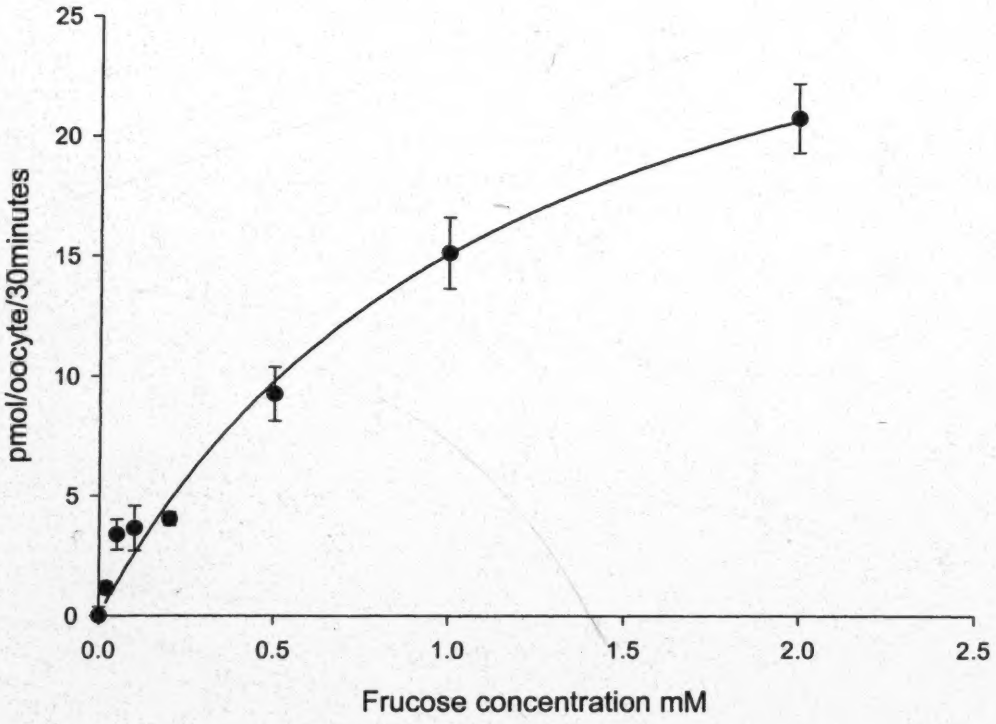

Fig. 3.22 Kinetics of fructose transport in human GLUT9. [^{14}C] D-Fructose uptake (30min at 22°C) was determined 3 days after injection of *Xenopus laevis* oocytes with mRNA (20ng). Data represent mean uptake into 10-12 individual oocytes corrected for uptake into water-injected oocytes. A curve was fit by non linear regression for a single Michaelis-Menten component with a K_m of 1.1 mM and a V_{max} of 32 pmol·oocytes^{-1}·30min^{-1}.

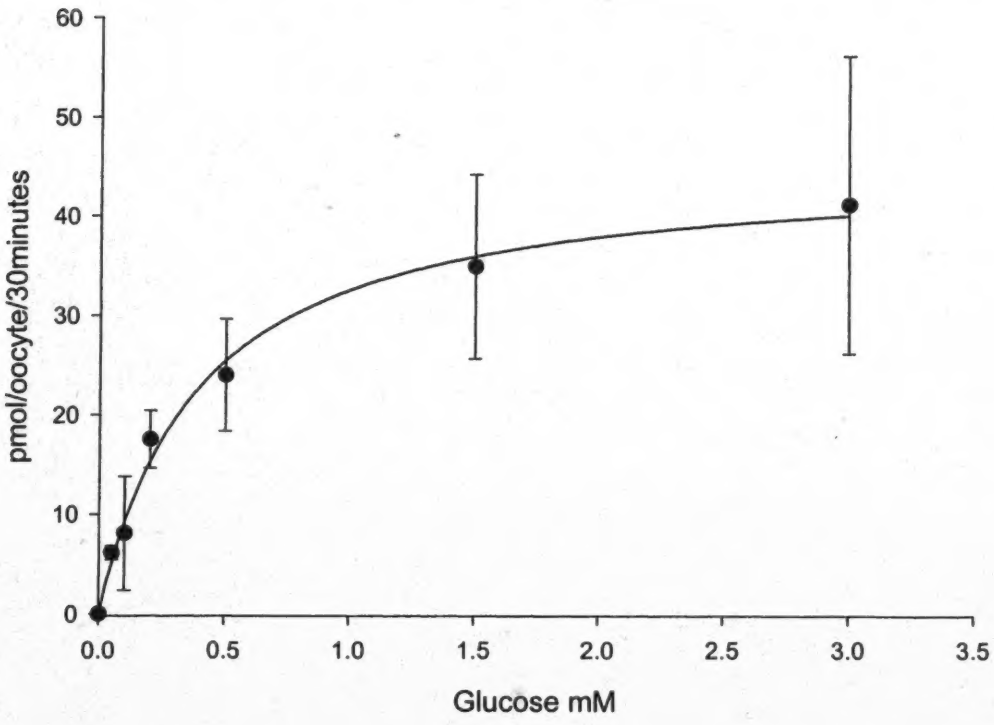

Fig. 3.23 Kinetics of glucose transport in human GLUT9 . [^{14}C] D-Glucose uptake (30min at 22°C) was determined 3 days after injection of *Xenopus laevis* oocytes with mRNA (20ng). Data represent mean uptake into 10-12 individual oocytes corrected for uptake into water-injected oocytes. A curve was fit by non linear regression for a single Michaelis-Menten component with a K_m of 0.40 mM and a V_{max} of 45 pmol, oocytes^{-1}, 30min^{-1}.

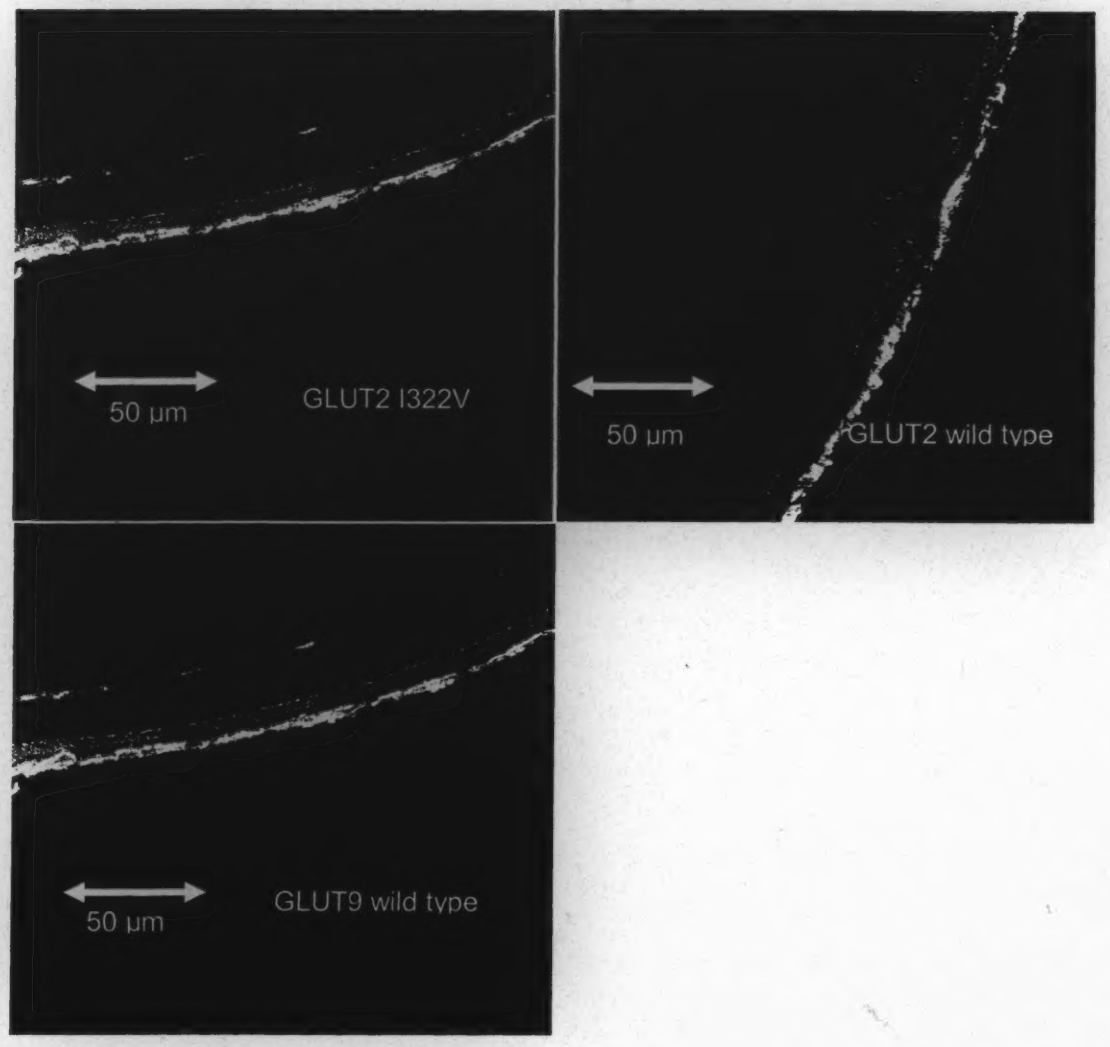

Fig. 3.24 Expression of wild type and mutant GLUT transporters in *Xenopus* oocytes Stage 5 *Xenopus* oocytes expressing wild type or mutant GLUT 2, 9 and GLUT I322V mutant mRNA (20 ng), or injected with water were frozen, sectioned and stained with specific IgG followed by fluorescin-conjugated goat anti rabbit IgG. Sections were visualized with a Zeiss LSM510 confocal microscope.

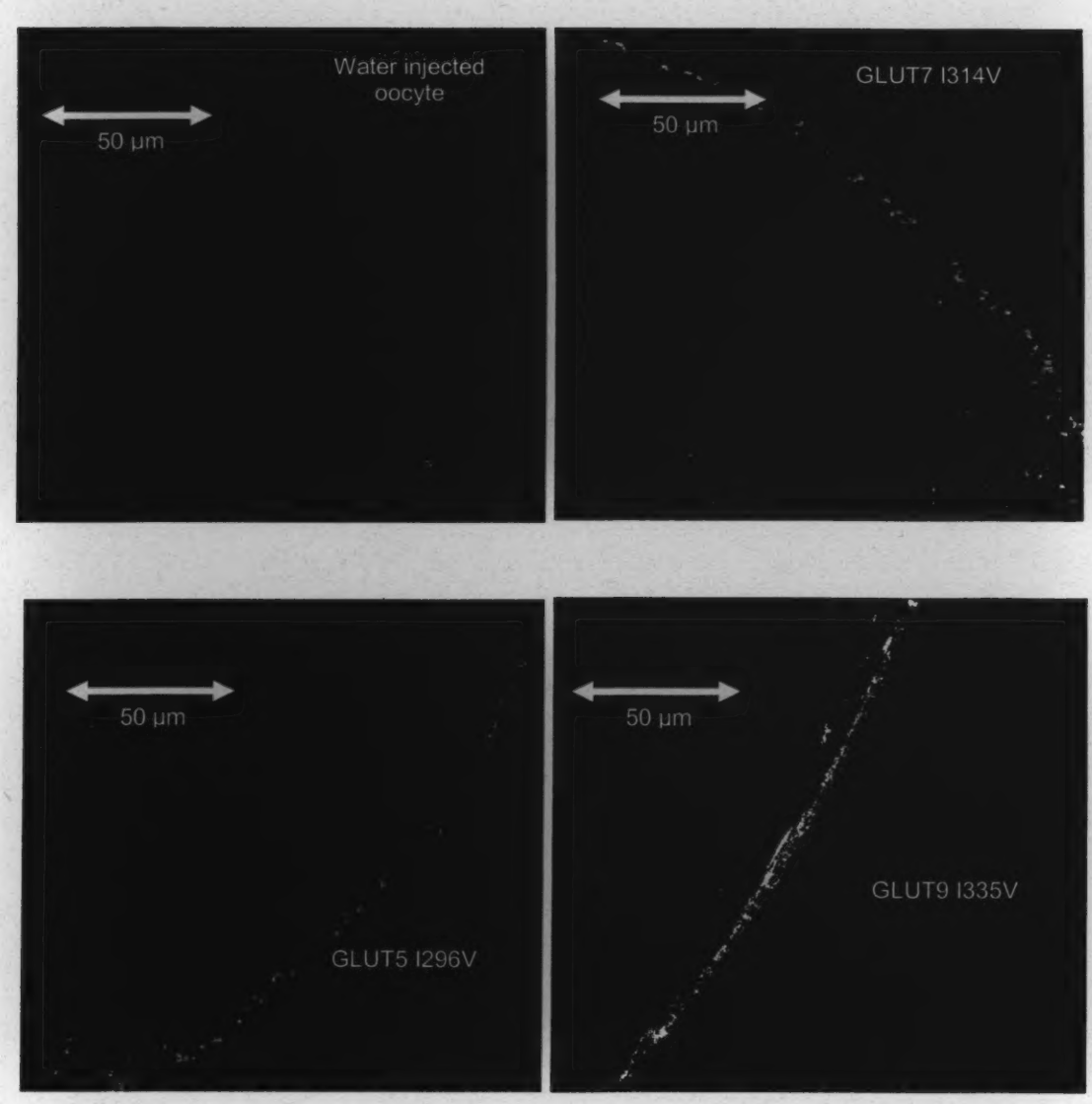

Fig. 3.25 Expression of wild type and mutant GLUT transporters in *Xenopus* oocytes. Three days after injection with wild type or mutant GLUT mRNA, oocytes were used to prepare plasma membranes for GLUT protein visualization using indirect immunofluorescence laser confocal microscopy. Stage 5-6 *Xenopus* oocytes expressing wild type or mutant GLUT 2, 5, 7 and 9 mRNA (20 ng), or injected with water were frozen, sectioned and stained with specific IgG followed by fluorescein-conjugated goat anti rabbit IgG. Sections were visualized with a Zeiss LSM510 confocal microscope at 40x/immersion magnification.

Fig. 3.26 Glucose and fructose transport mediated by hGLUT2 wild type and the I322V mutant. Stage 5-6 *Xenopus* oocytes were injected with hGLUT2 or GLUT2 I316V mRNA (20 ng) or water 3 days before determinations of uptake of [^{14}C] D-fructose or D-glucose (100 μM). Bars represent mean net uptake (30 min at 22 °C) into 10-12 oocytes injected with mRNA.

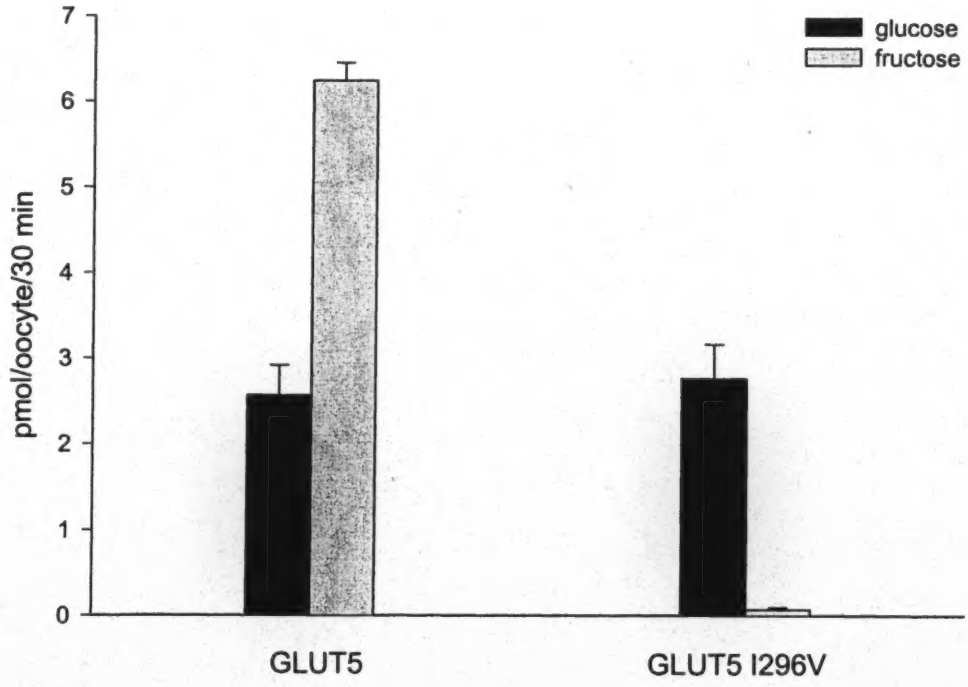

Fig. 3.27 Glucose and fructose transport mediated by hGLUT5 wild type and the I296V mutant. Stage 5-6 *Xenopus* oocytes were injected with hGLUT5 or GLUT5 I296V mRNA (20 ng) or water 3 days before determinations of uptake of [^{14}C] D-fructose or D-glucose (100 μM). Bars represent mean net uptake (30 min at 22 °C) into 10-12 oocytes injected with mRNA corrected for the uptake into water injected oocytes under identical conditions.

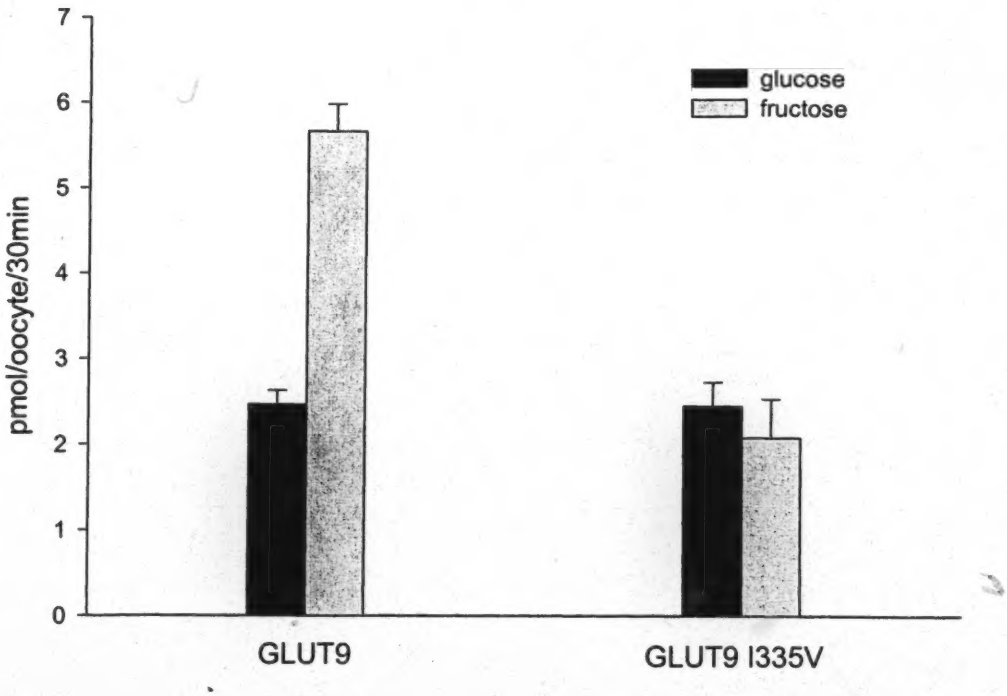

Fig. 3.28 Glucose and fructose transport mediated by hGLUT9 wild type and the I335V mutant. Stage 5-6 *Xenopus* oocytes were injected with hGLUT9 or GLUT9 I335V mRNA (20 ng) or water 3 days before determinations of uptake of [^{14}C] D-fructose or D-glucose (100 μM). Bars represent mean net uptake (30 min at 22 °C) into 10-12 oocytes injected with mRNA corrected for the uptake into water injected oocytes under identical conditions.

characteristics of glucose uptake in all the mutants. The uptake of glucose in GLUT5 I296V was determined over a concentration range 0.025-5 mM and, when corrected for the uptake into water injected oocytes, exhibited Michaelis-Menten kinetics with a Km of 360 ± 102 μM similar with one expressed by the wild type, (Fig. 3.29)

I have previously shown that the mutation of the Ile 322 to Val in the human GLUT2 produces the loss of fructose uptake while the glucose uptake remains untouched. Analysis of the mediated glucose uptake by the GLUT2 I322V mutant revealed a Michaelis-Menten kinetics with a Km of ~ 1mM which appears to represent a somewhat higher affinity compared to that of the wild type GLUT2 (Fig. 3.30).

Based on the observation that wild type hGLUT9 is a high affinity glucose transporter I tested if the mutation of the Ile 335 to Val would produce an effect on glucose transport as it did on that of fructose. Therefore, I determined the glucose uptake kinetic parameters for GLUT9 I335V mutant, which revealed a Km of ~64 μM, which is basically very similar to that of wild type (Fig. 3.31).

3.4 Importance of the amphipathic NXI/V motif in substrate selectivity.

Unlike the other members of class II, the hGLUT11 sequence contains at the homologous position to GLUT7's I314 a valine residue. Interestingly, the two residues, adjacent to V299 are not conserved in hGLUT11 *c.f.* its orthologs. The fructose transporting members of class II and GLUT2 have an NAI and an NGI motif at the equivalent position. The remaining members of class I present an NAV motif in the same region. In contrast the motif in hGLUT11 is DSV and represents a very interesting

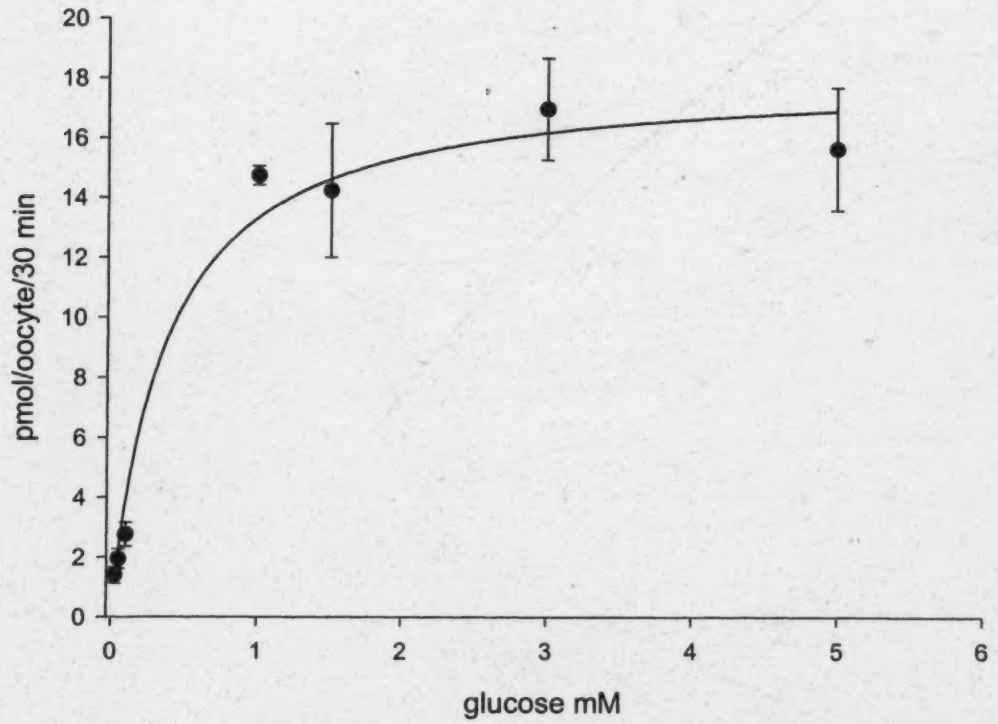

Fig. 3.29 Kinetics of glucose transport in GLUT5 I296V mutant . [^{14}C] D-Glucose uptake (30 min at 22°C) was determined 3 days after injection of *Xenopus laevis* oocytes with mRNA (20 ng). Data represent mean uptake into 10-12 individual oocytes corrected for uptake into water-injected oocytes. A curve was fitted by non-linear regression for a single Michaelis-Menten component with a K_m of 0.36 mM and a V_{max} of 18 pmol·oocytes^{-1}·30 min^{-1}.

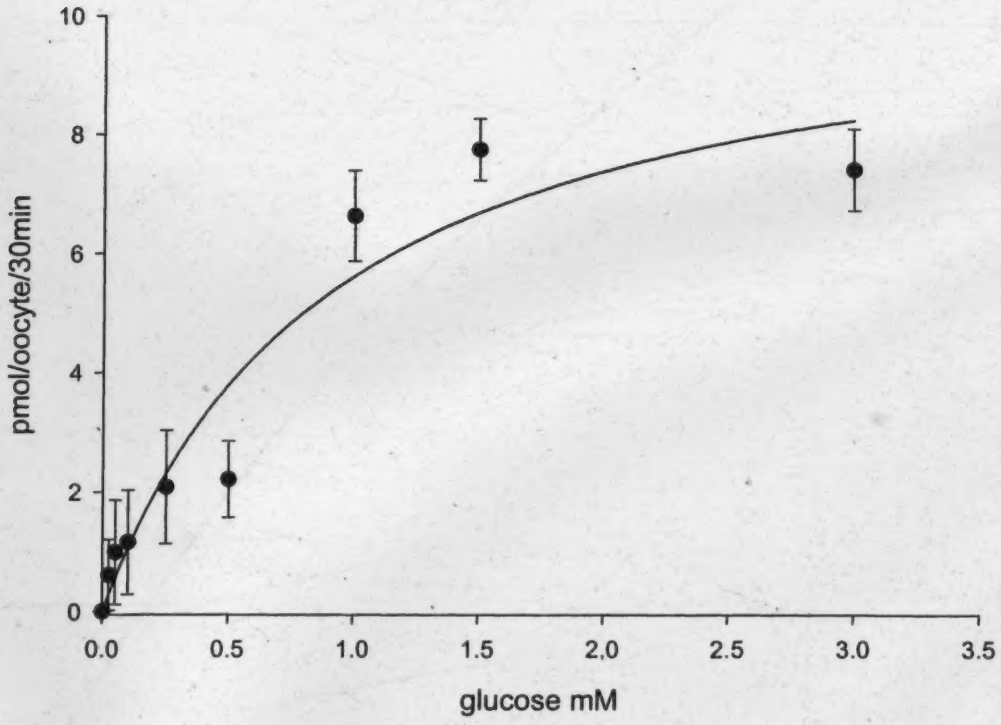

Fig. 3.30 Kinetics of glucose transport in GLUT2 I322V mutant . [^{14}C] D-Glucose uptake (30min at 22°C) was determined 3 days after injection of *Xenopus laevis* oocytes with mRNA (20ng). Data represent mean uptake into 10-12 individual oocytes corrected for uptake into water-injected oocytes. A curve was fit by non linear regression for a single Michaelis-Menten component with a K_m of 0.92 mM and a V_{max} of 10pmol·oocytes^{-1}· 30min^{-1}.

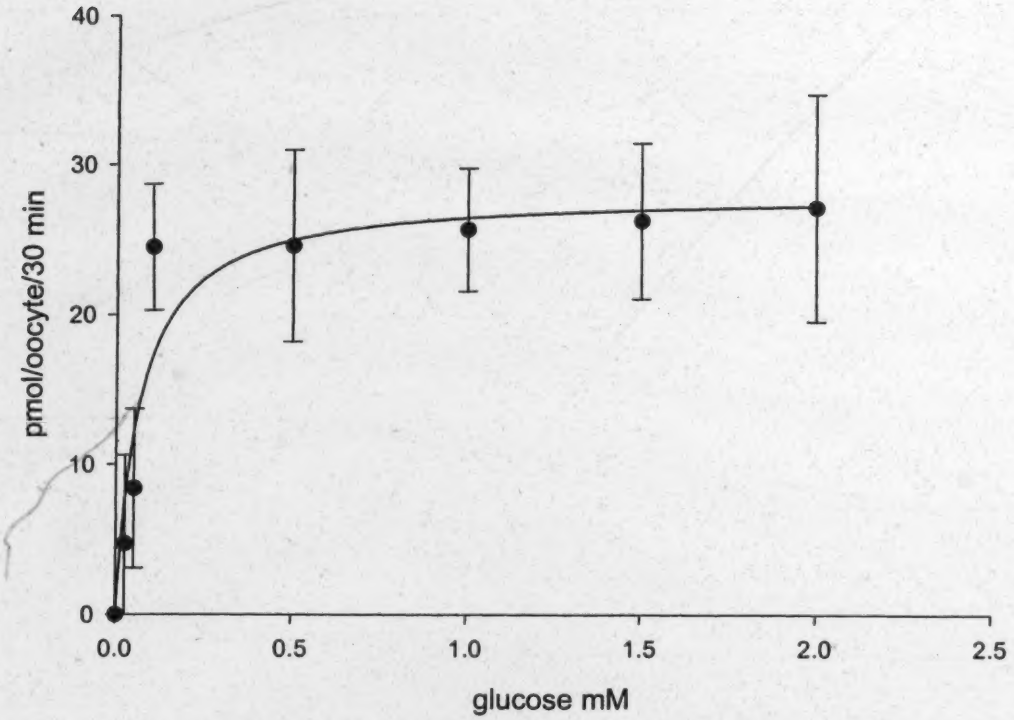

Fig. 3.31 Kinetics of glucose transport in GLUT9 I335V mutant. [^{14}C] D-Glucose uptake (30 min at 22°C) was determined 3 days after injection of *Xenopus laevis* oocytes with mRNA (20 ng). Data represent mean uptake into 10-12 individual oocytes corrected for uptake into water-injected oocytes. A curve was fit by non linear regression for a single Michaelis-Menten component with a K_m of 0.640 mM and a V_{max} of 28 pmol·oocytes^{-1}· 30min^{-1}.

functional and structural "intermediary link "between the first two phylogenetic classes. As can be seen in figure 3.32 (class I and II alignments) this conserved substitution is located at the exofacial border of the TM7 where I showed the putative substrate selectivity filter in the fructose transporting members is located. All the other members of the class I and II GLUT's contain two very similar motifs, NAV (class I) and NAI in class II which correlates with their functional properties regarding the transport of fructose. This finding was of particular interest based on the fact that the substrate specificity of all the hGLUT11 isoforms had the same pattern of fructose-glucose transporter as the class II GLUT's, (Fig. 3.33). The kinetic parameters for both glucose and fructose were determined using a wide range of concentrations as displayed in figures 3.34 & 3.35.

Hence, hGLUT11 maintains the same physiologic pattern that characterizes all the other glucose/fructose transporters, being a relatively high affinity transporter. The calculated Km for glucose was ~ 108 μM, and for fructose the Km was ~116 μM. Not only does the substrate specificity correlate with the phylogenetic relationship but the kinetic behaviour does it as well. As can be seen in figures 3.36 & 3.37, GLUT11 is defined as a high affinity glucose/fructose transporter, which is consistent with the behaviour of GLUT 5, 7 and 9.

Giving the essential role of the GLUT7's Ile 314 (and the homologous positions in GLUT 2, 5 and 9) the conserved substitution of the Ile with Val in GLUT11 created an interesting dilemma.

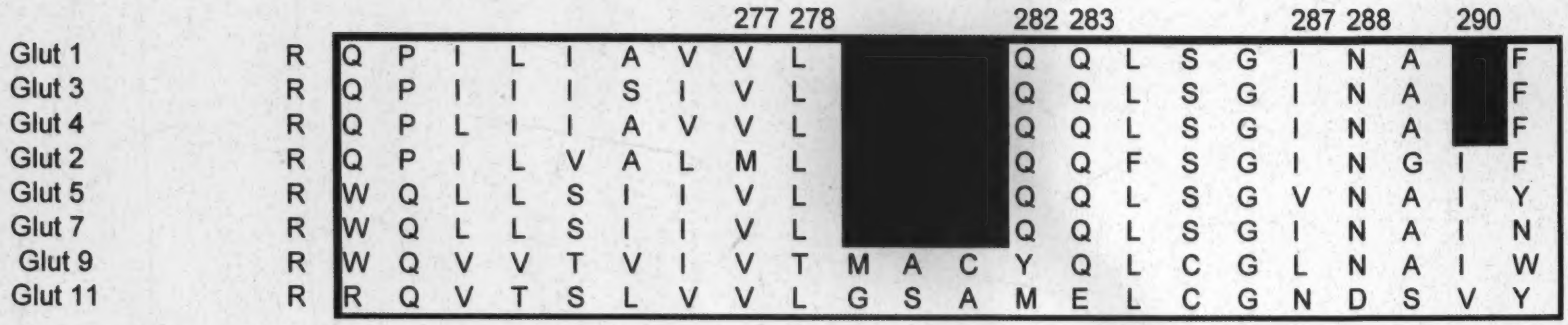
277 278
282 283
287 288
290
Glut 1 R Q P I L I A V V L Q Q L S G I N A F
Glut 3 R Q P I I I S I V L Q Q L S G I N A F
Glut 4 R Q P L I I A V V L Q Q L S G I N A F
Glut 2 R Q P I L V A L M L Q Q F S G I N G I F
Glut 5 R W Q L L S I I V L Q Q L S G V N A I Y
Glut 7 R W Q L L S I I V L Q Q L S G I N A I N
Glut 9 R W Q V V T V I V T M A C Y Q L C G L N A I W
Glut 11 R R Q V T S L V V L G S A M E L C G N D S V Y

Fig. 3.32. Class I and II alignments. Comparison of GLUTs class II memebers primary sequences to the class I members ones in the TM7 region . Sequences were aligned using Clustal X software and written from N to C-termini. Based on the putative membrane topology of this helix, its C-terminus end faces the extracellular side of the membrane (see figure1).

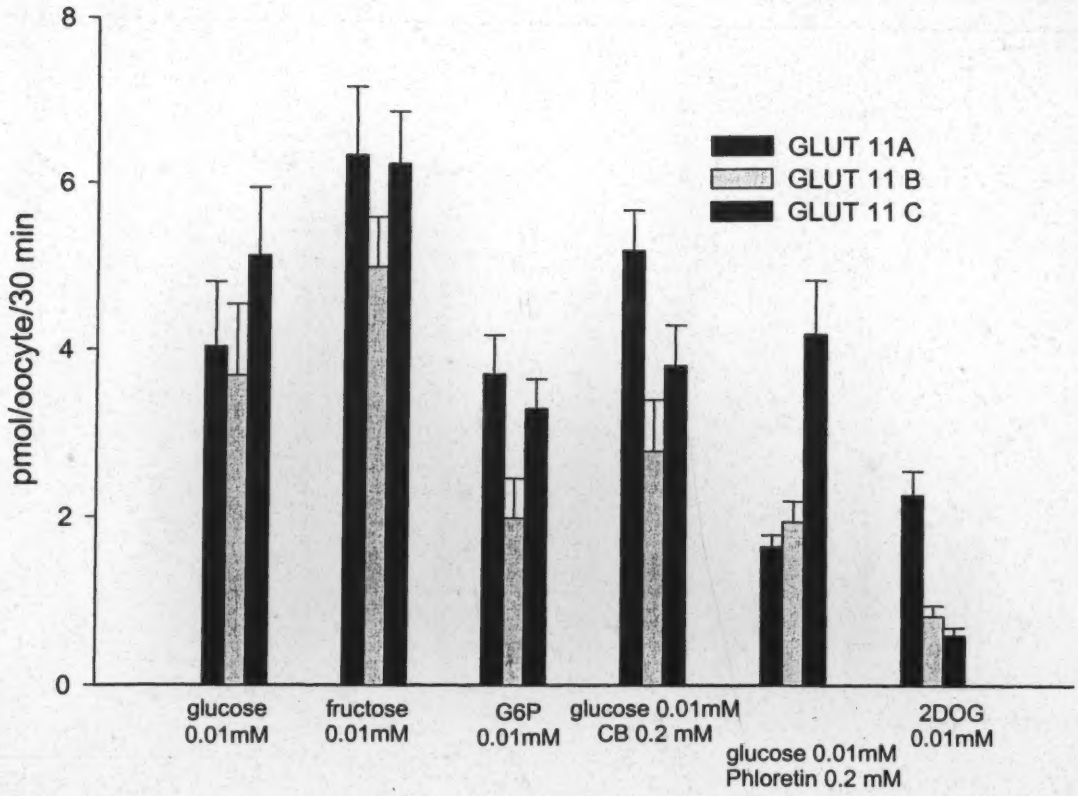

Fig 3.33 GLUT11 isoforms A, B and C mediated hexose fluxes in *Xenopus* oocytes. Oocytes were injected with GLUT11 isoforms mRNA or water 4 days before the measurement of uptake of radiolabelled substrates (100 μM). Bars represent uptake measured over 30 min into 8–10 oocytes injected with mRNA (hatched bars), water (open bars), and net uptake (filled bars). Error bars represent the standard error of the mean.

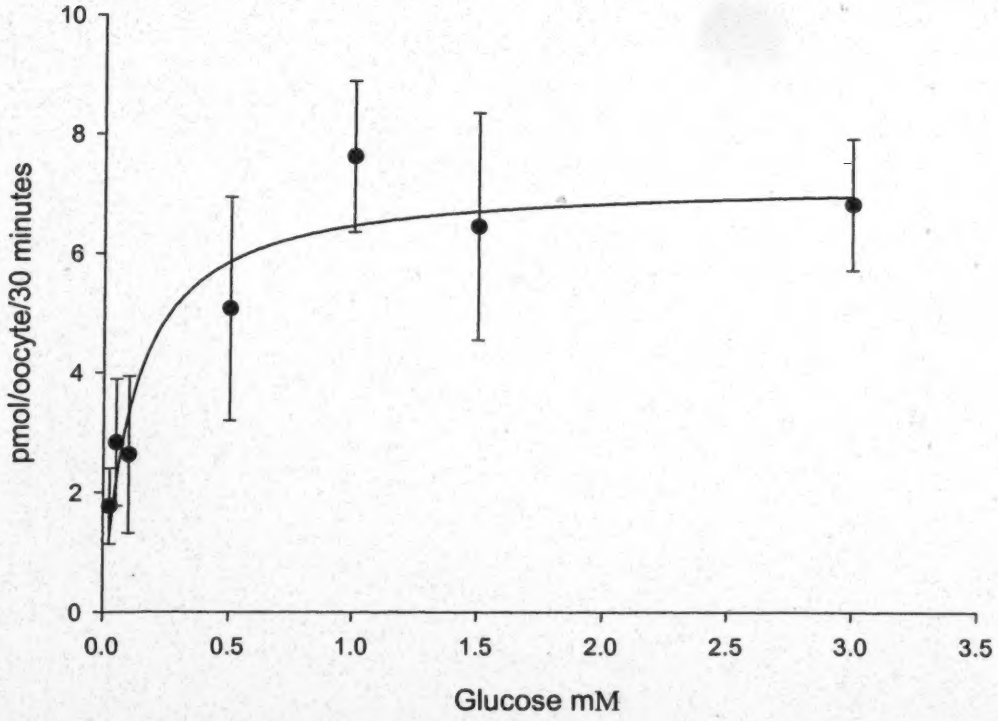

Fig. 3.34 Kinetics of glucose transport in GLUT11 wild type. [^{14}C] D-Glucose uptake (30min at 22°C) was determined 3 days after injection of *Xenopus laevis* oocytes with mRNA (20ng). Data represent mean uptake into 10-12 individual oocytes corrected for uptake into water-injected oocytes. A curve was fit by non-linear regression for a single Michaelis-Menten component with a K_m of 0.17 mM and a V_{max} of 7.2 pmol·oocytes^{-1}·30min^{-1}.

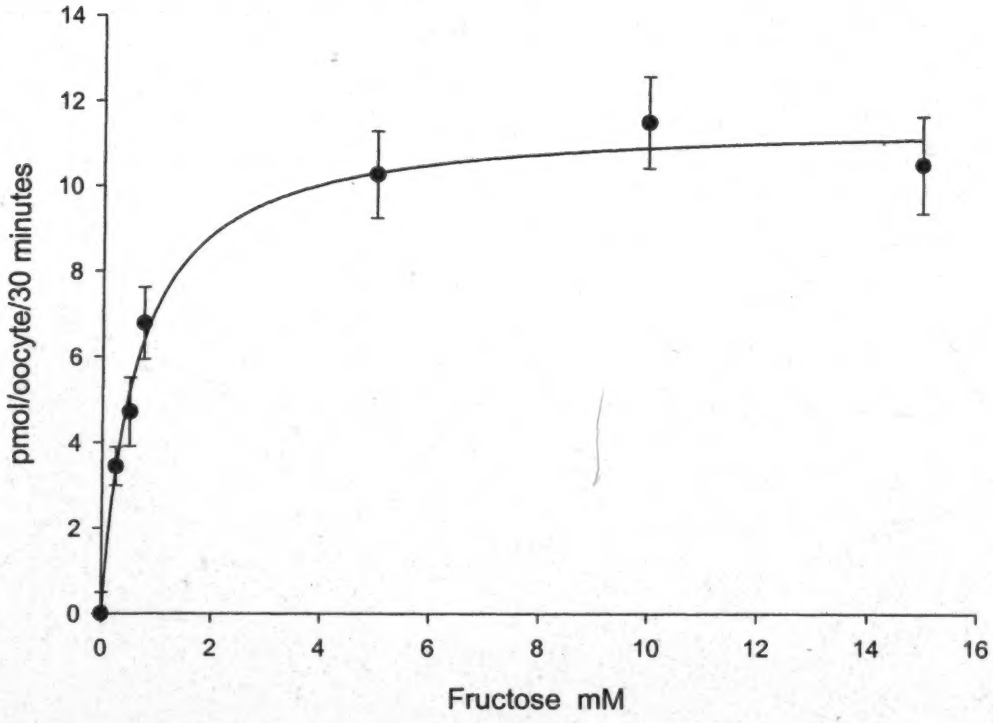

Fig. 3.35 Kinetics of fructose transport in human GLUT11 wild type. [^{14}C] D-Fructose uptake (30 min at 22°C) was determined 3 days after injection of *Xenopus laevis* oocytes with mRNA (20 ng). Data represent mean uptake into 10-12 individual oocytes corrected for uptake into water-injected oocytes. A curve was fit by non linear regression for a single Michaelis-Menten component with a K_m of 0.06 mM and a V_{max} of 11 pmol·oocytes^{-1}·30 min^{-1}.

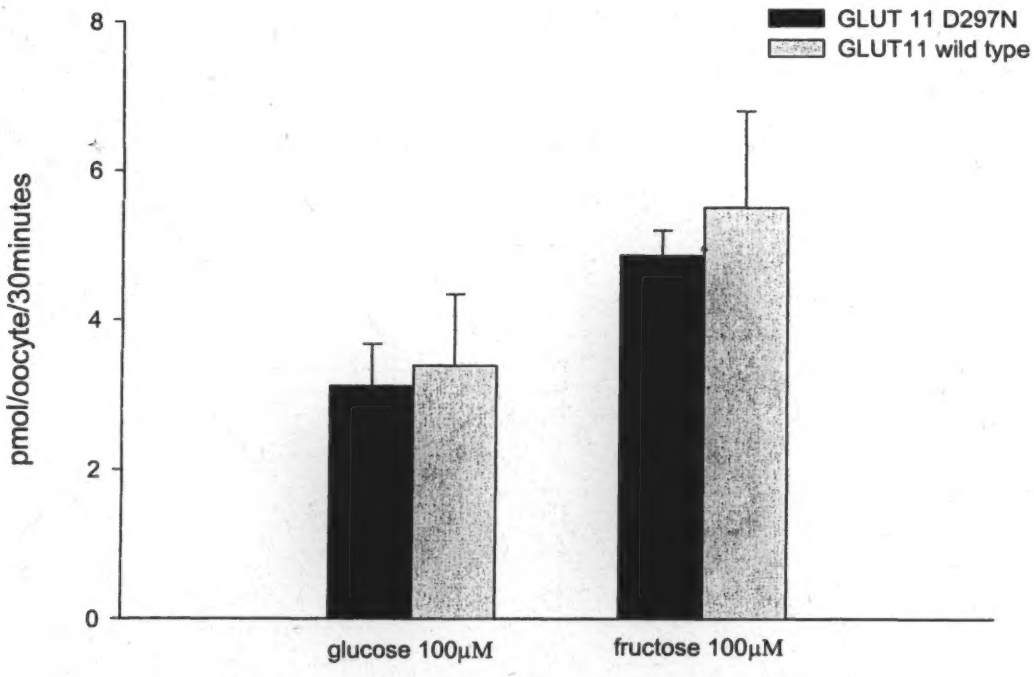

Fig. 3.36 Glucose and fructose transport mediated by GLUT11 wild type and D297N mutant. Stage 5-6 *Xenopus* oocytes were injected with hGLUT11 or GLUT11 D297N mRNA (20 ng) or water 3 days before determinations of uptake of [^{14}C] D-fructose or D-glucose (100 μM). Bars represent mean net uptake (30 min at 22 °C) into 10-12 oocytes injected with mRNA corrected for the uptake into water injected oocytes under identical conditions.

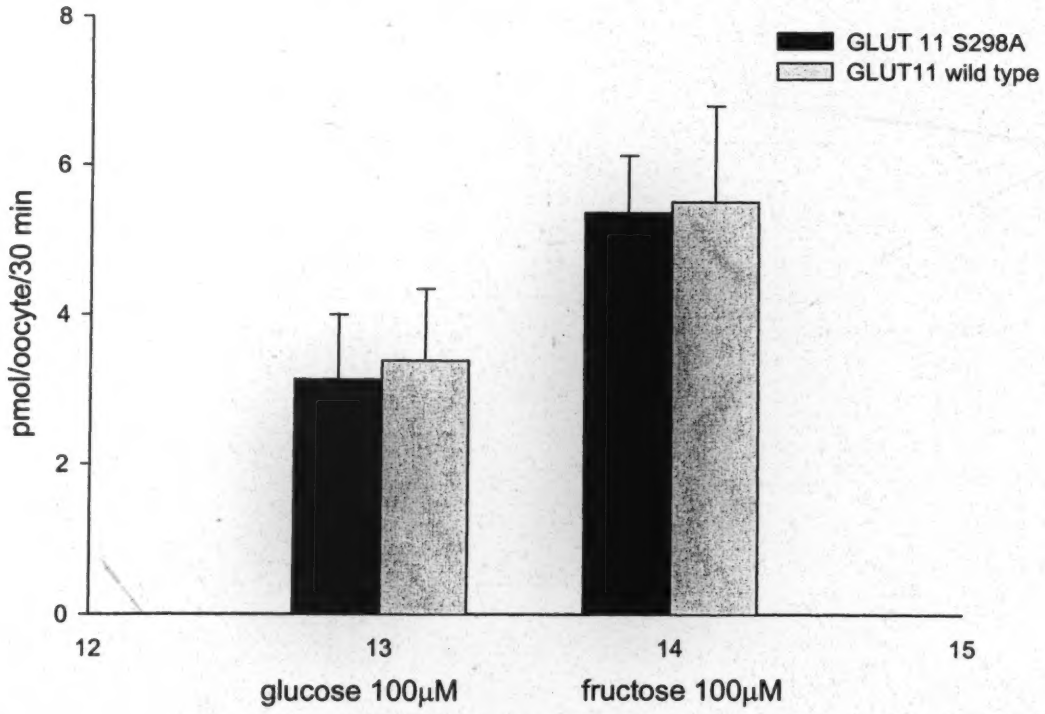

Fig. 3.37 Glucose and fructose transport mediated by GLUT11 wild type and S298A mutant. Stage 5-6 *Xenopus* oocytes were injected with hGLUT11 or GLUT11 S298A mRNA (20ng) or water 3 days before determinations of uptake of [^{14}C] D-fructose or D-glucose (100 μM). Bars represent mean net uptake (30 min at 22 °C) into 10-12 oocytes injected with mRNA corrected for the uptake into water injected oocytes under identical conditions.

To identify the potential role of Val 299 in the functionality of hGLUT11[1] the role of the neighbouring residues, Asp297, Ser298 were also investigated. Individual mutations of the D297 to Asn and S298 to Ala were performed and the substrate specificity of the mutants was determined. As seen in figures 3.36 and 3.37 the fructose and glucose transporting properties remained unchanged when those two mutations were made individually. Interestingly, when the unique mutation of V299 to Ile was made, both glucose and fructose uptakes were very significantly reduced compared to the levels recorded in the wild type, as shown in figure 3.38. Next the double mutant D297N S298A was investigated, which resulted in a similar glucose and fructose uptake to that of the wild type (Fig. 3.39). However, the triple mutant D297N S298A V299I almost completely returned the uptake of both glucose and fructose to the levels of the wild type.

[1] Portions of this subchapter have been previously published and are reproduced with permission from : Scheepers A, Schmidt S, **Manolescu A**, Cheeseman CI, Bell A, Zahn C, Joost HG, Schurmann A. *Characterization of the human SLC2A11 (GLUT11) gene: alternative promoter usage, function, expression, and subcellular distribution of three isoforms, and lack of mouse orthologue.* Mol Membr Biol. 2005;22(4):339-51.

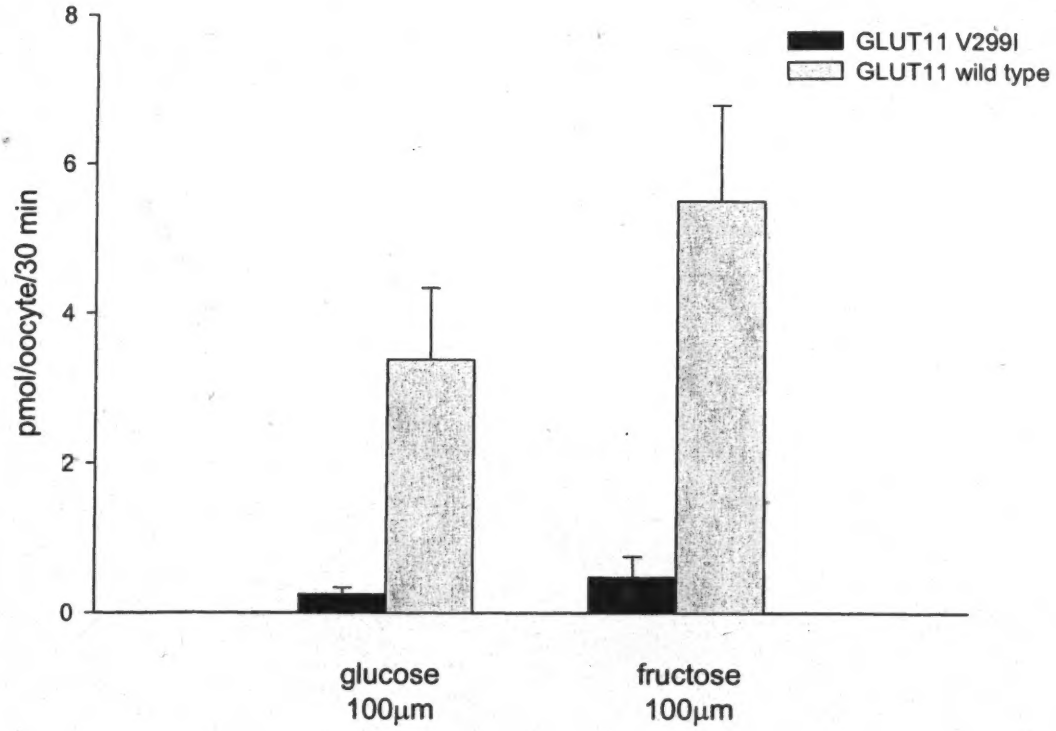

Fig. 3.38 Glucose and fructose transport mediated by GLUT11 wild type and V299I mutant. Stage 5-6 *Xenopus* oocytes were injected with hGLUT11 or GLUT11 V299I mRNA (20 ng) or water 3 days before determinations of uptake of [^{14}C] D-fructose or D-glucose (100 μM). Bars represent mean net uptake (30 min at 22 °C) into 10-12 oocytes injected with mRNA corrected for the uptake into water injected oocytes under identical conditions.

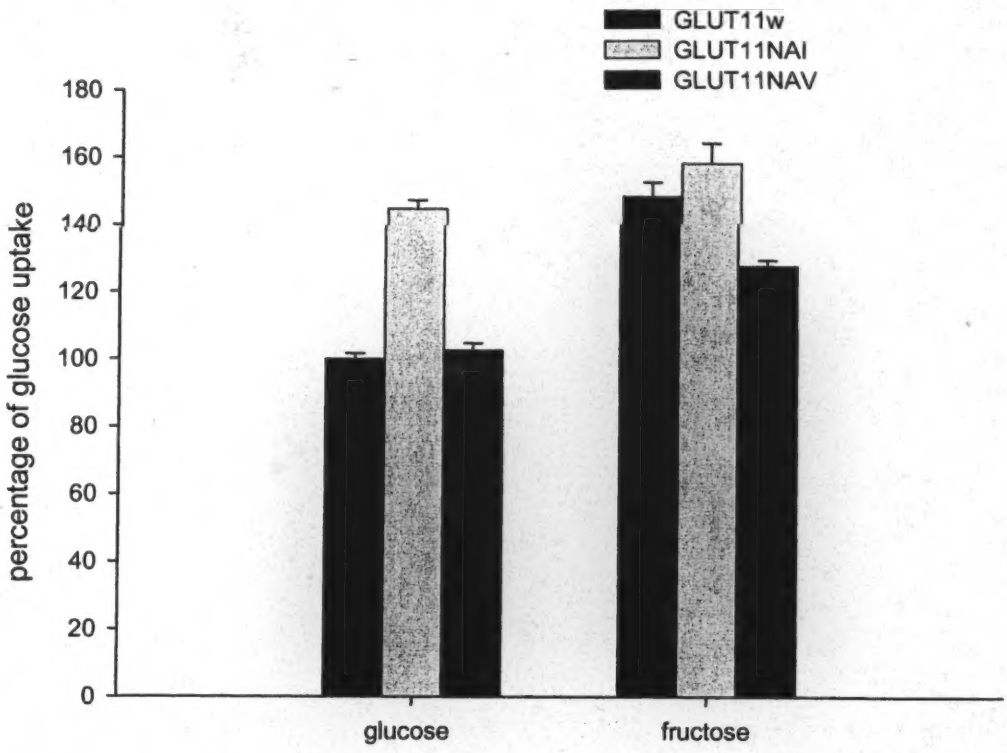

Fig. 3.39 Glucose and fructose transport mediated by GLUT11 wild type and NAI and NAV mutants. Stage 5-6 *Xenopus* oocytes were injected with hGLUT11, NAI or NAV mutants mRNA (20 ng) or water 3 days before determinations of uptake of [^{14}C] D-fructose or D-glucose (100 μM). Bars represent percentage of GLUT11 wild type glucose uptake (30 min at 22 °C) into 10-12 oocytes injected with mRNA corrected for the uptake into water injected oocytes under identical conditions.

3.5 Three-dimensional molecular modeling of the fructose selectivity filter.

In collaboration with Drs. Salas-Burgos and Fischbarg, I modelled the human GLUT7 protein. The modeling results predicted that the Ile 314 residue faces the pore and is in close proximity to the Trp89 residue from the adjacent TM2, (Fig. 3.40 and 3.41).

This 3-D model strongly supports my experimental data and in the same time is consistent with the latest putative models of the GLUT1 protein[107, 161]. This structural conservation in the folding pattern of the class II GLUT's emphasizes once more the importance of the Ile 314 and its homologous positions as a part of an highly amphipathic region of TM7 that plays a critical role within the exofacial side of the GLUT's aqueous pore.

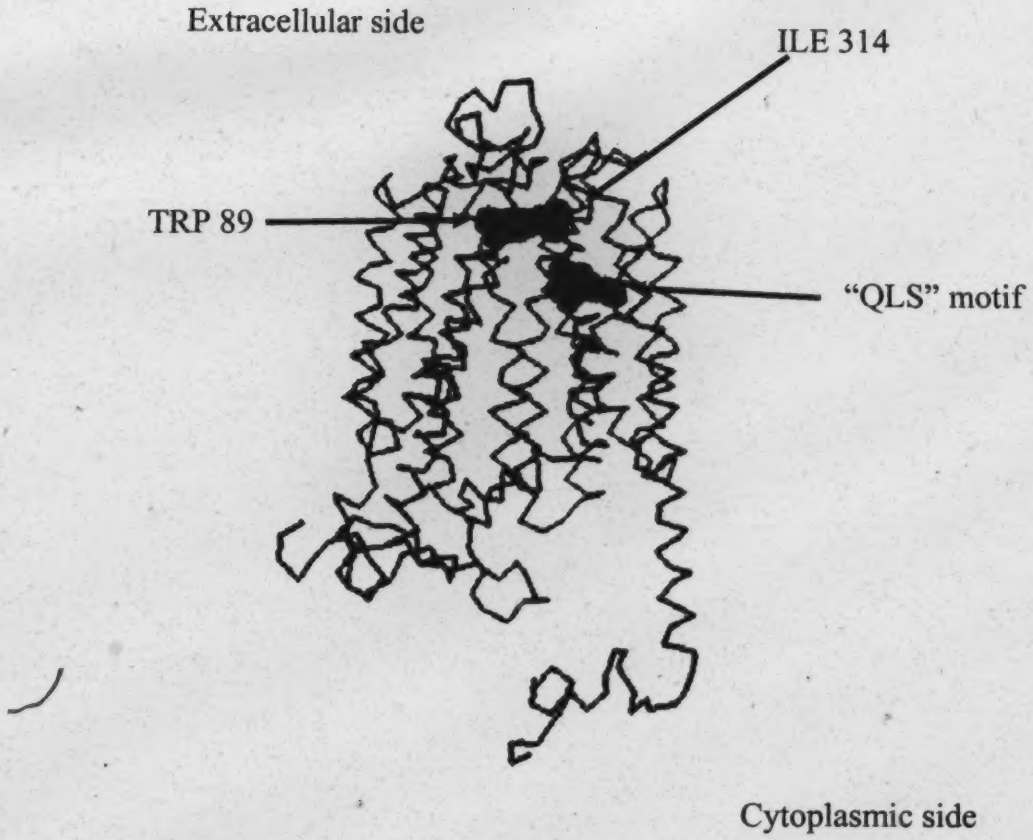

Fig. 3.40 Putative 3D structural model of hGLUT7 protein. The primary amino acid sequence for hGLUT7 was analyzed using the GLUT1 1SUK model coordinates. This template structure was subject to 10 ns molecular dynamics simulation in water/octane and ions, using the force field OPLS. This run was NPT, with Berendsen coupling for temperature and pressure. All bonds were constrained using the LINCS algorithm for the protein and SETTLE for water in the GROMACS suite. The resulting structure was then built and refined with Modeller.

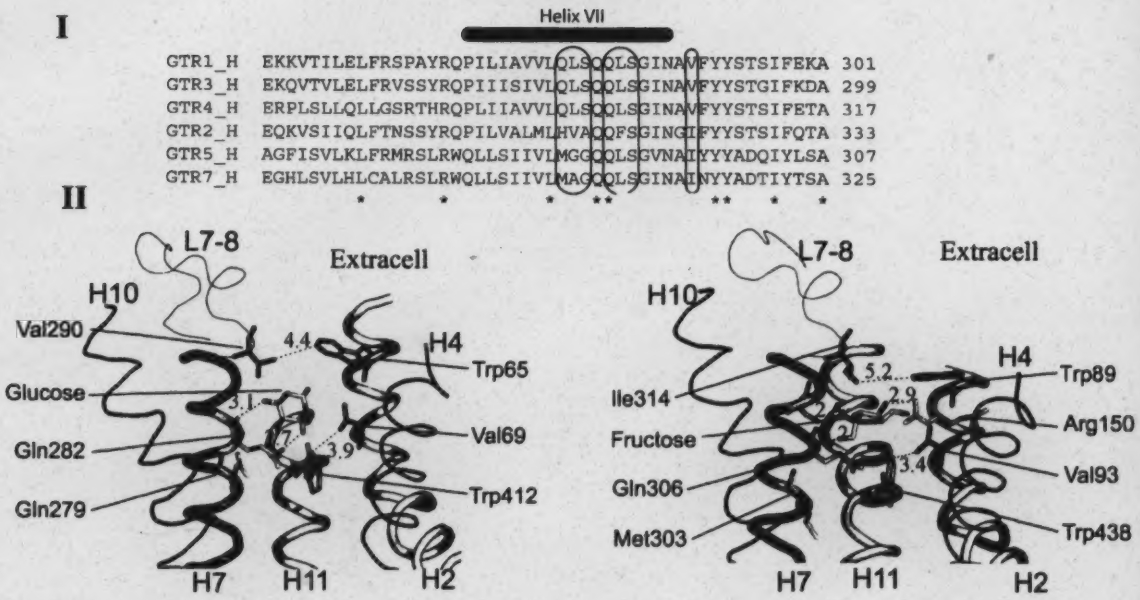

Fig. 3.41 I. Glucose in the GLUT1 transport channel. β-D-glucose is shown interacting with Gln282. The green residues mark hydrogen-bonding sites on the channel and the cluster Val169/Trp412 is represented in red and orange, respectively. Distances are given in Å. **II. Fructose in the GLUT7 transport channel.** Fructose forms hydrogen bonds with Gln306 and Arg150. The images in panel II were done with pymol and the helix colors are consistent with those in the description of the original helix packing.

Chapter 4.

Discussion.

4.1 Cloning and characterization of human GLUT7

The sequence alignment of GLUT5 and 7 shows that the two human proteins are 68% similar and 53% identical. GLUT7 appears to contain many of the so called "signature sequences" that are believed to be typical of the GLUT family of proteins. The proline-containing motif (PESPR) between transmembrane segments (TMs) 6 and 7 is present in both GLUT5 and 7. There are two QLS motifs within TM7 of GLUT1, 3, and 4, and the one equivalent to position 279–281 of GLUT1 has been suggested to be part of the glucose selectivity binding site[165]. This first motif is missing from GLUT2 (replaced with HVA), which is a low-affinity glucose and fructose transporter, and from the fructose transporter GLUT5 (replaced with MGG). The second QLS motif present in TM7 is found at positions 283–285 in GLUT1 as well as in equivalent positions in 3, 4, and 5 and is also present in GLUT7. It has previously been proposed that QLS 279–281 forms a high-affinity bond with the C-1 hydroxyl on glucose and is part of the exofacial recognition site. Additionally, replacement of the HVA by QLS motif in GLUT2 largely removed its ability to transport fructose, and the replacement of QLS by HVA motif into GLUT3 equivalent region induced low-affinity fructose transport[165]. However, the absence of either HVA or QLS at this site in GLUT7, which binds both glucose and fructose with very high affinity (K_m < 1.0 mM), would suggest that other residues that line the pore must also be involved in the recognition of substrates.

It is of interest that although GLUT1 contains two tryptophan residues at 388 and 412, both GLUT5 and 7 have only the one tryptophan at the position equivalent to 412.

This "di-tryptophan motif" has been shown to be involved in the CB binding site. Although GLUT5 has previously been shown to be insensitive to this fungal inhibitor we can now report that GLUT7 is also not inhibited by CB. This additional finding certainly lends support for the role of these two tryptophans in the binding of CB to GLUT proteins. Similarly, just as GLUT5 is insensitive to inhibition by phloretin[166], so is GLUT7, which sets these class II transporters apart from those in class I.

The vast majority of membrane proteins are glycosylated, and GLUT7 appears to be no exception given that the bands detected on the Western blots are relatively diffuse, typical of glycosylated proteins. The GLUT proteins belonging to classes I and II all appear to be glycosylated on the first putative extracellular loop found between the TMs 1 and 2. In contrast, preliminary data for class III indicates glycosylation on loop 9 between TMs 9 and 10[167], although the functional significance of this is not known. Examination of the primary sequence of GLUT7 indicates that within the first putative extracellular loop there are three asparagine residues that could provide a site for N-linked glycosylation. N46 is probably too close to the cell membrane, leaving the two most likely sites as N59 and N69, and of these two N59 appears to be the most conserved within the class I and II proteins.

Of considerable interest is the substrate specificity of this GLUT7 isoform, which can transport both glucose and fructose. None of the other hexoses tested appeared to be substrates, including galactose, 2DOG, and xylose. This inability to handle galactose and 2DOG is surprising given that the other GLUT which can recognize both glucose and

fructose is GLUT2, for which galactose and 2DOG are also a substrates. This would indicate that comparison between these three transporters should lead to some insights regarding the key residues involved in determining their substrate selectivity.

The GLUT7 affinity for glucose is also very high compared with the majority of GLUTs, having a K_m of 0.3 mM, which is almost an order of magnitude lower than that of GLUT5 for fructose[168] and two orders of magnitude lower than that of GLUT2[169,170,171]. The only other GLUT that has been shown to have such a low K_m is GLUT10, when 2DOG is used as the substrate[172]. Similarly, the ability of GLUT7 to transport fructose at a comparable rate for the same concentration as glucose (0.1 mM) and the IC_{50} of 60 μM for the inhibition of glucose transport by fructose shows that GLUT7 also has a high affinity for fructose. It is currently not clear why GLUT7 would have such a high affinity for its substrates, but presumably it must be related to the physiological role this protein plays in the small intestine.

The distribution of GLUT7 appears to be limited to the more distal region of small intestine, the ileum, which contrasts with the expression of SGLT1, GLUT5, and GLUT2. These latter hexose transporters are found predominantly in the jejunum with a much lower abundance in the ileum[169,173,174,175]. The presence of the message for GLUT7 in the testis and prostate is of interest given that the need for fructose as a substrate for sperm is well documented and GLUT7 can transport both glucose and fructose[158]. Additional work needs to be done to determine just where in these tissues the transporter is expressed.

Although is not possible at this stage to definitively assign a physiological role for GLUT7 in the intestine, it is possible to draw some inferences from the data currently available. The low K_m for this transporter suggests that it deals with low ambient concentrations of its substrates, glucose and fructose. Therefore, although it does not seem likely that GLUT7 plays a key role in taking up glucose from the diet in the initial stages of digestion and absorption, it may be important toward the end of the meal when luminal concentrations of glucose and fructose in the ileum are low. There is a rare genetic disease in humans, glucose/galactose malabsorption, in which point mutations in the SGLT1 lead to failure of the protein to be inserted into the brush-border membrane[176,177,178]. This results in malabsorption of the hexoses (glucose and galactose) taken up by this transporter. The uptake of fructose in the jejunum, however, which enters via different pathways, appears to be relatively normal in these patients. There are at least two known possible routes of entry for fructose across the brush-border membrane: via GLUT5, which is specific for fructose, and via the newly identified pathway of transiently expressed apical GLUT2[47]. GLUT5 appears to be expressed in a constitutive manner and is not regulated by the presence of luminal hexoses during the course of a meal[179], although its expression can adapt to maintained changes in the diet. In contrast, GLUT2 is inserted into the jejunal brush-border membrane within minutes when glucose is present in the intestinal lumen[180,181]. This effect appears to be mediated by the initial uptake of glucose via SGLT1 and so will not operate in glucose/galactose malabsorbers in whom SGLT1 is nonfunctional.

Could GLUT7 play a significant role in absorbing fructose and glucose in these patients? This seems unlikely for two reasons. First, GLUT7 appears to be a high-affinity transporter, which usually means a low V_{max} and hence low capacity. Thus, it is unlikely that GLUT7 would have the required capacity that can already be achieved via GLUT2 and 5, which have much higher K_m values, unless GLUT7 is present in high abundance. Second, if GLUT7 were able to handle a significant component of the nutrient load of fructose, then it should also be able to absorb significant amounts of glucose and so, at least partially, compensate for the absence of SGLT1 in patients with glucose/galactose malabsorption. This does not appear to be the case. Clearly, additional work is required to determine the contribution that GLUT7 makes to the absorption of the nutrient carbohydrate load in the small intestine.

4.2 Structural and functional role of GLUT7 I314 residue.

While glucose is the primary substrate for the majority of the GLUT proteins, a small number were also known to be able to recognize fructose. GLUT2, a member of the class I GLUTs, can transport both glucose and fructose with low affinity. Similarly, GLUT5 (a class II protein) can mediate fructose and glucose uptake but with higher affinity. Recently, it was reported that the newly cloned GLUT7, another member of class II, can also transport both fructose and glucose[158]. Comparison of the sequence alignment of GLUTs 1-7 in the putative TM7 region showed that, in the position equivalent to V290 of GLUT1, GLUTs 2, 5, 7 have an Ile residue while, in contrast, the other class I GLUTs (1, 3, & 4), which transport glucose but not fructose, have a Val at this position.

This raised a legitimate question in regard to a possible significant role of this position in the permeation process through the GLUT7 "pore". GLUT7 as well as GLUT2 transport both fructose and glucose[158] and we wondered if the replacement of Ile with Val would in any way affect their transport properties. Both residues are of similar size, but Ile with an extra $-CH_3$ group has a molecular volume of 168 $Å^3$ whereas Val is 145 $Å^3$. Their hydrophobicity index is however quite different, 2.5 for Ile and 1.5 for Val (Kyte and. Doolite scale).

The previous literature data regarding GLUT1 putative structure[105, 161] as well as our own three dimensional model of the GLUT7 present the same conclusion. Ile314 in GLUT7 and Val 290 in GLUT1 are lining the aqueous pore and placed at the

extracellular extremity of the TM7. ***Is this conserved substitution critically important for fructose transport? If yes, how exactly does Ile influence the fructose recognition?*** To answer these questions it seems reasonable to try to understand the reasons for which the GLUTs' biologically active conformation requires the presence of Ile 314 in the close proximity of the aqueous pore.

4.2.1 Folded structure of membrane proteins.

To better understand the forces and factors that govern and influence the protein conformation within the membrane I looked at the physical basis of protein folding. This approach is justified by the simple observation that the physical and chemical interactions which influence the spatial distribution of a protein's amino acid residues, during the maturation of the protein, are going to be present and further influence the protein within the membrane. Additionally, protein folding process is a very dynamic process in which multiple external factors (such as temperature, pressure, pH, etc) influence the interaction between certain residues which results in a final, viable and mature, configuration. Similarly, the membrane transport process is a very dynamic event in which the conformation of the protein goes through state transitions influenced by the same physical factors which influence the intracellular protein folding. The protein's conformation within the membrane determines the functional characteristics of the transporter, and this is one of the most important rate limiting steps in the kinetic behaviour of transport proteins. Protein folding has been incompletely viewed as the process through which the nascent protein achieves a stable, mature conformation and

was considered complete once the protein was expressed in the membrane. Biophysical studies of membrane transporters have definitely shown that the structure of membrane proteins continues to undergo conformational transformations in the presence or absence of substrate and that protein topology can influence its functional properties[182]. Therefore, aside of any semantic incompatibility, the protein folding process and the topological folding of the transport protein within the membrane are very similar events.

Physicochemical studies of the protein folding have a long history[183,184,185] and their predictions have been confirmed by more recent crystallographic and adjacent physiological studies[186,187]. This confirmation offers the validation for the predictive power of protein folding theory, showing that an accurate and careful mathematical analysis of protein structure can give valuable information regarding the three dimensional configuration and mechanism of function.

Protein folding describes the three dimensional conformation of the polypeptide backbone, by listing two dihedral angles per amino acid residue. Analysis of folded proteins reveals that the folded structure is very compact and the secondary and tertiary structures are not in conflict respecting the physical features of a Hamiltonian model, which is known as the minimal frustration principle[188]. The location of atoms in proteins can be determined in favorable cases, to an accuracy of slightly less than 3 Å using X-ray crystallography. This specificity of structure arises from the heterogeneity of the protein chain. The differing energies associated with positioning different residues near or far from each other or from solvent enable some structures to be more stable than others. For example, if a sequence is chosen at random, the specificity of structure is still

small — a variety of globally different structures have very low energies, but within a few k_BT of each other[189]. This mathematical observation has been the bane of computational protein structure prediction using energy functions.

4.2.2 Structure-substrate interaction

Regardless of the number of binding sites involved in hexose translocation, the mechanism by which GLUT proteins catalyze sugar transport is thought to involve a mutual interaction between these protein structures and the substrate molecule. Firstly, the structural changes that take place within the protein during the transport process directly influence the way in which substrate molecule is guided, tilted and passed along the transporter's pore, allowing for the formation of interactions between specific pore-lining residues and critical hydroxyl groups of the hexose ring[190,191]. Conversely, there is evidence for substrate-induced conformational changes, which emerged from studies using hexose analogues which stabilize either the outward- or inward–facing conformational states[192,193]. Ligands that bind to the outward-facing conformation, such as 4,6-O-ethylidene-D-glucose and bismannose compounds, induce a conformation which protects the protein from proteolysis by trypsin[194,195] and thermolysin[196]. This protection from proteases is reversed by inhibitors such as propyl-β-D-glucoside and phenyl- β-D-glucoside and cytochalasin B, which bind to the inward facing conformation[197]. From these data it becomes clear that the functionality of the SLC2A proteins is critically regulated by two main categories of factors. The specific conformations achieved by the protein in the membrane during the transport process and

secondly, by the chemical structure of the translocated substrate. Thus, the conformation of the transporter within the membrane determines the pattern of substrate passage and reciprocally, the nature of the substrate could influence the biologically active configuration of the transporter.

Substitution of Val for Ile in GLUT7[198] dramatically altered the substrate specificity of the protein almost completely eliminating the ability to transport fructose, while having no effect on the recognition or capacity to move glucose. The other transport characteristics were also identical to the wild type behavior, GLUT7 I314V showing no affinity for 2DOG or galactose. Expression of the mutant in the oocyte membrane was also unaffected by this single amino acid substitution as determined by immunohistochemistry and Western blotting. These results clearly indicate that the recognition, binding and the translocation of the glucose through GLUT7 does not depend on the presence of the Ile at the 314 position.

Wild-type GLUT7 has the same affinity for glucose and fructose and these substrates can competitively inhibit transport of the other equally effectively. The simplest interpretation of these observations would be that there is a single binding site, which recognizes both hexoses. However, GLUT7 I314V experiments showed that this hydrophobic residue appears to be critical for the recognition of fructose, but not glucose. The uptake of glucose by the I313V mutant was unaffected by the presence of 10 mM fructose, suggesting that in some way this point-mutation prevents fructose from accessing or interacting with the binding site. The differences in the size and

hydrophobicity for Val and Ile are minor, with molecular volumes of 145 and 168 $Å^3$ and surface are of 155 and 175 $Å^2$ respectively, the global protein energy of GLUT7 is expected to vary very little when Val is substituted by Ile, about 10 K_bT. A lack of effect on the transport of glucose also indicates that this mutation in no-way interferes with the ability of the protein change its conformation between the inward and outward facing configurations.

4.2.3 Evolutionary and theoretical considerations regarding Ile/Val phenotype in GLUTs members.

Before anything else, to clarify the role of GLUT7 I314, it seems important to get the correct understanding of the evolutionary significance of this mutation and its impact on overall protein configuration within the membrane. One of the best tools in deciphering evolutionary events is the analysis of amino acid interactions that contribute to the final configuration of a protein.

Apparently not very significant, the effect of mutation of the Ile to Val could be better assessed and understood by applying the ***minimal frustration*** principle[199] to the conformation of the protein. A typical sequence of amino acids chosen at random would have a very uncharacteristic pattern of the energy landscape and the dynamics of all the states in which could characterize would be very disorganized. The exact ground state of such a sequence derives from competition of many conflicting energy contributions – "frustrated" interactions. Even a point mutation in the sequence could cause the lock of the structure in a new ground state[200]. Evolutionary-wise, this would be totally

impractical to an evolving line of organisms. If a particular random protein has already achieved a functionally viable three dimensional shape in an ancestral organism, a single mutation could destroy this useful shape. Natural selection over time would not keep such outcomes because of the biological functional constraints[201]. The strength of the evolution consists of selecting for sequences in which the interactions present in the functionally viable conformation are not in conflict, as in a random sequence but instead are mutually supportive and cooperatively lead to a low-energy structure[202]. Therefore the interactions are "minimally frustrated" or consistent. For an evolved protein the mutually supportive and minimally frustrated nature of the interactions in the native structure means that a collective coordinate measuring distance to the native structure by itself gives a good indication of the energy of a particular conformation. The energy will decrease, on average, as more structures are formed which are more similar to the native structure of the native protein.

Therefore, it could be said that the energy landscape is "funneled". The protein folding funnel is defined[203] as a collection of geometrically similar collapsed structures, some of which being thermodynamically stable with respect to the rest, though not necessarily with respect to the whole conformational space. The capacity of the protein to fold is indissolubly connected to the existence of the folding funnel and by transitivity to the very own its primary structure. An amino acid sequence having a single sizable folding funnel to a unique, stable conformation is said to be "foldable". Conversely, "non –foldable" amino acid sequences have multiple folding funnels and do no exhibit a single

minimum. It is widely known now, that the biologically active state of a protein is both a deep global energy minimum and has a funnel of low energy configurations leading toward it[204]. The funnel guides the molecule to fold to its stable native conformation in a time much less than that required exploring all the configurations, thus avoiding the so-called Levinthal paradox[205].

In nature, the folding funnel consists of folding trajectories that lead to the final active conformations. These folding routes connect a given initial collapsed conformation go through several transition states and eventually end in the final active conformation. This concept suggests that the process of folding is consistent among members of the same phylogenetic family in spite of the inherent natural diversity and as long as stability is maintained. For example, mild mutation will initially shift the folding routes and, if one set of routes to the native structure is completely blocked by a destabilizing mutation, another set of routes will take over as long as the final structure will be similarly stable. Additionally, the role of secondary structure versus tertiary structure formation in synthesis of the native state, the effect of changing secondary structure propensities in turn regions or regions of well-defined secondary structure, and the effect of sequence mutations such as destabilizing core mutations are factors that should be taken into account when analyzing the process of achieving the active conformation of the protein.

Super-secondary structures accommodate both local hydrogen bonding and packing requirements. If it were not for this relative lack of frustration in final, folded structures and secondary structure prediction schemes would fail spectacularly. Using the

minimal frustration principle it is possible to calculate[189] the energy of molecule of protein in a specific conformation which will enable one to identify the level of energy of given protein in a biologically active state. This information is very important to energetically differentiate between different conformational states of a protein in the membrane (i.e. active vs. inactive state or in the presence of different substrates.) Also, it becomes meaningful to calculate these levels in different membrane expressed, either functional or non-functional, mutants of the same protein in order to identify a specific physiological behavior driven by a point mutation.

To exemplify, suppose that we are given a particular protein with N amino acids that is in a specific conformation. The energy of this molecule could be calculated[188] if we take into account the different kinds of interactions which take place in protein folding. Firstly, the energy associated with the state of each amino acid residue could be written as $-\varepsilon_i(\alpha_i)$, where ε refers to the amino acid residue under consideration and α_i refers to the state of the ith amino acid. Secondly, there are interactions along the chain, e.g., hydrogen bonding in α helices. Using a standard approximation by taking this interaction to be between nearest-neighbor residue[205] so the energy of each bond of this type as $J_{i,i+1}(\alpha_i,\alpha_{i+1})$.

Finally, there are long range interactions, i.e., interaction between residues there are far apart along the chain. These occur when bends in the chain bring two amino acids close together, e.g. , by hydrophobic forces. This energy component could be written as - $K_{i,j}(\alpha_i,\alpha_j,r_i,r_j)$ where r_i is the position of the ith residue. Again, this type of

interaction becomes very important in the "transport architecture" in the new light brought by the recent crystallographic data. More our experimental data communicated in this paper comes to support these predictions.

Therefore the total energy of the protein could be written as:

$$E = -\sum_i \varepsilon_i(\alpha_i) - \sum_i J_{i,i+1}(\alpha_i, \alpha_{i+1}) - \sum_{i,j} K_{i,j}(\alpha_i, \alpha_{i+1}, r_i, r_{i+1})$$

Simplistically, we can view $-\sum_i \varepsilon_i(\alpha_i)$ as being related to the primary structure, the $\sum_i J_{i,i+1}(\alpha_i, \alpha_{i+1})$ being responsible for the secondary structure and $\sum_{i,j} K_{i,j}(\alpha_i, \alpha_{i+1}, r_i, r_{i+1})$ as being responsible for the tertiary structure.

From these equations becomes obvious that any disallowed mutation inserted in the primary amino acid sequence of a protein could have dramatic consequences on the final folding state. However, because the funneled energy landscape is responsible for the robust ability to fold, this process involves a variety of detailed mechanisms. For example, secondary structures may form before or after collapse, side chains may order before or after main chain topology, one domain of a protein may fold before another. This is why conserved substitution in key region of proteins belonging to the same phylogenetic family becomes important in structure/function relationship by selecting equivalent folding conformations which however, display different functional properties.

Corollary- According to the findings of protein folding studies, tertiary structure of a protein is mainly dependent on long range interactions between key amino acid

residues. Mutation of this key coordinates within the structure of a given protein could lead to important conformational and functional changes.

In view of this theoretical framework it makes more sense that the evolution selected a minimal mutation (Ile to Val or vice versa) in order to achieve stable and functional proteins with similar but although different functions. Therefore, at the expense of such a minimal structural change the functionality of different members of the GLUT proteins could be dramatically changed and in the same time the overall stable protein conformation be maintained. However, this particular case in which such a close substitution has such an important effect on the protein functionality implies that this position is of critical importance for the GLUT functionality.

One possible interpretation for the role of I314 is that the Ile would have a "pushing" effect on the water and fructose molecules within the pore due to its hydrophobicity. In the putative 3-D structure for GLUT7 and in the one for GLUT1[105] the side chain of I314/ V290 is projecting into the pore, potentially enabling it to exert hydrophobic interactions with the water shell surrounding the substrates as they enter the vestibule. In this regard, the length of the Ile side chain would appear to be critical, since substitution with a similarly hydrophobic but shorter residue abolished the fructose transport. It is possible that this interaction could create a funneling action on the fructose, appropriately orienting it, such that it is recognized by the ligand binding site. This hypothesis would indicate that a very specific orientation of fructose is required within the pore to allow fructose to interact with the binding site. In other words the

hydrophobic interaction between Ile and the substrate could tilt the fructose molecule in such a way in which would allow the binding sites to create H bonds with the –OH groups of the hexose ring. The role of Ile would be, therefore, to act as part of structure which would guide the hexose ring as it enters the vestibule of the pore enabling fructose recognition and permeation.

Another possible interpretation for the role of I314 could be that this residue subtly influences the conformation of the protein, such that the shape of the vestibule is altered sufficiently to affect the ability of fructose to access the exofacial binding site. Such an effect might be produced through the interaction between hydrophobic residues and structural water molecules within the protein structure.

This hypothesis finds a good theoretical ground in the studies of microscopic properties of water in narrow pores which are relevant to the function of ion channels and related membrane transport proteins. Furthermore, water not only interacts with the protein surface, but it can directly interact with the protein backbone and the side chains in the protein interior or even form clusters of two or more water molecules in hydrophobic cavities[206]. Buried water molecules have much longer mean resistance time than water in the first hydration shell and thus they constitute an integral part of the protein structure[207,208,209] at a given time. Hydrophobic residues are known to interact with water during protein folding and these interactions play a crucial role in achieving stable 3D structures[210,211]. More over, these residues manifest their structural role through the so called 'hydrophobic effect' or 'hydrophobic interaction' exerted by/between the

side chains of the non polar residues that are responsible for an appropriate and tight folding process. This theory[212] assumes that the non-polar residues, through side-chain-side-chain hydrophobic interactions, get 'buried' in the 3-D structure of the protein and the water molecules are cooperatively squeezed out from the hydrophobic core region[213] and ordering in the exterior making them available for future hydrogen bonds[214] on the expense of a loss of randomness in the system . The burying of hydrophobic groups within a folded protein molecule produces therefore a stabilizing entropy decrease of the 'dry' packed protein. The water molecules that were ordered by the protein when it was in the denatured state are now released, gaining freedom of motion. Consequently, internalizing hydrophobic groups increases the randomness of the whole system (protein plus water). This concept could also, be applied to the kinetic mechanism of membrane transporters. Thus, dynamics of hydrophobic residues within the 3D structure of membrane proteins produces an increase in overall enthalpy which creates a more active (unstable) protein. This energetic state is more prone to subsequent conformational changes hence, favoring the interaction with the substrate. Therefore, mutations of hydrophobic residues could affect the number of structural water molecules within the core of a protein and disrupt essential interactions mediated by ordered water contacts[215], resulting in either total destabilization or more subtle changes of architecture. Similarly, it could be assumed that hydrophobic residues influence the functional configuration of transport proteins when expressed within the membrane.

Accordingly, mutations can affect the number of the number of the structural water molecules within the core and disrupt essential main-chain interaction network

mediated by water contacts resulting in destabilization[216]. This destabilization can prevent the achievement of biologically active conformation determining either sequestration of the protein by cellular quality control mechanisms or expression in the membrane of a functionally defective protein. Similarly, mutations of hydrophobic residues could create a tighter or looser hydrophobic packing of the structure within the membrane hence influencing the kinetic properties of the transporter.

To further test this hypothesis we replaced I314 with Ser, which has a smaller size and length of the side chain (residual volume 89 $Å^3$ and surface area of 115 $Å^2$), and is a hydrophilic residue and consequently could not establish hydrophobic interactions. My data showed an increase in both glucose and fructose transport in the GLUT7 I314S mutant. The previously communicated data[73] shows that TM7 and 2 of GLUT1 form a "cleft" at the exofacial side of the aqueous pore. This particular structure would contribute to the particular tight hydrophobic packing of the exofacial vestibule responsible for the functional properties of GLUTs. Our own 3D model suggests that Ile314 (TM7) and W89 (TM2) are positioned in a close proximity and could form a hydrophobic interaction Ser is shorter than Ile and will not be able interact hydrophobically with W89, allowing TM's 7 and 2 to 'relax'. Thus, the vestibule would be opened up allowing easier entry of both substrates.

4.2.4 Examples of natural mutations of hydrophobic residues in GLUTs members.

There are many examples in the literature of significant effects on the functionality of SLCA2 proteins when hydrophobic residues are inserted into or removed from the sequence[217,218,219]. One of the most frequent missense mutations encountered in De Vivo syndrome (a GLUT1 deficiency syndrome, hypoglycorrhachia and reduced erythrocyte glucose transport) is replacement of the hydrophilic residue Thr 310 is by Ile[220]. This Thr 310 is conserved in human GLUT1 through GLUT9 and also across many other species [221], suggesting that this residue may play an important role in glucose permeation. Analysis of the T310I properties revealed that the mutation significantly reduced the glucose transport but interestingly did not abolish it. Moreover the osmotic water permeability of the mutant was paradoxically increased over that of the wild type. These results led to the hypothesis that the presence of the Ile at the 310 position in GLUT1 might influence the biologically active conformation of the protein[220].

A similar natural mutation replaces a Thr residue in position 110 with an Ile in one of the two polymorphisms described in the human GLUT2 gene in patients with NIDDM[218]. Interestingly, the presence of the Thr at the position 110 is unique to the GLUT2 isoform, while the other human GLUT isoforms, 1, 3, 4 & 5, have an Ile residue. However, the GLUT2 T110I mutant does not show a significant reduction in 2-deoxyglucose uptake activity, but the uptake of the natural substrates, glucose and fructose, was not measured[218].

A second interesting polymorphism found in Afro-American patients with gestational diabetes involves the replacement of Val197 with Ile their GLUT2 gene. The effect of this very conservative substitution is quite surprising given it only represents the replacement of hydrophobic Val with Ile, differing in structure by only a single methylene group. It must also be recognized that the substitution of Ile for Val is one of the most common amino acid changes observed at the equivalent positions of homologous proteins[222]. When a similar experimental mutation was introduced into human GLUT1 (V165I)[132] a severe reduction in glucose transport resulted. The authors did not offer a mechanistic explanation for the effects of this conservative substitution but did conclude that this position must lie in the glucose translocation pathway.

Moreover, a similar mutation has been described in the structure of the insulin dependent glucose transporter (human GLUT4) in a patient with NIDDM who developed insulin resistance. Analysis of their insulin receptor did not reveal any anomaly indicating that the insulin resistance was likely the result of a structural defect in the mutant GLUT4. The mutation replaces Val with Ile in position 383 which is conserved in GLUTs 2, 3 and 4 and is located just before TM10. Interestingly, in wild type GLUT 5 Ile replaces Val in this position and in GLUT1 there is a Leu residue.

From these examples becomes clear that generally the role of the hydrophobic residues and particularly Ile, in the biologically active conformation of the SLCA2 membrane proteins is more complex than just creating a hydrophobic well inside the pore, but their structural importance is not yet fully understood.

4.3 Physiological and phylogenetic classes of SLC2A proteins

Glucose is the primary substrate for the majority of *SLC*2A proteins and properties of the uptake process have been researched extensively, whereas those of fructose, were somehow, viewed as having a secondary role. This could be explained by the ubiquitous expression of GLUT1 which was identified in the majority of tissues and by the fact that glucose is thought to be, more or less, the universal energetic currency. Conversely, fructose with a less obvious physiological function, was shown to be transported by only one member of class I (GLUT2) and by two members of class II (GLUT5, and more recently, 7). GLUT2 can transport glucose and fructose with low affinity[169] whereas GLUT5 and 7 can mediate both of them with high affinity[158,170,223]. During my Ph.D. studies I also showed that both, the third and fourth members of class II, GLUT9, and respectively GLUT11 transport fructose and glucose with high affinity as well. Comparison of the sequence alignments of the class I and II members in the putative TM7, more specifically within *L278-QLSQQLSGGINAVFY-Y293* region showed that, in the position equivalent to V290 in GLUT1 all the members that transport glucose have a Val residue whereas most of those that transport both glucose and fructose have an Ile residue (GLUT2, 5, 7 and 9). This indicated a possible significant role in the structural functionality of the Ile at this position and also the fact that conserved substitution of Ile for Val within the highly conserved NAI/NAV motif might play a role in the substrate specificity of these proteins. I have previously shown that in GLUT 7, I314 is involved in maintaining the ideal conformation for fructose docking in the translocation process[224]

by creating the necessary space for the passage of the permeant. Moreover, the molecular modeling placed this position as facing the aqueous pore and within the outer facing vestibule in a very favorable position to influence the recognition of the substrate molecules as they enter the pore.

Based on the fact that both functionally and structurally GLUTs 2, 5, 7, and 9 share a significant similarity I investigated the role of the position equivalent to I314 of GLUT7 in these proteins. I have employed a similar approach by mutating Ile to Val and in all three proteins the ability to recognize fructose was significantly impaired when Val was substituted for Ile.

Just as for GLUT7, the ability of GLUT2 to transport glucose was unaffected by this substitution. GLUT5 widely known for its ability to transport fructose also lost its transport capability when the isoleucine at the equivalent position was mutated to valine. Moreover, I have shown for the first time that human GLUT5 can transport glucose and determine the kinetic parameters of this hexose transport. Consequently, I have proven that the mutation of Ile 296 to Val does not affect the glucose transporting capacities of GLUT5.

In a similar manner, the effect of the mutation of Ile 335 to Val was analyzed relative to the effect on GLUT9 transport properties. Not very surprisingly, the effect was almost a total decrease in fructose uptake with an intact glucose transport.

These observations are interesting because these four glucose transporters (GLUT 2, 5, 7, and 9) display similar properties in spite of the fact that they phyologenetically

belong to different classes. Moreover the conserved mutation of Ile 314 and all its homologue positions within the other members produced exactly the same consequences on the transport properties. At this point, I conjecture that based on the functionality of the GLUT proteins would be justified to group SLC2A proteins in "physiological hexose transporter classes" which cross phylogenetic boundaries. Thus, a physiologic class of glucose and fructose transporters which is composed of GLUT2, 5, 7, 9 and 11 could be identified. Similarly, the GLUTs that can only transport glucose and its derivatives (2DOG, 3OMG, etc.) could form a different physiologic class, namely GLUT1, 3, and 4. Sequences alignment of the these proteins within TM7 region reveals a more or less conserved *L278-QLSQQLSGGINA-V290 motif* considered to be important in maintaining the proper packing of the exofacial site of the pore in order to achieve the biologically active conformation.

4.4 Selectivity filter concept applied to the function of SLC2A proteins

As presented in the results section, I have presented data, which shows that GLUT11 is capable of transporting both glucose and fructose. However, the multiple sequence alignment of the TM7 regions reveals that in the homologue position to N311-A313-I314 motif in GLUT7, GLUT11 displays a DSV motif. This particular difference between the GLUT11 and the other members of the class II was quite intriguing as GLUT11 can transport both glucose and fructose. In all the members of the glucose fructose transporters, Ile 314 was conserved at the homologue position whereas in the glucose but not fructose transporting GLUTs this residue was replaced by Val. Thus, GLUT11 appears as a veritable structural and functional chimera by having conserved a Val residue at position 299 (homologue to Val290 of GLUT1) while displaying glucose-fructose transport properties[225]. This striking discrepancy between the structure and function drew our attention upon the immediate neighbors of Val 299 within the GLUT11 structure. GLUT11 is the only protein out of the first two phylogenetic classes which does not contain the NAV or NAI motif at the exofacial side of the TM7. The importance of the N288 (Asn residue from the NAV/I motif) in functionality and structure GLUT1 had been highlighted by two different studies[105,161] and it had been largely discussed in the previous paragraphs of this work. In contrast to all the other members of the class I and II, in N288 is replaced GLUT11 by an aspartate residue. This is followed by a Ser residue, which again is a very conserved mutation of an Ala/Gly residue that is displayed by all the other GLUTs at this position. Thus, GLUT11 displays

a unique motif D297S298V299 instead of a NAI/V at the exofacial side of the TM7 and in the same time preserves the glucose-fructose transport properties. Trying to "dissect" the functional signification of this structural deviation I designed a GLUT11 chimera, which would present instead of the native DSV motif a NAI or a NAV motif.

To meaningfully interpret the role of each component amino acid residue, I created individual mutants for each position in part. Hence, I tested functional properties of the GLUT11 D297N, S298A and V299I mutants. Replacement of the D297 with Asn did not produce any modification in the transport pattern, the mutant being able to transport both glucose and fructose with similar affinity to the wild type. This might be explained by the fact that Asp is the salt of the Asn and this mutation does not produce a dramatic change in the hydrophilic effect of the region. Interestingly, mutation of the Ser 298 to Ala did not produce a significant change in the intrinsic properties of the transporter. Alternatively, mutation of the Val 299 to Ile produced a dramatic reduction in the transport of both glucose and fructose. This marked reduction was then rescued when the chimeric protein contained the NAI motif.

These findings led us to hypothesize that the NAI/V motif at the border between TM7 and extracellular loop 4 might form a complex structure which could play an important role in selection and subsequent recognition of the substrate. At this point, based on the literature data and on my experimental results, I can only conjecture that the proximity of Asn to Ile or Val could create a structure wherein Ile or Val are part of a hydrophobic filter just above the substrate selectivity binding sites, among which Asn

could be included. This putative structure of the GLUTs aqueous pore, could be approximated by the shape of a **"martini glass"** presenting a largely open exofacial vestibule and then narrowing down towards the substrate binding sites region, lining the "stem" formed by the pore with a putatively less open intracellular vestibule. The advantage of this structure would be that the steric and physical-chemical selection of the substrate would be done within a very short distance which would increase the energetic efficiency of the transport process.

A strong argument in the support of functional importance of this pair of amino acid residues Asn and Ile or Val within the NXI/V motif is constituted by the extremely high evolutionary conservation. This motif is highly conserved cross species among orthologs of human hexose transporters[106,226]. Thus, the exofacial side of the putative TM7 of the hexose transporters from *Taenia Solium, Schistosoma Mansoni, Saccharomyces cerevisiae, Trypanosoma crusi*, *vivax*, and *brucei*, and *Plasmodium falciparum* contain, with small variations, the same NXI/V motif. This finding is of particular interest as it was proven[227] that the global pattern of co-evolutionary interactions between key amino acid residues within different members of a given species of protein is sparse, such as a small set of positions mutually coevolves among majority that are largely decoupled. Furthermore, the strongly coevolving residues are organized in such a way in which they create physically connected networks linking distant functional sites in the structure through packing interactions[228,229,230].

Using molecular dynamics and energy minimization algorithms in a system already used to model GLUT1[161], we have produced a putative 3D structure for GLUT7. The model was created using fixed coordinates of the already crystallized E. c*oli* protein GlpT and adjusted using homology modeling from the template after 10ns of simulations. The position of isoleucine 314 is shown as facing the aqueous pore and within the outer facing vestibule. There also appears to be a tryptophan residue on the other side of the vestibule, contributed by TM2 (W89), and the together they may form a narrowing as a consequence of a hydrophobic interaction (Fig 3.41). The docking model further suggests that for the hexose substrates to move forward into the channel they first have to pass through this narrow passage. This hypothesis would indicate that a very specific orientation of fructose or glucose is required to allow them to access the binding site/s within the channel. Interestingly, when we compare the GLUT7 structure with that of GLUT1 in which valine (V290) also can interact with the conserved tryptophan we see an even narrower passage (4.4 vs 5.2 Å). This is likely a consequence of the significant difference in the hydrophobicity of the two residues, isoleucine 2.5 vs 1.5 for valine. Finally, the docking simulation also predicts a quite different orientation for fructose compared to glucose as they bind below the vestibule suggesting that fructose needs a wider opening in order to be able to enter the pore and complete the transport cycle.

Based on my findings and on the three dimensional modeling of the hGLUT7 protein it seems that the Ile 314 and Trp 89 residue could create a selectivity filter at the extracellular entry into the aqueous pore. This putative selectivity filter could act as a

physical "slot" through which the substrate molecule would have to pass prior to accessing the substrate binding site(s). This type of structure has been well characterized in ion channels.

The concept of a selectivity filter within the structure of a facilitative transporter is not entirely new and the concept is strongly supported by evolutionary and phylogenetic arguments[231]. The crucial distinction between a channel and a 'gated-pore' is that, when the channel is open, more than one solute particle can cross the membrane before a conformational change closes it again. Typically, several thousand ions will flow through the channel in single file in the 1–10 ms during which it is open. With the 'gated-pore' model there has to be a sequence of conformational changes for each turnover of the catalyst, and this results in the transport of a defined, stoichiometric, number of particles; 1, 2 or at most 3 per turnover. However, the gated-pore concept, as published previously, refers to the alternating gating of the pore through conformational changes during the state transitions from outward- to inward facing conformation. My data suggests the existence of a selectivity filter which is positioned above the substrate binding site and which could "gate" the access of the substrate coming from the extracellular space while the transporter is open in the outward facing conformation.

Twelve transmembrane helices is a recurrent structural feature of gated-pore carriers belonging to the MFS. It prompts the question: is this the right size for gated-pore carriers, or are they this size because they are all related, the question of convergence versus divergence. It was suggested that 12 α-helices may be a "structural

paradigm" for these transport proteins[232], and was dubbed "the rule of 12". An alternative view postulates a "rule of 6", and sees the prototype solute ductor molecule as comprising of six helices, forming a pore capable of transmitting a disaccharide or a nucleotide triphosphate[233]. MFS proteins are believed to be the result of a gene duplication event[234,235] but there are suggestions that MFS proteins may have developed from an even more primitive ancestral precursor that contained only three transmembrane segments. The architecture of the 12 transmembrane helices is such that each set of six helices is located in a different half of the molecule, and consequently the two halves form a nearly flat interface at their boundary that constitutes the transport channel pathway.

The majority of known 'gated-pore' translocators contain 12 α-helices. Many are obviously related and form clearly defined families. Some of these families themselves show resemblances and can be grouped into superfamilies. But other families of 12-helix transporters appear very different and display no vestiges of a common evolutionary origin. When the high resolution structures of Lac Y and GlpT became available[186,187], it became clear that they shared remarkably similar folding patterns. However, their sequence identity is only 21% and their mechanism of action appears to be different because GlpT uses the downhill gradient of phosphate for an obligatory exchange with glycerol-Pi (an antiporter), whereas the LacY cotransports β-galactosides with protons (a symporter). However, despite these differences, both structures show highly similar folding, which is, in general, also similar to the proposed low resolution structure for OxlT[236], obtained using electron microscopy. There are some structural differences in

loop length and conformation of these proteins and some of the TMs of LacY may be more kinked than in GlpT. These findings suggest the intriguing possibility that the folding of these transporters constitutes the scaffold for all the MSF transporters with 12 helices. Although the folding is conserved, the specific function is obtained by varying sets of amino acid residues at the substrate binding and translocation domains. These observations are supported by previously published data which showed for other protein families that the folding appears to be conserved better than the sequences[237]. Therefore, the structures of GlpT and LacY are likely to be a paradigm for other MFS proteins. The substrate translocation pathway is located at the N- and C-terminal domain interface, formed by eight transmembrane α helices, with the substrate-binding site located at the domain interface.

The existence of a selectivity filter within the biologically active conformation of GLUT proteins has an interesting replica in the structure and function of the glycerol conducting channel[238]. The *E. coli* glycerol facilitator is a member of the aquaglyceroporins which belong to the Major Facilitator Superfamily. Thus, it could be considered to be a remote evolutionary "cousin" of the facilitative hexose transporters. However, the functional folding structure of this protein presents, to certain extent, a structural parallel with the structure of GLUTs. Moreover, GlpF, in spite of the fact that is categorized as a channel has a functional behavior which is closer to the kinetic pattern of facilitative transporters. Thus, GlpF is capable of accommodating only three molecules of glycerol at time and only in a single file manner, and then the substrate

molecules enters the channel pore where they are subsequently bound by specific binding sites. The folding structure of the GlpF protein respects the general "scaffold" of the aquaporins consisting of three general elements, an extracellular vestibule, a narrow selectivity filter and a cytoplasmic vestibule. One half of the selectivity filter wall is highly hydrophobic, whereas the other half is hydrophilic conferring a strong amphipathic character to the structure. The amphipathic nature of the substrate selectivity filter has a key role in substrate permeation. The hydrophobic face provides an ideal match for carbon backbone of the glycerol while the opposing hydrophilic face is equipped with hydrogen-bonding groups to replace waters of hydration in the vicinity of glycerol hydroxyl groups. Another unique characteristic is the conservation of a double NPA (Asn-Pro-Ala) motif present on helix 3 and 7 which create an intimate interface across the quasi two-fold axis in which proline rings are in Van der Waals contact, cupped between the proline and alanine side chains from the opposite helix. The NPA motifs are juxtaposed in such a way in which each asparagine chain is constrained by two hydrogen bonds that precisely orient side-chain NH's toward acceptors on the permeant substrate.

The glycerol molecules initially enter a large exofacial vestibule in a hydrated state and become progressively dehydrated due to the rather hydrophobic character of the vestibule, which strips off the water molecules from the substrate. This type of structure, wherein mostly hydrophobic residues "guard "the entrance into the pore is present in all of the aquaporin family members[239]. Interestingly, GLUTs' sequence alignments and the

putative 3-D structure models available, reveal that all the eight TMs believed to form the aqueous pore present almost exclusively hydrophobic residues at their exofacial ends. Thus, this arrangement creates a hydrophobic ring surrounding the entrance in the vestibule similar to the structure of aquaporins, and whose main role appears to be the exclusion of the primary hydration shell from the substrate molecule in order to facilitate a more efficient transport process.

Simulations of bundles of parallel alpha-helical peptides (e.g. alamethicin) have enabled the development of methodologies and concepts appropriate to study the role of water molecules in the anatomy of transport process through membrane proteins[240]. In the narrow channels formed by such bundles, water molecules exhibit reduced rotational and translation motion. This reduction in water mobility may be a general property of narrow pores. Narrow pores with a hydrophobic lining of the vestibule, although physically open, may not admit water molecules, acting as a 'hydrophobic gate' that prevents water and ion permeation. Such a gate could be opened either by widening the pore or making its lining more polar. Simulations have been used to explore the behaviour of water in GlpF, a member of the aquaporin family of water pores, and OmpA, a bacterial outer membrane protein. The results suggest that a continuous water wire is not formed within the amphipathic GlpF pore. Simulations of OmpA, in which polar residues line the channel, indicate that a small conformational change in one of the channel lining side chains may open the channel. In summary, comparison of the behavior of water and substrate molecules in different narrow transmembrane pores

suggests that an amphipathic pore is ideal for permeation, and that either a highly hydrophobic pore lining or a charged pore-lining region can act as a gate.

Based on these observations, it could be hypothesized that substrate stereoselectivity of this type of channels and transport membrane proteins is influenced by the specific arrangements of different species of hydrophobic amino acid residues within the entrance to the pore. This primary contact between the substrate and transporter could have several important roles. Firstly, it could act as "dryer" by stripping the water shell molecules from the substrate and hence, preparing the substrate molecule for the subsequent hydrophilic interactions with the substrate binding site/s. Secondly, the hydrophobic residues could play a very important role in the correct packing and folding of a membrane protein, contributing significantly to achieving the biologically active conformation. Thirdly, the nature of the helix-helix hydrophobic interactions is responsible for the adequate packing and shape of the pore creating the necessary space for the permeation of the substrate through the channel pathway. Lastly, the hydrophobic residues placed at the exofacial site of the pore could exert a steric hindrance effect upon the permeant and thus play a determinant role in tilting the substrate molecule plane to a specific angle, which would produce the ideal three dimensional orientations for entry into the pore. Ultimately, it could be concluded that all these effects, produced by the hydrophobic lining of the vestibule, have a common final result which consists of presenting the substrate molecule to the binding sites in an energy and temporally efficient manner.

4.5 Summary and conclusions

The newly cloned GLUT7 protein has proved to be a versatile transporter capable of transporting both glucose and fructose (but not galactose). This last GLUT member remaining to be characterized proved to be a veritable "Rosetta stone" for the SLC2A protein family. The characterization of this glucose transporter provided important information for our understanding of the structure/function of the hexose facilitative transporters.

Functional studies performed on the other class II isoforms revealed that all of these proteins are able to transport both glucose and fructose with similar affinity. Phylogenetic analysis of the whole SLC2 A family demonstrated that GLUT2 is located at a very close evolutionary distance from the class II orthologs. Functionally, GLUT 2 is also a glucose-fructose transporter, and the structural and functional similarity to the other class II members creates the premise for a new organization of these membrane transport proteins. Originating from one of the governing concepts of biological systems, according to which the structure defines the function and the function "tailors" the structure, I propose a new organization of the first eight members of SLC2A family. I hypothesized that five transport proteins, namely GLUTs 2, 5, 7, 9 and 11 could be grouped in a physiological class of glucose-fructose transporters that crosses the recognized phylogenetic arrangement. Similarly, GLUTs 1, 3, and 4 could be grouped in a class of transporters that transport glucose and not fructose.

This physiological organization better reflects the concept of the protein folding theory, which demonstrated that despite some differences within the amino acid structure, proteins that share similar function are very likely to fold in similar structure conserving the essential amino acid residues important in achieving the biologically active conformation. Comparison of the sequence alignments of all the GLUT proteins enabled me to identify within GLUT7's sequence a particular conserved isoleucine residue at position 314 within TM7 (≡ 290 in GLUT1). This residue is found in all GLUT members able to transport fructose (GLUT2, 5, 7, and 9). Conversely, all GLUTs that do not transport fructose have conserved a valine residue at the equivalent position. An interesting "anomaly" is represented by GLUT11 which transports fructose but has a Val residue in the GLUT7Ile314 homologues position. When I interchanged isoleucine 314 with a valine residue in GLUT7 fructose transport was reduced by up to 90%. Induction of the same mutation in all the other member of the physiological group had essentially the same result, namely reducing almost to zero the fructose transport properties of the mutants. Conversely the mutation of the Val290 (to Cys) within GLUT1 had previously been shown to produce a significant decrease in glucose transport[105]. Cross species sequence alignments revealed that the Ile 314 is conserved in all the hexose transporters able to transport fructose[106,226].

Molecular modeling and site directed mutagenesis results led me to hypothesize that Ile 314 (or its homologues) are involved in creating a filter like structure via hydrophobic interactions with a Trp residue present on an opposing α-helix, defining a particular packing of the extracellular vestibule of the transporter's pore. This interaction

places the extracellular ends of TM2 and 7 within a conformation that favors the entrance of fructose into the pore. Replacement of this Ile with Val (as is present in GLUT1 and its orthologs) reduces the space available for the entry of fructose and blocking its ability access the binding site(s) below. How exactly this proposed selectivity filter functions is not yet clear. A steric hindrance effect could play a role in the specific tilting of the substrate molecule when entering the vestibule or these residues might "dehydrate"the substrate molecules before entering the aqueous pore. Finally, these hydrophobic residues could influence the selection of the substrate by influencing the conformation of the protein such that it recognizes a specific substrate.

This type of structure has been well known and studied in special channel proteins such as aquaglyceroporins. These types of channels are known to present a substrate selectivity filter at the exofacial extremity of their pore, and this structure involves the abundant presence of hydrophobic residues. Interestingly, these channels present immediately subjacent to this exofacial hydrophobic layer the substrate binding site which is formed by a pair of highly conserved Asn residues. Interestingly enough, cross species analysis of the sequence alignments of hexose facilitators showed that Ile/Val placed at the extracellular border of the TM7 are actually part of a highly conserved motif NXI/V. This structural similarity does not appear to be random as the proximity of a putative substrate binding site in the immediate proximity of a selectivity filter would respect the minimal energetic requirements of an efficient transport process.

For next steps of my research I am looking to identify the other determinants of the hypothesized selectivity filter structure. The first, candidate is the Trp89 in the

structure of GLUT7. This Trp is one of the six Trp residues conserved in the structure of all hexose facilitators and its proposed interaction with Ile314 indicates that the functional importance has not been entirely elucidated. Subsequently, I identified several hydrophobic residues within the intracellular side of the aqueous pore and efforts are still needed to elucidate the role and/or the presence of a similar selectivity filter within the efflux component of the transport.

Another direction in which I would like to focus my future research is the identification of the other components of the substrate binding site. To date, only indirect evidence is available regarding the number of residues involved in the binding of the hexose molecules. Equally, appealing and exciting seems the investigation of the possibility of having specific binding sites for different substrates. Also, the strong available evidence of substrate induced conformational changes of the transporter structures opens a whole new area of research where the role of a structural-functional complex formed by the transporter and specific substrates molecules during the translocation process, becomes crucial for understanding of GLUTs mechanism of function. To answer all these questions, I would design a dual strategy that combines the use of glucose analogues, with controlled substituted radical groups, and targeted site directed mutagenesis of putative binding sites. In this way one could get more insight regarding the direct interaction between the substrate and transporter. This approach is very generous and potentially could offer abundant information that could lead to the identification of specific substrates for specific GLUT isoforms. Needless, to say such

results could easily provide invaluable diagnostic and treatment tools with direct application within a variety of pathologies ranging from diabetes to oncology.

Appendix

Summary of kinetic properties for wild type and mutant class II GLUTs.

Transporter	Substrate	Km	Vmax	Comment
Glut7	glucose	0.3 mM	20 pmol/30min	P88
"	fructose	0.09	9	P89
Glut7 I314-Val	Glucose 100 μM			=wt
Glut7 I314-Val	Fructose100 μM			1/5 of wt
"	glucose	0.1 mM or 33+/-26 uM	30	
"	Glucose + cold Fructose	No competition		
Glut 7	"	IC50 60 uM F.		
Glut7 I314-Ser	Glucose 100 μM	0.3 mM	22	= wt
"	Fructose100 μM	0.8 mM	31	+50% vs wt
Glut 5	Glucose	0.65 mM	22	
Glut 9	Glucose and fructose 100 μM			Equal transport rates
"	fructose	1.1 mM	32	
"	glucose	0.4 mM	45	
Glut2 I322-Val	Glucose and Fructose100 μM			G=wt F=1/4 of wt
	glucose	0.9	10	
Glut5 I296-Val	Glucose and Fructose100 μM			G=wt F=1/20 of wt
"	glucose	0.36	18	
Glut9 I335-Val	Glucose and Fructose100μM			G=wt F=1/2 of wt
"	glucose	64 uM	28	
Glut 11A	glucose	0.116	7	
	Fructose	0.6	11	
" D296N	Glucose and Fructose100uM			=wt
" S298A	"			=wt
"V299I	"			=1/10 of wt
" NAI	"			=wt
" NAV	"			=50-70% of wt

References:

[1] Newsholme, E. A. & Leech, A. R.: ***Biochemistry for the medical sciences,*** 1985; John Wiley and Sons, Chichester

[2] Mueckler M. ***Facilitative glucose transporters.*** Eur. J. Biochem. 1994; 219,713-725.

[3] Collander R, ***The permeability of plant protoplasts to non-electrolytes***. Trans. Faraday Soc 1937; 33: 985-990.

[4] Overton E. ***Uber die allgemeinen osmotischen Eigenschaften der Zelle, ihre vermuticlichen Ursachen und ihre Bedeutung fur die Physiologie.*** Vjschr.Naturf.Ges.Zurich 1899; 44: 88-135.

[5] Overton E.: ***Beitrage zur allgemeinen Muskel- und Nervenphysiologie.*** Pflug.Arch.ges.Physiol. 1902; 92:115-280,346-386.

[6] Collander R, ***Uber die Durchlassigkeit der Kupferferrozyanidniederschlagsmembran fur Nichtelektrolyte***. Kolloidchem.Beih. 1924;19:72-105.

[7] Michaelis, L: ***Die Permeabilitat von Membranen.*** Naturwissenschaften 1926; 14: 33-42.

[8] Kozawa, S. ***Beitrage zum arteigenen Verhalten der rotten Blutkorperchen.*** Biochem.Z. 1914; 60: 231-256

.

[9] Osterhout, W.J. ***Permeability in large plant cells and in models.*** Ergebn.Physiol. 1933; 35: 967-1021.

[10] Lundegardh, H. ***Investigation as to the absorption and accumulation of inorganic ions***. LantbrHogsk.Ann 1940; 8: 233-404.

[11] Widas W.F. ***Inability of diffusion to account for placental glucose transfer in the sheep and consideration of the kinetics of a possible carrier transfer***. J. Physiolo. 1952; 118: 23-29.

[12] Ussing H.H. ***Some aspects of the application of tracers in permeability studies***. Advanc. Enzymol. 1952; 13: 21-65.

[13] LeFavre P.G. ***Evidence of active transfer of certain non-electrolytes across the human red cell membrane***. J Gen.Physiol. 1948; 31: 505-527.

[14] Wilbrandt W., Rosenberg T. ***The concept of carrier transport and its corollaries in pharmacology***. Pharmacol Rev. 1961; 13:109-83.

[15] Danielli J.F. ***Morphological and molecular aspects of active transport***. Symp. Soc. Exp.Biol. 1954; 8: 502-504.

[16] Stein W.D., Danielli J.F. ***Structure and function in red cell membrane***. Disc. Faraday Soc. 1956; 21:238-251.

[17] LeFavre P.G. ***Sugar transport in the red blood cells: Structure-activity relationship in substrates and antagonists***. Pharmacol. Rev. 1961;13:39-70

[18] Ross E.J. ***The influence of insulin on the permeability of the blood-aqueous barrier to glucose.*** J Physiol. 1952;116(4):414-23.

[19] Helmreich E, Cori CF. ***Studies of tissue permeability. II. The distribution of pentoses between plasma and muscle.*** J Biol Chem. 1957; 224(2):663-79.

[20] Kasahara M, Hinkle PC. ***Reconstitution and purification of the D-glucose transporter from human erythrocytes.*** J Biol Chem. 1977; 252(20):7384-90.

[21] Baldwin SA, Baldwin JM, Gorga FR, Lienhard GE. ***Purification of the cytochalasin B binding component of the human erythrocyte monosaccharide transport system.*** Biochim Biophys Acta. 1979; 552(1):183-8.

[22] Wheeler TJ, Hinkle PC. ***Kinetic properties of the reconstituted glucose transporter from human erythrocytes.*** J Biol Chem. 1981; 256(17):8907-14.

[23] Singer, SJ. Thermodynamics, the structure of integral membrane proteins, and transport. J Supramol Struct. 1977; 6(3):313-23.

[24] Wang JF, Falke JJ, Chan SI. ***A proton NMR study of the mechanism of the erythrocyte glucose transporter activity.*** Proc Natl Acad Sci U S A. 1986; 83(10):3277-81.

[25] Helgerson AL, Carruthers A. ***Equilibrium ligand binding to the human erythrocyte sugar transporter. Evidence for two sugar-binding sites per carrier.*** J Biol Chem. 1987; 262(12):5464-75.

[26] Carruthers A. ***ATP regulation of the human red cell sugar transporter.*** J Biol Chem. 1986; 261(24):11028-37.

[27] Appleman JR, Lienhard GE. ***Rapid kinetics of the glucose transporter from human erythrocytes. Detection and measurement of a half-turnover of the purified transporter.*** J Biol Chem. 1985; ;260(8):4575-8.

[28] Gorga FR, Lienhard GE. ***Changes in the intrinsic fluorescence of the human erythrocyte monosaccharide transporter upon ligand binding.*** Biochemistry. 1982;21(8):1905-8.

Zoccoli MA, Lienhard GE. ***Monosaccharide transport in protein-depleted vesicles from erythrocyte membranes.*** J Biol Chem. 1977; 252(10):3131-5.

[30] Jarvis SM, Ellory JC, Young JD. ***Radiation inactivation of the human erythrocyte nucleoside and glucose transporters.*** Biochim Biophys Acta. 1986; 855(2):312-5.

[31] Hebert DN, Carruthers A. ***Glucose transporter oligomeric structure determines transporter function. Reversible redox-dependent interconversions of tetrameric and dimeric GLUT1.*** J Biol Chem. 1992; 267(33):23829-38.

[32] Pessino A, Hebert DN, Woon CW, Harrison SA, Clancy BM, Buxton JM, Carruthers A, Czech MP. ***Evidence that functional erythrocyte-type glucose transporters are oligomers.*** J Biol Chem. 1991; 266(30):20213-7.

[33] Lowe AG, Walmsley AR. ***The kinetics of glucose transport in human red blood cells.*** Biochim Biophys Acta. 1986; 857(2):146-54.

[34] Walmsley AR, Lowe AG. ***Comparison of the kinetics and thermodynamics of the carrier systems for glucose and leucine in human red blood cells.*** Biochim Biophys Acta. 1987; 901(2):229-38.

[35] Joost HG, Thorens B. ***The extended GLUT-family of sugar/polyol transport facilitators: nomenclature, sequence characteristics, and potential function of its novel members (review).*** Mol Membr Biol. 2001; 18(4):247-56.

[36] Mueckler M, Caruso C, Baldwin SA, Panico M, Blench I, Morris HR, Allard WJ, Lienhard GE, Lodish HF. ***Sequence and structure of a human glucose transporter.*** Science. 1985; 229(4717):941-5.

[37] Flier JS, Mueckler M, McCall AL, Lodish HF. ***Distribution of glucose transporter messenger RNA transcripts in tissues of rat and man.*** J Clin Invest. 1987; 79(2):657-61.

[38] Gould GW, Bell GI. ***Facilitative glucose transporters: an expanding family.*** Trends Biochem Sci. 1990; 15(1):18-23.

[39] Elliott KR, Craik JD. ***Sugar transport across the hepatocyte plasma membrane.*** Biochem Soc Trans. 1982; 10(1):12-3.

[40] Fukumoto H, Seino S, Imura H, Seino Y, Eddy RL, Fukushima Y, Byers MG, Shows TB, Bell GI. ***Sequence, tissue distribution, and chromosomal localization of mRNA encoding a human glucose transporter-like protein.*** Proc Natl Acad Sci U S A. 1988; 85(15):5434-8.

[41] Thorens B, Sarkar HK, Kaback HR, Lodish HF. ***Cloning and functional expression in bacteria of a novel glucose transporter present in liver, intestine, kidney, and beta-pancreatic islet cells.*** 1988; Cell. 21;55(2):281-90.

[42] Orci L, Thorens B, Ravazzola M, Lodish HF. ***Localization of the pancreatic beta cell glucose transporter to specific plasma membrane domains.*** Science. 1989; 245(4915):295-7.

[43] Chen C, Thorens B, Bonner-Weir S, Weir GC, Leahy JL. ***Recovery of glucose-induced insulin secretion in a rat model of NIDDM is not accompanied by return of the B-cell GLUT2 glucose transporter.*** Diabetes. 1992; 41(10):1320-7.

[44] Thorens B. ***GLUT2 in pancreatic and extra-pancreatic gluco-detection (review).*** Mol Membr Biol. 2001; 18(4):265-73.

[45] Thorens B, Cheng ZQ, Brown D, Lodish HF. ***Liver glucose transporter: a basolateral protein in hepatocytes and intestine and kidney cells.*** Am J Physiol. 1990; 259(6 Pt 1):C279-85.

[46] Marks J, Carvou NJ, Debnam ES, Srai SK, Unwin RJ. ***Diabetes increases facilitative glucose uptake and GLUT2 expression at the rat proximal tubule brush border membrane.*** J Physiol. 2003;553(Pt 1):137-45.

[47] Au A, Gupta A, Schembri P, Cheeseman CI. ***Rapid insertion of GLUT2 into the rat jejunal brush-border membrane promoted by glucagon-like peptide 2.*** Biochem J. 2002; 367(Pt 1):247-54.

[48] Nagamatsu S, Kornhauser JM, Burant CF, Seino S, Mayo KE, Bell GI. ***Glucose transporter expression in brain. cDNA sequence of mouse GLUT3, the brain***

facilitative glucose transporter isoform, and identification of sites of expression by in situ hybridization. J Biol Chem. 1992; 267(1):467-72.

[49] Haber RS, Weinstein SP, O'Boyle E, Morgello S. ***Tissue distribution of the human GLUT3 glucose transporter.*** Endocrinology. 1993; 132(6):2538-43.

[50] Kozka IJ, Clark AE, Reckless JP, Cushman SW, Gould GW, Holman GD. ***The effects of insulin on the level and activity of the GLUT4 present in human adipose cells.*** Diabetologia. 1995; 38(6):661-6.

[51] Cushman SW, Wardzala LJ. ***Potential mechanism of insulin action on glucose transport in the isolated rat adipose cell. Apparent translocation of intracellular transport systems to the plasma membrane.*** J Biol Chem. 1980; 255(10):4758-62.

[52] James DE, Brown R, Navarro J, Pilch PF. ***Insulin-regulatable tissues express a unique insulin-sensitive glucose transport protein.*** Nature. 1988; 333(6169):183-5.

[53] Kobayashi H, Mitsui T, Nomura S, Ohno Y, Kadomatsu K, Muramatsu T, Nagasaka T, Mizutani S. ***Expression of glucose transporter 4 in the human pancreatic islet of Langerhans.*** Biochem Biophys Res Commun. 2004; 314(4):1121-5.

[54] Garcia JC, Strube M, Leingang K, Keller K, Mueckler MM. ***Amino acid substitutions at tryptophan 388 and tryptophan 412 of the HepG2 (Glut1) glucose transporter inhibit transport activity and targeting to the plasma membrane in Xenopus oocytes.*** J Biol Chem. 1992; 267(11):7770-6.

[55] Schurmann A, Keller K, Monden I, Brown FM, Wandel S, Shanahan MF, Joost HG. ***Glucose transport activity and photolabelling with 3-[125I]iodo-4-azidophenethylamido-7-O-succinyldeacetyl (IAPS)-forskolin of two mutants at tryptophan-388 and -412 of the glucose transporter GLUT1: dissociation of the binding domains of forskolin and glucose.*** Biochem J. 1993;290 (Pt 2):497-501

[56] Kayano T, Burant CF, Fukumoto H, Gould GW, Fan YS, Eddy RL, Byers MG, Shows TB, Seino S, Bell GI. ***Human facilitative glucose transporters. Isolation, functional characterization, and gene localization of cDNAs encoding an isoform (GLUT5) expressed in small intestine, kidney, muscle, and adipose tissue and an unusual glucose transporter pseudogene-like sequence (GLUT6).*** J Biol Chem. 1990; 265(22):13276-82.

[57] Burant CF, Takeda J, Brot-Laroche E, Bell GI, Davidson NO. ***Fructose transporter in human spermatozoa and small intestine is GLUT5.*** J Biol Chem. 1992; 267(21):14523-6.

[58] Joost HG, Thorens B. ***The extended GLUT-family of sugar/polyol transport facilitators: nomenclature, sequence characteristics, and potential function of its novel members (review).*** Mol Membr Biol. 2001; 18(4):247-56.

[59] Phay JE, Hussain HB, Moley JF. ***Cloning and expression analysis of a novel member of the facilitative glucose transporter family, SLC2A9 (GLUT9).*** Genomics. 2000; 66(2):217-20.

[60] Augustin R, Carayannopoulos MO, Dowd LO, Phay JE, Moley JF, Moley KH. ***Identification and characterization of human glucose transporter-like protein-9 (GLUT9): alternative splicing alters trafficking.*** J Biol Chem. 2004; 279(16):16229-36.

[61] Doege H, Bocianski A, Scheepers A, Axer H, Eckel J, Joost HG, Schurmann A. ***Characterization of human glucose transporter (GLUT) 11 (encoded by SLC2A11), a novel sugar-transport facilitator specifically expressed in heart and skeletal muscle.*** Biochem J. 2001; 359:443-9.

[62] Doege H, Bocianski A, Joost HG, Schurmann A. ***Activity and genomic organization of human glucose transporter 9 (GLUT9), a novel member of the family of sugar-transport facilitators predominantly expressed in brain and leucocytes.*** Biochem J. 2000; 350 Pt 3:771-6.

[63] Ibberson M, Uldry M, Thorens B. ***GLUTX1, a novel mammalian glucose transporter expressed in the central nervous system and insulin-sensitive tissues.*** J Biol Chem. 2000; 275(7):4607-12.

[64] Doege H, Schurmann A, Bahrenberg G, Brauers A, Joost HG. ***GLUT8, a novel member of the sugar transport facilitator family with glucose transport activity.*** J Biol Chem. 2000; 275(21):16275-80.

[65] Carayannopoulos MO, Chi MM, Cui Y, Pingsterhaus JM, McKnight RA, Mueckler M, Devaskar SU, Moley KH. ***GLUT8 is a glucose transporter responsible for insulin-stimulated glucose uptake in the blastocyst.*** Proc Natl Acad Sci U S A. 2000; 97(13):7313-8.

[66] Reagan LP, Rosell DR, Alves SE, Hoskin EK, McCall AL, Charron MJ, McEwen BS. ***GLUT8 glucose transporter is localized to excitatory and inhibitory neurons in the rat hippocampus.*** Brain Res. 2002; 932(1-2):129-34.

[67] McVie-Wylie AJ, Lamson DR, Chen YT. ***Molecular cloning of a novel member of the GLUT family of transporters, SLC2A10 (GLUT10), localized on chromosome 20q13.1: a candidate gene for NIDDM susceptibility.*** 2001; Genomics.72(1):113-7.

[68] Rogers S, Chandler JD, Clarke AL, Petrou S, Best JD. ***Glucose transporter GLUT12-functional characterization in Xenopus laevis oocytes.*** Biochem Biophys Res Commun. 2003; 308(3):422-6.

[69] Wu X, Freeze HH. ***GLUT14, a duplicon of GLUT3, is specifically expressed in testis as alternative splice forms.*** Genomics. 2002 ; 80(6):553-7.

[70] Uldry M, Ibberson M, Horisberger JD, Chatton JY, Riederer BM, Thorens B. ***Identification of a mammalian H^+-myo-inositol symporter expressed predominantly in the brain.*** EMBO J. 2001; 20(16):4467-77.

[71] Zuniga FA, Shi G, Haller JF, Rubashkin A, Flynn DR, Iserovich P, Fischbarg J. ***A three-dimensional model of the human facilitative glucose transporter Glut1*** . J Biol Chem. 2001;30;276(48):44970-5..

[72] Hruz PW, Mueckler MM. ***Structural analysis of the GLUT1 facilitative glucose transporter (review). Mol Membr Biol.*** 2001;18(3):183-93

[73] Olsowski A, Monden I, Krause G, Keller K. ***Cysteine scanning mutagenesis of helices 2 and 7 in GLUT1 identifies an exofacial cleft in both transmembrane segments.*** *Biochemistry.* 2000 ;39(10):2469-74.

[74] Dwyer DS. ***Model of the 3-D structure of the GLUT3 glucose transporter and molecular dynamics simulation of glucose transport.*** *Proteins.* 2001;42(4):531-41.

[75] Carruthers A. ***Facilitated diffusion of glucose.*** Physiol Rev. 1990 ;70(4):1135-76.

[76] Erin K. Cloherty, Karen S. Heard, and Anthony Carruthers. ***Human Erythrocyte Sugar Transport is Incompatible with Available Carrier Models.*** Biochemistry. 1996;35(32):10411-21.

[77] Alvarez J, Lee DC, Baldwin SA, Chapman D. ***Fourier transform infrared spectroscopic study of the structure and conformational changes of the human erythrocyte glucose transporter.*** J Biol Chem 1987; 262(8):3502-9.

[78] Chin JJ, Jung EK, Jung CY. ***Structural basis of human erythrocyte glucose transporter function in reconstituted vesicles.*** J Biol Chem 1986; 261(16):7101-4.

[79] Jung EK, Chin JJ, Jung CY. ***Structural basis of human erythrocyte glucose transporter function in reconstituted system. Hydrogen exchange.*** J Biol Chem 1986; 261(20):9155-60.

[80] Hresko RC, Kruse M, Strube M, Mueckler M. ***Topology of the Glut 1 glucose transporter deduced from glycosylation scanning mutagenesis.*** J Biol Chem. 1994; 269(32):20482-8.

[81] Cairns MT, Alvarez J, Panico M, Gibbs AF, Morris HR, Chapman D, Baldwin SA. ***Investigation of the structure and function of the human erythrocyte glucose transporter by proteolytic dissection.*** Biochim Biophys Acta. 1987; 905(2):295-310.

[82] Joost HG, Thorens B. ***The extended GLUT-family of sugar/polyol transport facilitators: nomenclature, sequence characteristics, and potential function of its novel members (review).*** Mol Membr Biol. 2001; 18(4):247-56.

[83] Asano T, Katagiri H, Takata K, Lin JL, Ishihara H, Inukai K, Tsukuda K, Kikuchi M, Hirano H, Yazaki Y. ***The role of N-glycosylation of GLUT1 for glucose transport activity.*** J Biol Chem. 1991; 266(36):24632-6.

[84] Gould GW, Holman GD. ***The glucose transporter family: structure, function and tissue-specific expression.*** Biochem J. 1993;295 (Pt 2):329-41.

[85] Zeng H, Parthasarathy R, Rampal AL, Jung CY. ***Proposed structure of putative glucose channel in GLUT1 facilitative glucose transporter.*** Biophys J. 1996; 70(1):14-21.

[86] Dwyer DS. ***Model of the 3-D structure of the GLUT3 glucose transporter and molecular dynamics simulation of glucose transport.*** Proteins. 2001; 42(4):531-41.

[87] Zuniga FA, Shi G, Haller JF, Rubashkin A, Flynn DR, Iserovich P, Fischbarg J. ***A three-dimensional model of the human facilitative glucose transporter Glut1.*** J Biol Chem. 2001; 276(48):44970-5.

[88] Lemieux MJ, Huang Y, Wang DN. ***Glycerol-3-phosphate transporter of Escherichia coli: structure, function and regulation.*** Res Microbiol. 2004;155(8):623-9.

[89] Abramson J, Iwata S, Kaback HR. ***Lactose permease as a paradigm for membrane transport proteins (Review).*** Mol Membr Biol. 2004;21(4):227-36

[90] Mueckler M, Caruso C, Baldwin SA, Panico M, Blench I, Morris HR, Allard WJ, Lienhard GE, Lodish HF. ***Sequence and structure of a human glucose transporter.*** Science. 1985; 229(4717):941-5.

[91] Vidaver GA. ***Inhibition of parallel flux and augmentation of counter flux shown by transport models not involving a mobile carrier.*** J Theor Biol. 1966;10(2):301-6.

[92] Barnett JE, Holman GD, Munday KA. ***Structural requirements for binding to the sugar-transport system of the human erythrocyte.*** Biochem J. 1973;131(2):211-21.

[93] Rees WD, Holman GD. ***Hydrogen bonding requirements for the insulin-sensitive sugar transport system of rat adipocytes.*** Biochim Biophys Acta. 1981 ;646(2):251-60.

[94] Barnett JE, Holman GD, Chalkley RA, Munday KA. ***Evidence for two asymmetric conformational states in the human erythrocyte sugar-transport system.*** Biochem J. 1975;145(3):417-29.

[95] Holman GD, Rees WD. ***Side-specific analogues for the rat adipocyte sugar transport system.*** Biochim Biophys Acta. 1982;8;685(1):78-86.

[96] Yang J, Dowden J, Tatibouet A, Hatanaka Y, Holman GD. ***Development of high-affinity ligands and photoaffinity labels for the D-fructose transporter GLUT5.*** Biochem J. 2002;367(Pt 2):533-9.

[97] Koumanov F, Yang J, Jones AE, Hatanaka Y, Holman GD. ***Cell-surface biotinylation of GLUT4 using bis-mannose photolabels.*** Biochem J. 1998;330 (Pt 3):1209-15.

[98] Tatibouet A, Yang J, Morin C, Holman GD. ***Synthesis and evaluation of fructose analogues as inhibitors of the D-fructose transporter GLUT5.*** Bioorg Med Chem. 2000;8(7):1825-33.

[99] Mueckler M, Weng W, Kruse M. ***Glutamine 161 of Glut1 glucose transporter is critical for transport activity and exofacial ligand binding.*** J Biol Chem. 1994;269(32):20533-8.

[100] Hashiramoto M, Kadowaki T, Clark AE, Muraoka A, Momomura K, Sakura H, Tobe K, Akanuma Y, Yazaki Y, Holman GD, et al. ***Site-directed mutagenesis of GLUT1 in helix 7 residue 282 results in perturbation of exofacial ligand binding.*** J Biol Chem. 1992;267(25):17502-7

[101] Seatter, MJ, De La Rue, SA, Porter, LM, Gould, GW. ***The QLS motif in transmembrane helix VII of the glucose transporter (GLUT) family interacts with C-1 position of D-glucose and is involved in substrate selection at the exofacial binding site***. Biochem. 1998; 37:1322-1326.

[102] Wellner M, Monden I, Mueckler MM, Keller K. ***Functional consequences of proline mutations in the putative transmembrane segments 6 and 10 of the glucose transporter GLUT1.*** Eur J Biochem. 1995;227(1-2):454-8.

[103] Hresko RC, Kruse M, Strube M, Mueckler M. ***Topology of the Glut 1 glucose transporter deduced from glycosylation scanning mutagenesis.*** J Biol Chem. 1994; 269(32):20482-8.

[104] Olsowski A, Monden I, Krause G, Keller K. ***Cysteine scanning mutagenesis of helices 2 and 7 in GLUT1 identifies an exofacial cleft in both transmembrane segments***. *Biochemistry.* 2000 ;39(10):2469-74.

[105] Hruz PW, Mueckler MM. ***Cysteine-scanning mutagenesis of transmembrane segment 7 of the GLUT1 glucose transporter.*** J Biol Chem. 1999; 274(51):36176-80.

[106] Doege H, Schurmann A, Ohnimus H, Monser V, Holman GD, Joost HG. ***Serine-294 and threonine-295 in the exofacial loop domain between helices 7 and 8 of glucose transporters (GLUT) are involved in the conformational alterations during the transport process.*** Biochem J. 1998;329 (Pt 2):289-93.

[107] Mueckler M, Makepeace C. ***Analysis of transmembrane segment 8 of the GLUT1 glucose transporter by cysteine-scanning mutagenesis and substituted cysteine accessibility.*** Biol Chem. 2004;279(11):10494-9.

[108] Wandel S, Schurmann A, Becker W, Summers SA, Shanahan MF, Joost HG. ***Mutation of two conserved arginine residues in the glucose transporter GLUT4 supresses transport activity, but not glucose-inhibitable binding of inhibitory ligands.*** Naunyn Schmiedebergs Arch Pharmacol.1995;353(1):36-41.

[109] Mueckler, M., and C. Makepeace. ***Analysis of transmembrane segment 10 of the Glut1 glucose transporter by cysteine-scanning mutagenesis and substituted cysteine accessibility.*** *J. Biol. Chem.* . 2002 277:3498–3503

[110] Hruz PW, Mueckler MM. ***Cysteine-scanning mutagenesis of transmembrane segment 11 of the GLUT1 facilitative glucose transporter.*** Biochemistry;39(31):9367-72. 2000

[111] Heinze M, Monden I, Keller K. ***Cysteine-scanning mutagenesis of transmembrane segment 1 of glucose transporter GLUT1: extracellular accessibility of helix positions.*** Biochemistry.2004;43(4):931-6.

[112] Schirmer T, Keller TA, Wang YF, Rosenbusch JP. ***Structural basis for sugar translocation through maltoporin channels at 3.1 A resolution.*** Science. 1995;267(5197):512-4.

[113] Forst D, Welte W, Wacker T, Diederichs K. ***Structure of the sucrose-specific porin ScrY from Salmonella typhimurium and its complex with sucrose.*** Nat Struct Biol. 1998;5(1):37-46.

[114] Garcia JC, Strube M, Leingang K, Keller K, Mueckler MM. ***Amino acid substitutions at tryptophan 388 and tryptophan 412 of the HepG2 (Glut1) glucose transporter inhibit transport activity and targeting to the plasma membrane in Xenopus oocytes.*** J Biol Chem. 1992; 267(11):7770-6.

[115] Schurmann A, Keller K, Monden I, Brown FM, Wandel S, Shanahan MF, Joost HG. ***Glucose transport activity and photolabelling with 3-[125I]iodo-4-azidophenethylamido-7-O-succinyldeacetyl (IAPS)-forskolin of two mutants at***

tryptophan-388 and -412 of the glucose transporter GLUT1: dissociation of the binding domains of forskolin and glucose. Biochem J. 1993;290 (Pt 2):497-501

[116] Tamori Y, Hashiramoto M, Clark AE, Mori H, Muraoka A, Kadowaki T, Holman GD, Kasuga M. ***Substitution at Pro385 of GLUT1 perturbs the glucose transport function by reducing conformational flexibility.*** J Biol Chem. 1994;269(4):2982-6.

[117] Williams KA, Deber CM. ***Proline residues in transmembrane helices: structural or dynamic role?*** Biochemistry. 1991;30(37):8919-23.

[118] Vilsen B, Andersen JP, Clarke DM, MacLennan DH. ***Functional consequences of proline mutations in the cytoplasmic and transmembrane sectors of the Ca^{2+}-ATPase of sarcoplasmic reticulum.*** J Biol Chem.1990;264(35):21024-30.

[119] Kawakami T, Akizawa Y, Ishikawa T, Shimamoto T, Tsuda M, Tsuchiya T. ***Amino acid substitutions and alteration in cation specificity in the melibiose carrier of Escherichia coli.*** J Biol Chem. 1988;263(28):14276-80.

[120] Consler TG, Tsolas O, Kaback HR. ***Role of proline residues in the structure and function of a membrane transport protein.*** Biochemistry. 1991;30(5):1291-8.

[121] Brandl CJ, Deber CM. ***Hypothesis about the function of membrane-buried proline residues in transport proteins.*** Proc Natl Acad Sci U S A. 1986 Feb;83(4):917-21.

[122] Chou PY, Fasman GD. ***Prediction of the secondary structure of proteins from their amino acid sequence.*** Adv Enzymol Relat Areas Mol Biol. 1978;47:45-148.

[123] Pawagi AB, Deber CM. ***Ligand-dependent quenching of tryptophan fluorescence in human erythrocyte hexose transport protein.*** Biochemistry. 1990;29(4):950-5.

[124] Deisenhofer J, Epp O, Miki K, Huber R, Michel H. ***X-ray structure analysis of a membrane protein complex. Electron density map at 3 A resolution and a model of the chromophores of the photosynthetic reaction center from Rhodopseudomonas viridis.*** J Mol Biol. 1984;180(2):385-98.

[125] von Heijne G. ***Proline kinks in transmembrane alpha-helices.*** J Mol Biol. 1991;218(3):499-503.

[126] Wellner M, Monden I, Mueckler MM, Keller K. ***Functional consequences of proline mutations in the putative transmembrane segments 6 and 10 of the glucose transporter GLUT1.*** Eur J Biochem. 1995;227(1-2):454-8.

[127] Mori H, Hashiramoto M, Clark AE, Yang J, Muraoka A, Tamori Y, Kasuga M, Holman GD. ***Substitution of tyrosine 293 of GLUT1 locks the transporter into an outward facing conformation.*** J Biol Chem. 1994;269(15):11578-83.

[128] Lebron JA, Bennett MJ, Vaughn DE, Chirino AJ, Snow PM, Mintier GA, Feder JN, Bjorkman PJ. ***Crystal structure of the hemochromatosis protein HFE and characterization of its interaction with transferrin receptor.*** Cell. 1998;93(1):111-23.

[129] Mueckler M, Makepeace C. ***Analysis of transmembrane segment 8 of the GLUT1 glucose transporter by cysteine-scanning mutagenesis and substituted cysteine accessibility.*** J Biol Chem.

[130] Alisio A, Mueckler M. ***Relative proximity and orientation of helices 4 and 8 of the GLUT1 glucose transporter.*** J Biol Chem. 2004;279(25):26540-5.

[131] Mueckler M, Makepeace C. ***Transmembrane segment 5 of the Glut1 glucose transporter is an amphipathic helix that forms part of the sugar permeation pathway.*** J Biol Chem. 1999;274(16):10923-6.

[132] Mueckler M, Makepeace C. ***Identification of an amino acid residue that lies between the exofacial vestibule and exofacial substrate-binding site of the Glut1 sugar permeation pathway***. J Biol Chem. 1997;272(48):30141-6.

[133] Kaback HR, Wu J. ***From membrane to molecule to the third amino acid from the left with a membrane transport protein.*** Q Rev Biophys. 1997;30(4):333-64

[134] Yan RT, Maloney PC. ***Residues in the pathway through a membrane transporter.*** Proc Natl Acad Sci U S A. 1995;92(13):5973-6.

[135] Dayhoff M.O., Schwartz R. and Orcutt B.C. ***Atlas of protein sequence and structure.*** 1978 Vol. 5, Suppl. 3, Ed. M. O. Dayhoff.

[136] Feng, D.-F. and Doolittle, R.F. ***Progressive sequence alignment as a prerequisite to correct phylogenetic trees.*** J.Mol.Evol. 1987; 25, 351-360.

[137]Higgins, D.G. and Sharp, P.M. ***Fast and sensitive multiple sequence alignments on a microcomputer.*** CABIOS 5, 1989; 151-153.

[138] Higgins, D.G. and Sharp, P.M. ***CLUSTAL: a package for performing multiple sequence alignments on a microcomputer.*** Gene 73, 1988; 237-244.

[139] Wilbur, W.J. and Lipman, D.J. ***Rapid similarity searches of nucleic acid and protein data banks.*** PNAS USA 1983; 80, 726-730.

[140] Hess, B., Bekker, H., Berendsen, H. J. C., and Fraaije, J. G. E. M. ***LINCS: a linear constraint solver for molecular simulations.*** Journal of Computational Chemistry. 1997; 18, 1463-1472

[141] Miyamoto, S., , Kollman, P. A. ***SETTLE: an analytical version of the SHAKE and RATTLE algorithms for rigid water models.*** Journal of Computational Chemistry. 1992; 13, 952-962

[142] Lindahl, E., Hess, B., van der Spoel, D. ***GROMACS 3.0: a package for molecular simulation and trajectory analysis*** J. Mol. Mod. 2001; **7**, 306-317.

[143] Henikoff S, Henikoff JG. ***Automated assembly of protein blocks for database searching.*** Nucleic Acids Res. 1991;19(23):6565-72.

[144] Preston, R. A., and S. A. Baldwin. ***GLUT 1: identification of exofacial lysine-residues***. Biochem. Soc. Trans. 1993; 21:309–312

[145] Xiang, Z., and B. Honig. ***Extending the accuracy limits of prediction for side-chain conformations***. J. Mol. Biol. 200; 1311:421–430

[146] Sali, A., and T. L. Blundell. ***Comparative protein modelling by satisfaction of spatial restraints***. J. Mol. Biol. 1993; 234:779–815

[147] Laskowki, R. A., M. W. MacArthur, D. S. Moss, and J. M. Thornton. ***PROCHECK: a program to check the stereochemical quality of protein structures***. J. Appl. Crystallog. 199326:283–291

[148] van Aalten, D. M., R. Bywater, J. B. Findlay, M. Hendlich, R. W. Hooft, and G. Vriend.. ***PRODRG, a program for generating molecular topologies and unique molecular descriptors from coordinates of small molecules.*** J. Comput. Aided Mol. Des. 1996; 10:255–262

[149] Altschul, S., T. Madden, A. Schaffer, J. Zhang, Z. Zhang, W. Miller, and D. Lipman.. ***Gapped BLAST and PSI-BLAST: a new generation of protein database search programs***. Nucleic Acids Res. 1997; 25:3389–3402

[150] Kleywegt, G. J., and T. A. Jones.. ***Detection, delineation, measurement and display of cavities in macromolecular structures***. Acta Crystallogr. 1994; D50:178–185.

[151] Kleywegt, G. J., and T. A. Jone. ***xdlMAPMAN and xdlDATAMAN—programs for reformatting, analysis and manipulation of biomacromolecular electron-density maps and reflection data sets***. Acta Crystallogr. 1996; D52:826–828

[152] Kleywegt, G. J., and T. A. Jones. ***Software for handling macromolecular envelopes***. Acta Crystallogr. . 1999; D55:941–944

[153] Humphrey, W., A. Dalke, and K. Schulten.. ***VMD: visual molecular dynamics***. J. Mol. Graph. 1996.; 14:33–38

[154] Morris, G. M., Goodsell, D. S., Halliday, R. S., Huey, R., Hart, W. E., Belew, R. K.,Olson, A. J. ***Distributed automated docking of flexible ligands to proteins: parallel applications of AutoDock 2.4.*** *J. Computational Chemistry* 1998;19(14), 1639-1662

[155] Gurdon JB, Lane CD, Woodland HR, Marbaix G. ***Use of frog eggs and oocytes for the study of messenger RNA and its translation in living cells.*** Nature. 1971; 233(5316):177-82.

[156] Hediger MA, Ikeda T, Coady M, Gundersen CB, Wright EM. ***Expression of size-selected mRNA encoding the intestinal Na/glucose cotransporter in Xenopus laevis oocytes.*** Proc Natl Acad Sci U S A. 1987; 84(9):2634-7.

[157] Dumont JN. ***Oogenesis in Xenopus laevis (Daudin). I. Stages of oocyte development in laboratory maintained animals.*** J Morphol. 1972; 136(2):153-79.

[158] Li Q, Manolescu A, Ritzel M, Yao S, Slugoski M, Young JD, Chen XZ, Cheeseman CI. ***Cloning and functional characterization of the human GLUT7 isoform SLC2A7 from the small intestine.*** Am J Physiol Gastrointest Liver Physiol. 2004;287(1):G236-42.

[159] Manolescu A, Salas-Burgos AM, Fischbarg J, Cheeseman CI. ***Identification of a hydrophobic residue as a key determinant of fructose transport by the facilitative hexose transporter SLC2A7(GLUT7).*** J Biol Chem. 2005 Sep 26; [Epub ahead of print]

[160] Mueckler M, Makepeace C. ***Analysis of transmembrane segment 8 of the GLUT1 glucose transporter by cysteine-scanning mutagenesis and substituted cysteine accessibility***. J Biol Chem. 2004 12;279(11):10494-9

[161] Salas-Burgos A, Iserovich P, Zuniga F, Vera JC, Fischbarg J. ***Predicting the three-dimensional structure of the human facilitative glucose transporter glut1 by a novel evolutionary homology strategy: insights on the molecular mechanism of substrate***

migration, and binding sites for glucose and inhibitory molecules. Biophys J. 2004;87(5):2990-9

[163] Burant CF, Takeda J, Brot-Laroche E, Bell GI, Davidson NO. ***Fructose transporter in human spermatozoa and small intestine is GLUT5.*** J Biol Chem. 1992;267(21):14523-6.

[164] Augustin R, Carayannopoulos MO, Dowd LO, Phay JE, Moley JF, Moley KH. ***Identification and characterization of human glucose transporter-like protein-9 (GLUT9): alternative splicing alters trafficking.*** J Biol Chem. 2004;279(16):16229-36

[165] Seatter, MJ, De La Rue, SA, Porter, LM, Gould, GW. ***The QLS motif in transmembrane heix VII of the glucose transporter (GLUT) family interacts with C-1 position of D-glucose and is involved in substrate selection at the exofacial binding site.*** Biochem. 1998; 37:1322-1326.

[166] Corpe CP, Basaleh MM, Affleck J, Gould G, Jess TJ, and Kellett GL. ***The regulation of GLUT5 and GLUT2 activity in the adaptation of intestinal brush-border fructose transport in diabetes.*** Pflugers Arch , 1996; 432: 192-201

[167] Wu X, Li W, Sharma V, Godzik A, and Freeze HH. ***Cloning and characterization of glucose transporter 11, a novel sugar transporter that is alternatively spliced in various tissues***. Mol Genet Metab 2002; 76: 37-45,.

[168] Cheeseman CI. ***Role of intestinal basolateral membrane in absorption of nutrients***. Am J Physiol 1992; 263: R482-R488.

[169] Cheeseman CI. ***GLUT2 is the transporter for fructose across the rat intestinal basolateral membrane.*** Gastroenterology, 1993; 105: 1050-1056.

[170] Johnson JH, Newgard CB, Milburn JL, Lodish HF, and Thorens B. ***The high Km glucose transporter of islets of Langerhans is functionally similar to the low affinity transporter of liver and has an identical primary sequence***. J Biol Chem, 1990; 265: 6548-6551.

[171] Keller K and Mueckler ***M. Different mammalian facilitative glucose transporters expressed in Xenopus oocytes.*** *Biomed Biochim Acta* 49: 1201-1203, 1990.

[172] Dawson PA, Mychaleckyj JC, Fossey SC, Mihic SJ, Craddock AL, and Bowden DW. ***Sequence and functional analysis of GLUT10: a glucose transporter in the Type 2 diabetes-linked region of chromosome 20q12-13.1***. Mol Genet Metab, 2001; 74: 186-199.

[173] Davidson NO, Hausman AM, Ifkovits CA, Buse JB, Gould GW, Burant CF, and Bell GI. ***Human intestinal glucose transporter expression and localization of GLUT5.*** Am J Physiol, 1992; 262: C795-C800.

[174] Hwang ES, Hirayama BA, and Wright EM. ***Distribution of the SGLT1 Na+/glucose cotransporter and mRNA along the crypt-villus axis of rabbit small intestine***. Biochem Biophys Res Commun, 1991 181: 1208-1217

[175] Thorens B, Cheng ZQ, Brown D, and Lodish HF. ***Liver glucose transporter: a basolateral protein in hepatocytes and intestine and kidney cells***. Am J Physiol 1990; 259: C279-C285,

[176] Lam JT, Martin MG, Turk E, Hirayama BA, Bosshard NU, Steinmann B, and Wright EM. ***Missense mutations in SGLT1 cause glucose-galactose malabsorption by trafficking defects***. Biochim Biophys Acta, 1999 1453: 297-303

[177] Maenz, DD, & Cheeseman, CI. ***Effect of hyperglycemia on D-glucose transport across the brush-border and basolateral membranes of rat small intestine***. Biochim. Biophys. Acta. , 1986;860: 277-285.

[178] Turk E, Zabel B, Mundlos S, Dyer J, and Wright EM. ***Glucose/galactose malabsorption caused by a defect in the Na+/glucose cotransporter***. Nature, 1991; 350: 354-356.

[179] Helliwell PA, Richardson M, Affleck J, and Kellett GL. ***Regulation of GLUT5, GLUT2 and intestinal brush-border fructose absorption by the extracellular signal-regulated kinase, p38 mitogen-activated kinase and phosphatidylinositol 3-kinase intracellular signalling pathways: implications for adaptation to diabetes.*** Biochem J , 2000 350 Pt 1: 163-169

[180] Kellett GL. ***The facilitated component of intestinal glucose absorption***. J Physiol , 2001;531: 585-595

[181] Kellett GL and Helliwell PA. ***The diffusive component of intestinal glucose absorption is mediated by the glucose-induced recruitment of GLUT2 to the brush-border membrane.*** Biochem J 2000;350 Pt 1: 155-162,

[182] Levy Y, Wolynes PG, Onuchic JN. ***Protein topology determines binding mechanism.*** Proc Natl Acad Sci U S A.101(2):511-6. 2004

[183] Anfinsen CB. ***Principles that govern the folding of protein chains.*** Science. 1973;181(96):223-30.

[184] Creighton TE. ***Toward a better understanding of protein folding pathways.*** Proc Natl Acad Sci U S A. 1988 85(14):5082-6.

[185] Go N. ***Theoretical studies of protein folding.*** Annu Rev Biophys Bioeng. 1983;12:183-210

[186] Lemieux MJ, Huang Y, Wang DN. ***Glycerol-3-phosphate transporter of Escherichia coli: structure, function and regulation.*** Res Microbiol. 2004;155(8):623-9.

[187] Abramson J, Iwata S, Kaback HR. ***Lactose permease as a paradigm for membrane transport proteins (Review).*** Mol Membr Biol. 2004;21(4):227-36

[188] Bryngelson JD, Wolynes PG. ***Spin glasses and the statistical mechanics of protein folding.*** Proc Natl Acad Sci U S A. 1987;84(21):7524-8.

[189] Hardin C, Eastwood MP, Prentiss M, Luthey-Schulten Z, Wolynes PG. ***Folding funnels: the key to robust protein structure prediction.*** J Comput Chem. 2002;23(1):138-46.

[190] Hashiramoto M, Kadowaki T, Clark AE, Muraoka A, Momomura K, Sakura H, Tobe K, Akanuma Y, Yazaki Y, Holman GD. ***Site-directed mutagenesis of GLUT1 in helix 7 residue 282 results in perturbation of exofacial ligand binding.*** J Biol Chem. 1992;267(25):17502-7

[191] Rees WD, Holman GD. ***Hydrogen bonding requirements for the insulin-sensitive sugar transport system of rat adipocytes.*** Biochim Biophys Acta. 1981;646(2):251-60.

[192] Barnett JE, Holman GD, Munday KA. ***Structural requirements for binding to the sugar-transport system of the human erythrocyte.*** Biochem J. 1973;131(2):211-21.

[193] Barnett JE, Holman GD, Chalkley RA, Munday KA. ***Evidence for two asymmetric conformational states in the human erythrocyte sugar-transport system.*** Biochem J. 1975; 145(3):417-29.

[194] Gibbs AF, Chapman D, Baldwin SA. ***Proteolytic dissection as a probe of conformational changes in the human erythrocyte glucose transport protein.*** Biochem J. 1988;256(2):421-7.

[195] Clark AE, Holman GD. ***Exofacial photolabelling of the human erythrocyte glucose transporter with an azitrifluoroethylbenzoyl-substituted bismannose.*** Biochem J. 1990;269(3):615-22.

[196] Holman GD, Rees WD. ***Photolabelling of the hexose transporter at external and internal sites: fragmentation patterns and evidence for a conformational change.*** Biochim Biophys Acta. 1987 ;897(3):395-405.

[197] King AP, Tai PK, Carter-Su C. ***Cytochalasin B interferes with conformational changes of the human erythrocyte glucose transporter induced by internal and external sugar binding.*** Biochemistry. 1991;30(49):11546-53

[198] Manolescu A, Salas-Burgos AM, Fischbarg J, Cheeseman CI. ***Identification of a hydrophobic residue as a key determinant of fructose transport by the facilitative hexose transporter SLC2A7(GLUT7).*** Biol Chem. 2005 Sep 26; [Epub ahead of print].

[199] Go N. ***Theoretical studies of protein folding.*** Annu Rev Biophys Bioeng. 1983;12:183-210.

[200] Bryngelson JD, Onuchic JN, Socci ND, Wolynes PG. ***Funnels, pathways, and the energy landscape of protein folding: a synthesis.*** Proteins. 1995;21(3):167-95

[201] Onuchic JN, Luthey-Schulten Z, Wolynes PG. ***Theory of protein folding: the energy landscape perspective.*** Annu Rev Phys Chem. 1997;48:545-600

[202] Taketomi H, Ueda Y, Go N. ***Studies on protein folding, unfolding and fluctuations by computer simulation. I. The effect of specific amino acid sequence represented by specific inter-unit interactions.*** Int J Pept Protein Res. 1975;7(6):445-59.

[203] Leopold PE, Montal M, Onuchic JN. ***Protein folding funnels: a kinetic approach to the sequence-structure relationship.*** Proc Natl Acad Sci U S A. 1992;89(18):8721-5

[204] Dill KA, Chan HS. ***From Levinthal to pathways to funnels.*** Nat Struct Biol. 1997;4(1):10-9.

[205] Poland D, Scheraga HA, ***Theory of helix-coil transitions in polymers***. Academic, New York. 1970

[206] Savage H, Wlodawer A. ***Determination of water structure around biomolecules using X-ray and neutron diffraction methods.*** Methods Enzymol. 1986;127:162-83

[207] Otting G, Liepinsh E, Wuthrich K. ***Protein hydration in aqueous solution.*** Science. 1991 15;254(5034):974-80.

[208] Denisov VP, Halle B. ***Hydrogen exchange and protein hydration: the deuteron spin relaxation dispersions of bovine pancreatic trypsin inhibitor and ubiquitin.*** J Mol Biol. 1995 ;245(5):698-709.

[209] Garcia AE, Hummer G. ***Water penetration and escape in proteins.*** Proteins. 2000;38(3):261-72.

[210] Kauzmann, W. ***Some factors in the interpretation of protein denaturation.*** Adv. Prot. Chem. 1959 14, 1–59.

[211] Dill, K. A. ***Dominant forces in protein folding***. Biochemistry. 1990 Aug 7;29(31):7133-55..

[212] Hartley, G., (1936) ***Aqueous solutions of paraffin-chain salts,*** Hermann & Cie., Paris, as quoted in Tanford, C. (1973) ***The Hydrophobic Effect: Formation of Micelles and Biological Membranes,*** p viii, John Wiley & Sons, New York

[213]Levy Y, Onuchic JN. ***Water and proteins : A love-hate relationship.*** Proc Natl Acad Sci U S A. 2004;101(10):3325-6.

[214] W.Kauzmann.***Factors in interpretation of protein denaturation***..Adv.Prot.Chem. 1959.14,1-59

[215] Covalt, J. C., Roy, M. & Jennings, P. A. ***Core and surface mutations affect folding kinetics, stability and cooperativity in IL-1 beta: does alteration in buried water play a role?*** J.Mol Biol. 2001;307(2):657-69..

[216] Covalt JC Jr, Roy M, Jennings PA. ***Core and surface mutations affect folding kinetics, stability and cooperativity in IL-1 beta: does alteration in buried water play a role?*** J Mol Biol. 2001;307(2):657-69.

[217] Mueckler M, Weng W, Kruse M. ***Glutamine 161 of Glut1 glucose transporter is critical for transport activity and exofacial ligand binding*** J Biol Chem. 1994;269(32):20533-8.

[218] Mueckler M, Kruse M, Strube M, Riggs AC, Chiu KC, Permutt MA. ***A mutation in the Glut2 glucose transporter gene of a diabetic patient abolishes transport activity.*** *J Biol Chem*. 1994;269(27):17765-7.

[219] Kusari J, Verma US, Buse JB, Henry RR, Olefsky JM. ***Analysis of the gene sequences of the insulin receptor and the insulin-sensitive glucose transporter (GLUT-4) in patients with common-type non-insulin-dependent diabetes mellitus***. J Clin Invest. 1991;88(4):1323-30

[220] Iserovich P, Wang D, Ma L, Yang H, Zuniga FA, Pascual JM, Kuang K, De Vivo DC, Fischbarg J. ***Changes in glucose transport and water permeability resulting from the T310I pathogenic mutation in Glut1 are consistent with two transport channels per monomer.*** *J Biol Chem*. 2002 Aug 23;277(34):30991-7.

[221] Bell GI, Kayano T, Buse JB, Burant CF, Takeda J, Lin D, Fukumoto H, Seino S. ***Molecular biology of mammalian glucose transporters.*** Diabetes Care. 1990.13(3):198-208.

[222] Schulz,G.E., and Schirmer,R.H., (1979) ***Principle of Protein Structure***, Springer-Verlag, New York.

[223] Davidson, N. O., Hausman, A. M., Ifkovits, C. A., Buse, J. B., Gould, G. W., Burant, C. F., and Bell, G.I. ***Human intestinal glucose transporter expression and localization of GLUT5.*** Am J Physiol 1992 **262**(3 Pt 1), C795-800

[224] Manolescu A, Salas-Burgos AM, Fischbarg J, Cheeseman CI. ***Identification of a hydrophobic residue as a key determinant of fructose transport by the facilitative hexose transporter SLC2A7(GLUT7).*** J Biol Chem. 2005 Sep 26; [Epub ahead of print]

[225] Scheepers A, Schmidt S, Manolescu A, Cheeseman CI, Bell A, Zahn C, Joost HG, Schurmann A. ***Characterization of the human SLC2A11 (GLUT11) gene: alternative promoter usage, function, expression, and subcellular distribution of three isoforms, and lack of mouse orthologue.*** Mol Membr Biol. 2005;22(4):339-51.

[226] Manning SK, Woodrow C, Zuniga FA, Iserovich P, Fischbarg J, Louw AI, Krishna S. ***Mutational analysis of the hexose transporter of Plasmodium falciparum and development of a three-dimensional model.*** J Biol Chem. 2002;277(34):30942-9.

[227] Socolich M, Lockless SW, Russ WP, Lee H, Gardner KH, Ranganathan R. ***Evolutionary information for specifying a protein fold.*** Nature. 2005;437(7058):512-8.

[228] Lockless, S. W. & Ranganathan, R. ***Evolutionarily conserved pathways ofenergetic connectivity in protein families***. Science 1999; 286, 295—299).

[229] Hatley, M. E., Lockless, S. W., Gibson, S. K., Gilman, A. G. & Ranganathan, R..***Allosteric determinants in guanine nucleotide-binding proteins***. Proc. Natl Acad.Sci. USA 100, 14445—14450 (2003).

[230] Shulman, A. I., Larson, C., Mangelsdorf, D. J. & Ranganathan, R. ***Structural determinants of allosteric ligand activation in RXR heterodimers***. Cell 2004; 116, 417—429 .

[231] Ian C. West. ***Ligand conduction and the gated-pore mechanism of transmembrane transport.*** Biochim Biophys Acta. 1997 ;1331(3):213-34.

[232] Maloney P.C ***A consensus structure for membrane transport.*** Res. Microbiol. 141 (1990), pp. 374–383

[233] M.H. Saier, Jr.. ***Evolution of permease diversity and energy-coupling mechanisms: An introduction*** Res. Microbiol. 1990; 141, pp. 281–286

[234] Henderson, P. J., and M. C. Maiden.. ***Homologous sugar transport proteins in Escherichia coli and their relatives in both prokaryotes and eukaryotes.*** Phil. Trans. R. Soc. Lond. B Biol. Sci. 1990. **326:**391-410

[235] Rubin, R. A., S. B. Levy, R. L. Heinrikson, and F. J. Kezdy. ***Gene duplication in the evolution of the two complementing domains of gram-negative bacterial tetracycline efflux proteins***. Gene. 1990. **87:**7-13.

[236] Hirai T, Heymann JA, Shi D, Sarker R, Maloney PC, Subramaniam S. ***Three-dimensional structure of a bacterial oxalate transporter.*** Nat Struct Biol. 2002 (8):597-600

[237] Rupasinghe S, Baudry J, Schuler MA. ***Common active site architecture and binding strategy of four phenylpropanoid P450s from Arabidopsis thaliana as revealed by molecular modeling.*** Protein Eng. 2003;16(10):721-31.

[238] Fu D, Libson A, Miercke LJ, Weitzman C, Nollert P, Krucinski J, Stroud RM. ***Structure of a glycerol-conducting channel and the basis for its selectivity.*** Science. 2000;290(5491):481-6.

[239] Agre P, King LS, Yasui M, Guggino WB, Ottersen OP, Fujiyoshi Y, Engel A, Nielsen S. ***Aquaporin water channels--from atomic structure to clinical medicine.*** J Physiol. 2002;542(Pt 1):3-16

[240] Sansom MS, Bond P, Beckstein O, Biggin PC, Faraldo-Gomez J, Law RJ, Patargias G, Tieleman DP. ***Water in ion channels and pores--simulation studies.*** Novartis Found Symp. 2002;245:66-78; discussion 79-83, 165-8.